Analysis of the Immune Cell Infiltrates and Biomarkers during acute Gastrointestinal Graft vs Host Disease

Dissertation
zur Erlangung des Doktorgrades
der Biomedizinischen Wissenschaften
(Dr. rer. physiol.)
der
Fakultät für Medizin
der Universität Regensburg

vorgelegt von
Sakhila Ghimire
aus **Kathmandu, Nepal**
im Jahr **2016**

The present work was carried out from April 2013 to September 2016 at the Department of Internal Medicine III at the University Hospital Regensburg.

Die vorliegende Arbeit entstand im Zeitraum von April 2013 bis September 2016 an der Klinik und Poliklinik für Innere Medizin III des Universitätsklinikums Regensburg.

I dedicate this doctoral thesis to my mother and my motherland.

जननी जन्मभूमिश्च स्वर्गादपि गरीयसी

Mother and motherland are superior to Heaven

TABLE OF CONTENTS

List of Figures

List of Tables

List of Abbreviations

aGI-GvHD	acute Gastro Intestinal Graft vs. Host Disease
aGvHD	acute Graft versus Host Disease
AML	Acute myeloid leukemia
ANOVA	Analysis of variance
APCs	Antigen Presenting Cells
APS	Ammonium persulfate
ATG	Anti Thymocyte Globulin
BM	Bone Marrow
BW	Body Weight
CARD	Caspase Recruitment Domain
CD	Cluster of Differentiation
cDNA	complementary DNA
cGvHD	chronic Graft versus Host Disease
CLL	Chronic lymphocytic leukemia
CY	Cyclophosphamide
DANN	Deoxyribonucleic acid
DAPI	4',6-diamidino-2-phenylindole
DCs	Dendritic cells
DMSO	Dimethyl sulfoxide
dNTPs	2'-deoxyribonucleosid-5'-triphosphate
dsDNA	Double stranded DNA
ECL	Enhanced chemiluminescence
ECP	Extracorporeal Photophoresis
EDTA	Ethylene diamine tetra acetic acid
ELISA	Enzyme-linked immunosorbent assay
FCS	Fetal calf serum
FFPE	Formalin fixed-paraffin-embedded
FITC	Fluorescein isothiocyanate
Flu	Fludarabine
Foxp3	Forkhead Box Protein 3
GAPDH	Glyceraldehyde 3-phosphate dehydrogenase
G-CSF	Granulocyte colony stimulating factor
GM-CSF	Granulocyte -monocyte colony-stimulating factor
GvHD	Graft versus Host Disease
GvL	Graft versus Leukemia
GvT	Graft versus Tumor
Gy	Gray
HLA	Human Leukocyte Antigen
HRP	Horse radish peroxidase
HSCs	Hematopoietic Stem Cells
HSCT	Hematopoietic Stem Cell Transplantation

I3S	Indoxyl 3-sulfate
IDO	Indoleamine 2,3-dioxygenase
IFNγ	interferon gamma
Ig	Immunoglobulin
IL	Interleukin
IL-17	Interleukin-17
ILCs	Innate Lymphoid Cells
iTregs	induced Tregs
IκB	Inhibitor of kappa B
LPS	Lipopolysaccharide
MA	Myeloablative
mHags	Minor Histocompatibility Antigens
MHC	Major Histocompatibility Complex
miRs/miRNAs	micro RNAs
MMF	Mycophenolate Mofetil
MP	Methyl prednisolone
mRNA	messenger RNA
MUD	Mutual Unrelated Donor
NF-κB	Nuclear factor κB
NK	Natural Killer
NKT	Natural Killer T cell
NMA	Non-Myeloablative
NOD2	Nucleotide oligomerization domain 2
nTregs	natural Tregs
PAMP	Pathogen associated molecular pattern
PBS	Phosphate buffered saline
PBSC	Peripheral Blood Stem Cells
PCR	Polymerase chain reaction
PRR	Pathogen recognition receptor
qRT-PCR	Quantitative real-time PCR
Reg3a	Regenerating islet-derived protein 3 alpha
RIC	Reduced intensity conditioning
RISC	RNA-Induced Silencing Complex
RNA	Ribonucleic acid
RORγT	Retinoic acid receptor related orphan receptor 3
RT	Room temperature
rRNA	ribosomal RNA
s.e.m	standard error of mean
SCID	Severe combined immunodeficient
SDS-PAGE	Sodium dodecyl sulfate polyacrylamide gel electrophoresis
SNP	Single nucleotide polymorphism
T-bet	T-box transcription factor
TBI	Total Body Irradiation
TBS	Tris buffer saline
TBST	TBS + Tween 20
TCR	T Cell Receptor
TGF	Transformation Growth Factor

TLI	Total Lymphocyte Irradiation
TLR	Toll Like Receptor
TNF	Tumor Necrosis Factor
Tregs	Regulatory T cells

X

1 Introduction

Since the early beginnings, in the 1950's, hematopoietic stem cell transplantation (HSCT) is being performed as the major curative therapy for several life-threatening hematological and genetic disorders. Huge advances have been made in the past 60 years for successful transplantation and to increase the quality of life of patients, yet, complete success is hard to achieve due to the frequent occurrence of a secondary disease called graft versus host disease (GvHD). The number of allogenic hematopoietic cell transplantations continues to increase with more than 25,000 allogenic transplantations performed annually[1].

1.1   Hematopoietic Stem Cell Transplantation (HSCT)

Hematopoietic stem cells (HSCs) are pluripotent stem cells in the bone marrow (and fetal liver) that can give rise to all lineages of blood cells, including lymphocytes[2]. Mature blood cells are produced continuously by differentiation and expansion of hematopoietic stem cells. These stem cells have a unique capacity of self-renewal: they produce some daughter cells that do not differentiate, but replace and maintain the stem cell pool throughout individual's life. Leukemic cells arise from malignant stem cells that usually originate via mutation of normal stem cells. Most of the leukemic cells have limited capacity for proliferation and are continuously replenished by leukemic stem cells. Only 1 in 1 million leukemic blasts appears to be a true stem cells, according to the capacity to propagate and sustain human leukemia in immunologically susceptible mice[3]. Chemotherapy may eradicate the majority of leukemic blasts; leukemic stem cells, however, are quiescent and insensitive to therapy[4], and will result in recurrence. Some malignant stem cells survive even a lethal dose of total-body irradiation (TBI) and chemotherapy which is given as a preparative regimen for HSCT. The recurring malignant cells may be eliminated by immunologically active donor T cells and this phenomenon is called Graft vs Leukemia (GvL) effect[5]. Therefore HSCT

serves as promising therapy to get rid of leukemia and keep the immune system in balance but at the cost of GvHD.

HSCT is an intensive curative therapy for several malignant and non-malignant diseases[1]. Following conditioning with irradiation or chemotherapy to eradicate leukemic cells and render the recipient receptive of new stem cells, patients are given infusion of hematopoietic stem cells from a suitable donor[6].

Table 1.1 summarizes some diseases commonly treated with allogenic hematopoietic stem cell transplantation[7].

Table 1.1: Diseases Commonly Treated with Allogenic Hematopoietic Stem Cell Transplantation

Cancers	Other Diseases
Acute myeloid leukemia	Aplastic anemia
Acute lymphoblastic leukemia	Paroxysmal nocturnal hemoglobinuria
Chronic myeloid leukemia	Fanconi's anemia
Myelodysplastic syndrome	Blackfan-Diamond anemia
Myeloproliferative disorders	Thalassemia major
Non-Hodgkin's lymphoma	Sickle cell anemia
Hodgkin's disease	Severe combined immunodeficiency
Chronic lymphocytic leukemia	Wiskott-Aldrich syndrome
Multiple myeloma	Inborn errors of metabolism
Juvenile chronic myeloid leukemia	

1.1.1   Selection of stem cell donors

In order to achieve successful stem cell transplantation, it is crucial that both donor and recipient have a high degree of match in Human Leukocyte Antigen (HLA), a highly polymorphic protein that differs from individual to individual, encoded by Major Histocompatibility Complex (MHC). Class I HLA (A,B & C) are expressed on almost all nucleated cells and platelets whereas class II HLA proteins (DR, DQ & DP) are primarily expressed on cells that arise from hematopoietic stem cells such as B cells, monocytes and dendritic cells, but can be induced on other cell types during immune response[1]. The HLA system

encodes structurally homologous cell surface glycoproteins which present peptides to the immune cells that trigger an immune response and are encoded by chromosome 6, characterized by a high degree of allelic polymorphism. The strongest transplant reactions occur when the HLA of the donor and the recipient are incompatible[7]. Therefore the best donor for HSCT would be an HLA matched sibling. When a recipient does not have any siblings, a matched unrelated donor (MUD) is chosen based on at least HLA-A, -B, -C and –DRB1 alleles. Allele compatibility for the HLA-A/B/C/DRB1//DQB1 loci is defined as a 10/10 match and considered as the standard donor requested by many transplant centers[8]. Despite HLA identity between donor and recipient, almost 40% of patients receiving HLA-identical grafts develop GvHD due to genetic differences that lie outside of the HLA-loci, in terms of minor histocompatibility antigens (mHags)[1]. mHags are immunogenic peptides derived from polymorphic cellular proteins. These peptides bind to HLA antigens and are recognized by allogenic T cells.

1.1.2   Sources of Stem Cells

HSCs can be obtained either directly from bone marrow, from peripheral blood or from umbilical cord blood. Since marrow stem cells detach continuously and circulate in the peripheral blood, peripheral blood stem cells (PBSCs) are the most convenient source of hematopoietic stem cells. In allogenic stem cell transplantation, PBSCs are thought to have better and rapid hematopoietic reconstitution and have the potential to reduce disease recurrence[9] . However, PBSCs contain more T lymphocytes than the bone marrow, thus increase the incidence and prolong the treatment of chronic GvHD (cGvHD)[10,11].

The use of cord blood as an alternative to donor stem cells has provided a promising alternative when transplantation is urgent or when the suitable donor is not found[7]. Blood from the umbilical cord and placenta of newborn child is rich in hematopoietic stem cells but the numbers of cells are limited. Infection is a common problem after cord blood transplantation since hematological and immune reconstitution is slower in cord blood transplantation. However this type of transplantation requires less-stringent HLA matching[12] compared to marrow or peripheral blood.

1.1.3   Conditioning therapy for HSCT

For successful HSCT, a first criterion is that the graft gets enough space and support for cell proliferation and differentiation. Therefore, the existing host stem cells must be eradicated in order for donor stem cells to engraft properly for which conditioning therapy is necessary prior to HSCT. Secondly, it is crucial that recipients are immunocompromised to prevent rejection of the incoming donor cells by the host immune system. The administered conditioning regimen suppresses the host immune system and thus, allows donor stem cells to home in the bone marrow microenvironment without the risk of graft rejection. Finally and most importantly, the conditioning therapy eradicates the underlying disease and provides long-term disease control or at least reduces leukemic cells to a level which allows final elimination by GvL effects. This is particularly important for patients with hematological malignancies.

Although there is no full agreement on meticulous classification of conditioning treatments, generally accepted definitions are of three types: myeloablative conditioning, non-myeloablative and reduced-intensity conditioning[13]. The diagrammatic overview of conditioning is shown below in Figure 1.1.
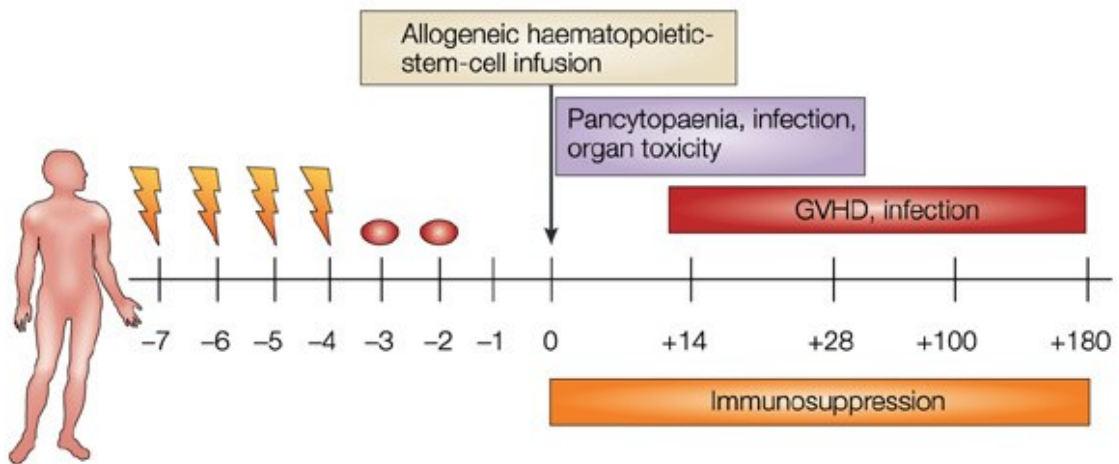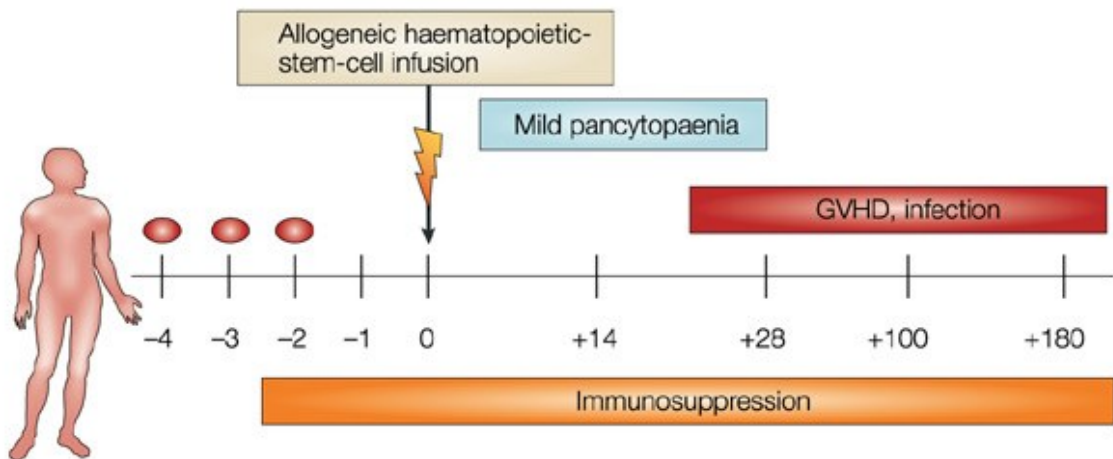
Figure 1.1: Overview of myeloablative and non-myeloablative conditioning regimens
Lightning bolts in yellow represent total body irradiation and the ovals in red represent chemotherapy[5].

Myeloablative (MA) conditioning is of high-dose intensity consisting of a single agent or combination of agents that eradicate the patient's hematopoietic cells in the bone marrow and induce long-lasting trilineage aplasia. This strategy includes TBI and/or alkylating agents, at doses that will not allow autologous hematologic recovery resulting in profound pancytopaenia within days from the time of administration[13]. Pancytopaenia is life-threatening and fatal unless patients' hematopoiesis is restored by infusion of hematopoietic stem cells.

Non-myeloablative (NMA) conditioning can be defined as a regimen that will cause minimal cytopenia, little early toxicity and does not require hematopoietic

stem cell support[13,14]. Nevertheless, NMA conditioning regimens are immunosuppressive to the extent that, when followed by granulocyte-colony stimulating factor (G-CSF) mobilized PBSC or BM infusion, donor lymphohematopoietic cells can engraft with at least mixed donor/recipient chimerism[15]. The final elimination of host hematopoiesis is then achieved by graft-versus-hematopoietic and GvL effects of the donor immune cells resulting eventually in full donor chimerism[14].

Reduced intensity conditioning (RIC) regimens try to fill the gap between MA and NMA conditioning therapies and are used for the majority of patients nowadays. The concept of RIC is based on the idea of preventing the high toxicity and mortality associated with MA conditioning regimens in patients with advanced age or relevant comorbidities[16]. The goal of RIC is not always complete tumor eradication and thus, complete destruction of host hematopoiesis but sufficient control of the underlying disease by cytotoxic therapy followed by the immune-mediated effects of donor graft cells[16].

Table 1.2 summarizes the current, most frequently used conditioning regimens for allogeneic HSCT.

Table 1.2: Frequently used Conditioning Regimens in various Transplant Centre Worldwide

Intensity	Regimen	Comments
Myeloablative	CY/TBI	Profound pancytopenia, require stem cell support, substantial nonhematological toxicities
	BU/CY	
Non-myeloablative	FLU/TBI	Minimal cytopenia, do not require stem cell support
	TLI/ATG	
	Low dose TBI	
Reduced-Intensity	FLU/MEL	Intermittent cytopenia, reduced nonhematological toxicities
	FLU/BU	
	FLU/CY	

Abbreviations: CY = cyclophosphamide; TBI = total body irradiation; BU = busulfan; FLU = fludarabine; TLI = total lymphoid irradiation; ATG = anti-thymocyte globulin; MEL = melphalan.

1.2 Graft versus Host Disease (GvHD)

GvHD is the most recognized complication after HSCT. The first recognition of GvHD was in 1956 in a murine model. Barnes *et al.*. demonstrated that irradiated mice infused with the allogenic marrow and spleen cells recovered from radiation injury and aplasia but they developed diarrhea, weight loss, skin changes and liver abnormalities. Mice subsequently died due to "secondary disease"[17]. This phenomenon was subsequently recognized as graft versus host disease (GvHD). A decade later, in 1966, Billingham postulated three crucial requirements for the development of GvHD:

i) the transplanted graft must contain immunologically competent cells,

ii) the recipient must be incapable of rejecting or eliminating transplanted cells and,

iii) the recipient must express tissue antigen that are not present in the transplant donor thus the recipient antigen be recognized as foreign by donor cells[18].

Today it is realized that the immunocompetent cells are T lymphocytes that are present in the stem cell inoculum and are required to mount an effective immune response[19]. A normal immune system is able to reject T cells from a foreign donor, but when the patient immune system is compromised by the use of various immune-ablative agents (chemotherapy and/or radiotherapy), the recipient is incapable of rejecting transplanted cells[20]. Previously it was believed that acute GvHD occurs within day 100 after transplantation and chronic GvHD occurs beyond day 100 and that the most affected organs at the onset of GvHD are skin (81%), gastrointestinal tract (54%) and liver (50%)[21]. Now it is clear that acute GvHD can occur after day 100 as late acute GvHD (e.g. after cessation of immunosuppression or after donor lymphocyte infusion) or cause an overlap syndrome of both acute and chronic GvHD[22].

1.2.1 Pathophysiology of acute GvHD: a three-step model

Acute GvHD has been attributed to three stages. Initially there is tissue damage due to conditioning which in turn activates the host antigen presenting cells (APCs). Secondly, APCs activate donor T cells, also known as afferent phase.

Finally, in the efferent phase, cellular and inflammatory factors work together to destroy the target organs.

a. conditioning-mediated tissue damage: damaged host tissue release danger signals that includes pro-inflammatory cytokines like tumor necrosis factor (TNF) and interleukin-1 (IL-1)[23], which can activate host APCs, ultimately activating donor T cells infused in the stem cell inoculum[24,25]. Conditioning-mediated damage to the GI tract remains the main concern as the GI tract allows systemic translocation of microbial products like lipopolysaccharide (LPS) and pathogen associated molecular patterns (PAMPs) that greatly amplify host APC activation[26], leading to T cell activation.
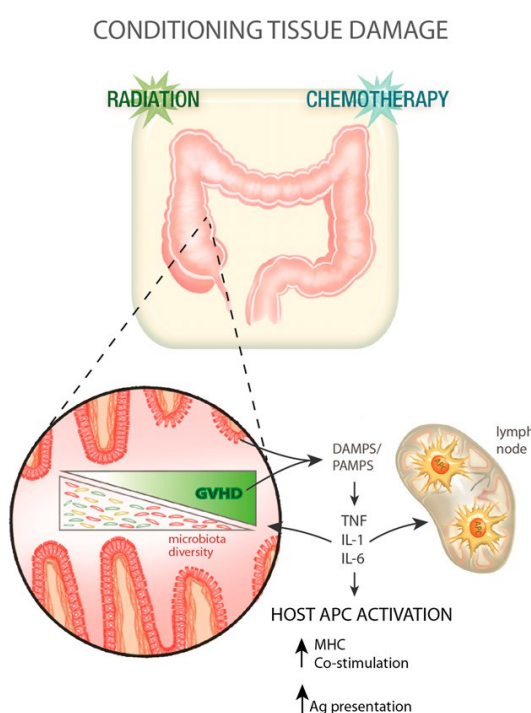
Figure 1.2: Conditioning mediated tissue damage (phase I)
Radiotherapy and/or chemotherapy damage the gastrointestinal mucosa which causes the translocation of DAMPS and PAMPS leading to the release of pro-inflammatory cytokines[27].

b. donor T cell activation (the afferent phase): graft versus host disease occurs when donor T cells become activated and respond to HLA differences on recipient's cells[1]. Experimental models have proved that the host APCs are necessary and sufficient to activate donor T cells and initiate GvHD[25,28]. Donor T cell can recognize alloantigen either on host APC, known as direct antigen presentation[29] or on donor APCs, known as indirect presentation[30]. T cell response depends on the disparity between the donor and the recipient with

regard to major and minor HLA[1]. CD4^{+} T cells respond to the variations in MHC class II molecules (HLA-DR, DQ, DP) and CD8^{+} T cells respond to the variations in MHC class I molecules (HLA-A, B, C)[31]. Even though the transplantation is carried out with a HLA matched donor, GvHD occurrence has been reported to occur due to differences in minor HLA[32].
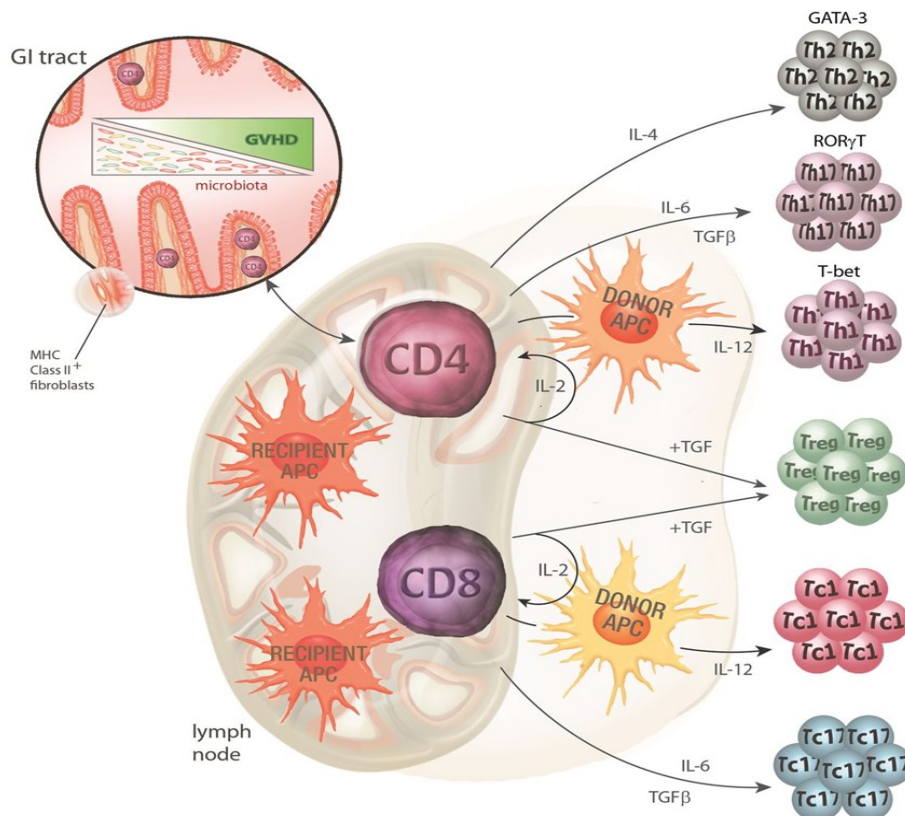
Figure 1.3: Donor T cell priming and differentiation (phase II)
Both donor and recipient APCs are actively involve in antigen presentation. Activation of T cells in the presence of various cytokines determines the fate of T cell differentiation. Th2, Th17 and Th1 marked by the transcription factors GATA-3, RORyt and T-bet respectively[27].

c. target cell apoptosis (the efferent phase): in this phase, both innate and adaptive immune cells work synergistically to aggravate the T cells mediated inflammation. Cellular mediators such as cytotoxic T lymphocytes (CTLs) and natural killer (NK) cells use Fas/Fas ligand (FasL) pathway and perforin/granzyme pathway to lyse the target cells[33,34]. Furthermore, inflammatory cytokines synergize with CTLs, resulting in further tissue injury and possible target organ dysfunction[1]. In addition, microbial products like LPS, which are released during conditioning, leak through a damaged intestinal mucosa and skin, and stimulate mononuclear cells (monocytes/macrophages) to secret inflammatory cytokines.

This leads to amplification and propagation of the so-called "cytokine storm"[1] and to the destruction of epithelial cells mostly in the GI tract.
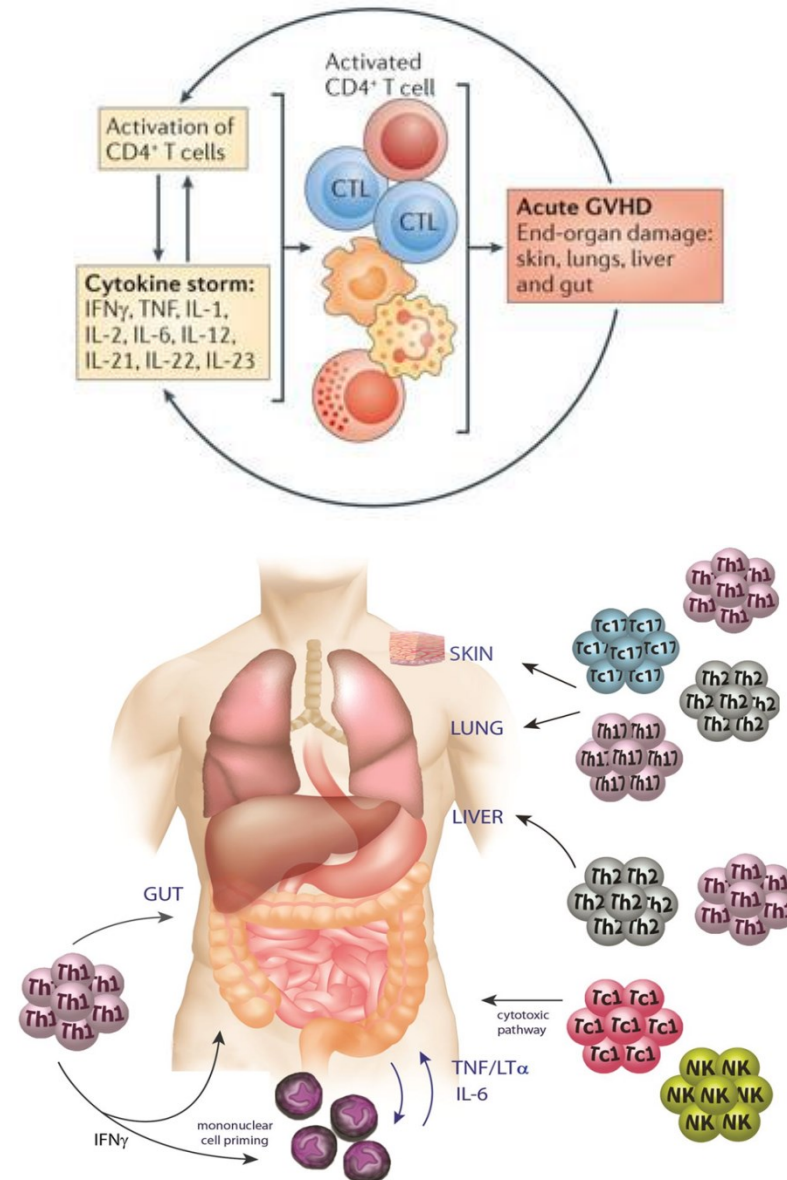
Figure 1.4: Target cell apoptosis: the effector phase (phase III)
Liver, lung, skin and most pronouncedly gut are the target tissue of T cells[27,35].

In the last 10 years, this concept has been largely extended and a more differentiated view has been adapted. It became clear that the microbiota of epithelial tissues are major players influencing epithelial integrity and local immune tolerance by commensal bacteria and millions of metabolites are produced to maintain epithelial homeostasis [36,37].

In context with the concept of microbiota as important players, researchers have recognized the increasing importance of regulatory immune cells which normally balance immune reactions. Regulatory T cells expressing the transcription factor

Foxp3 occur as natural, thymus derived regulatory cells and are able to prevent alloreactions[38]. On epithelial surfaces, induced peripheral Tregs try to dampen acute inflammation[39]. Foxp3^{+} T cells act in cooperation with numerous newly identified regulatory populations such as invariant NKT cells[40], myeloid derived suppressor cells and a whole new set of innate immune cells such as innate lymphoid cells[41].

.

1.3 Regulatory T cells (Tregs) in GvHD

Tregs are a subset of CD4^{+} T cells whose function is to suppress immune responses and maintain self-tolerance[42]. A transcription factor called FOXP3, a member of the fork head family of transcription factors, is critical for the development and function of Tregs and is used as a definite marker to identify Tregs[42,43]. Tregs are produced in the thymus as a functionally mature subpopulation of T cells and can also be induced from naive T cells in the periphery[44].

Natural Tregs (nTregs), derived from the thymus are characterized by the co-expression of CD4, CD25 and Foxp3, collectively represented as CD4^{+}CD25^{+}Foxp3^{+} Tregs[45]. Induced or adaptive Tregs (iTregs) are generated in the peripheral lymphoid organs in presence of transforming growth factor beta (TGF-B)[46].

1.3.1 Tregs in immune balance

Tregs are known to downregulate immune responses by a) production of inhibitory cytokines and b) a contact-mediated effect on APCs. Tregs produce the anti-inflammatory cytokine- interleukin 10 (IL-10), that inhibits the production of IL-12 by activated DCs and macrophages[47,48]. IL-10 also inhibits the expression of co-stimulators and class II MHC molecules on DCs and macrophages thus inducing tolerance of immune system[47-49]. Another anti-inflammatory cytokine produced by Tregs, TGF-β, inhibits the proliferation and effector functions of T cells and the activation of macrophages. TGF-β also regulates the differentiation

of functionally distinct subsets of T cells, stimulates production of immunoglobulin A (IgA) antibodies, promotes tissue repair after local immune and inflammatory reactions subside, conferring Tregs mediated immune reconstitution[47-50]. Tregs play a major role in regulation of epithelial inflammation and are strongly influenced by the interaction with the epithelial microbial environment[36,51].

1.3.2   Tregs in pre-clinical model of Stem Cell Transplantation.

Tregs play an indispensable role in both solid organ transplant tolerance and in allograft tolerance after HSCT. In rodents and humans, a subpopulation of thymus derived naïve CD4^{+} T cells that co-express the IL-2Ralpha chain, CD25, has potent suppressor activity. Tregs mediate transplantation tolerance in experimental models of skin, solid organs[52] as well as tolerance to bone marrow allografts[53]. HSCT and conditioning can cure malignant and non-malignant hematological disorders ,but at the same time the treatment efficacy is highly limited due to GvHD[1]. Regulatory T cells have received considerable attention in recent science due to their ability to suppress the proliferation of conventional T cells and prevent GvHD in animal models when added to donor grafts containing conventional T cells, hence suppressing GvHD[54]. Using a mouse model, Edinger and co-workers have shown that CD4^{+}CD25^{+} Tregs suppress GvHD after bone marrow transplantation without abrogating the graft versus-leukemia (tumor) (GvL or GvT) effect[38] supporting the importance of Tregs in allogenic HSCT. It has been demonstrated that the adoptive transfer of Tregs preserved thymic and lymphoid architecture of the host and hence accelerate post-transplant T cell immune reconstitution in a murine GvHD model[55].

Tregs are long believed to be a subset of CD4^{+} T cell compartment. Recently, CD8^{+} Treg population was reported and ws shown to be capable of suppressing T cell responses in an experimental model of autoimmunity[56]. In terms of GvHD, Robb *et al.*. demonstrated that CD8^{+}Foxp3^{+} Tregs suppressed GvHD and attenuated GvHD mortality after bone marrow transplantation (BMT) in mice model[57].

1.3.3 Tregs in clinical Hematopoietic Stem Cell Transplantation

Many researchers have focused on evaluating the status of Tregs after HSCT, since they play an important role in the amelioration of GvHD. Using peripheral blood of patients after transplantation, Li et al. demonstrated that the frequency of CD4^{+}CD25^{+} Tregs was significantly downregulated in patients with severe acute or chronic GvHD [58]. They also showed that a decreased level of CD4^{+}CD25^{+} Tregs was correlated to increased severity of GvHD [58]. While majority of studies focused on blood-derived Tregs, there is little information on Tregs isolated from intestinal tissues due to the lack of availability of repeated gut biopsies without diagnostic purpose. Using immunoenzymatic labeling, Rieger et al. were the first to demonstrate that the infiltrating Tregs decreased the signs of acute and chronic GvHD in intestinal mucosa [59]. They showed that the acute and chronic GvHD patients had a complete lack of counter regulation indicated by a Foxp3^{+}/CD8^{+} T cell ratio in patients with GvHD identical to that of healthy individuals, while this ratio was increased in patients without GvHD[59].

However, for the first time, Lord et al. demonstrated a contradictory result showing that Foxp3^{+} cells were nither decreased in blood nor in gastrointestinal tissues and that the frequency of Tregs did not correspond to the disease incidence or severity [60]. They rather found that the Foxp3^{+} cells were significantly upregulated in GvHD intestinal mucosa when compared to non GvHD mucosa[60]. This finding is further supported by Ratajczak et al. who observed an increased proportion of CD4^{+}Foxp3^{+} cells in Grade 2-4 GvHD patients compared to grade 0-1 GvHD patients[61]. Part of these conflicting results is again due to the lack of possibility to discriminate between natural and induced Tregs. It may well turn out that nTregs are decreased in GvHD while iTregs try to compensate for exaggerated inflammation.

1.3.4 Approaches to induce regulatory T cells after HSCT

Tregs are crucial to induce tolerance and maintain immune homeostasis. A major challenge to use Tregs as a therapy is their relative scarcity in blood (0.5-1% of CD4^{+}CD25 bright T cells)[62]. In 2011, Hippen et al. showed two individual reports

regarding generation of induced Tregs in large scale[63] and *ex vivo* expansion of natural Tregs[64], both method focused on the development of large scale expansion protocols for Tregs with higher cellular yield so that they can ultimately be used as GvHD therapy or for GvHD-prevention[63,64]. Using chronic GvHD subjects, Matsuika and co-workers reported that daily administration of low-dose IL-2 induced selective expansion of functional Tregs, improved cGvHD, restored CD4$^+$ T cells homeostasis, and promoted the re-establishment of immune tolerance[65]. This suggests that low-dose IL-2 could be a potential therapy to restore immune balance after HSCT.

Furusuwa and colleagues reported that the clostridia products like short chain fatty acid (SCFA) especially butyrate can induce the differentiation of colonic Tregs *in-vitro* and *in vivo* in mice[66] providing strong evidence of the necessity of host-microbiome interaction to establish immunological tolerance and homeostasis in gut. Moreover, Mathewson and colleagues reported that restoring clostridia metabolites or the strain itself modulated intestinal epithelial cell integrity and mitigated GvHD in mice[36]. Of note, Baban and colleagues reported indoleamine 2,3-dioxygenase (IDO) as a potent inducer of Tregs and an inhibitor of Th1 cell subset[67]. Later it was reported that Tregs generation by IDO takes place via aryl hydrocarbon receptor (AhR)[68]. Interestingly, it was recently observed that AhR engages in long-term regulation of systemic inflammation only in presence of IDO[69] suggesting a triangular positive feedback loop between Tregs, IDO and AhR. AhR is a ligand activated transcription factor that is activated in presence of xenobiotic compounds and bacterial metabolites such as indole and its derivate[70]. Taken together, these findings strongly suggest that right balance of gut microbiome is crucial to induce Tregs for intestinal tolerance.

1.3.5 Tregs in GvHD: First-In-Man Clinical Trial

The first clinical trial reported was an adoptive transfer of ex-vivo expanded CD4$^+$CD25$^+$CD127- Tregs after HLA-identical sibling HSCT. Transfer of Tregs resulted in a reduction of the steroids administered, increase in levels of circulating Tregs and a decrease in inflammatory cytokine levels in the peripheral blood (PB)[71]. Another "first-in-human" clinical trial was reported in double

umbilical cord blood transplantation (UCBT) in 23 patients, who received *in-vitro* expanded Tregs derived from partially HLA-matched third-party UCB units. There was an almost significant reduction of the incidence of grade II-IV acute GvHD controls without transfusion of Tregs. No toxicities were observed, no infections, relapse or early mortality which suggested that UCB Tregs could be a potential tool for preventing acute GvHD[72]. Taken together these early trials suggest the potential of Tregs as candidates to ameliorate GvHD and establish immune reconstitution after transplantation in larger clinical trials.

1.4   Indoleamine-2,3 dioxygenase (IDO) in GvHD

IDO is an intracellular enzyme that catalyzes the first and rate-limiting step of essential amino acid tryptophan catabolism[73]. This immunosuppressive enzyme is expressed by APCs and parenchymal cells and is further inducible by inflammation[74]. Depletion of tryptophan and the increase of tryptophan metabolites (namely kynurenines) via IDO inhibit T cell proliferation and ultimately favor T cell apoptosis. Moreover, tryptophan starvation and the presence of kynurenines induces the conversion of naïve T cells and regulatory T cells[75]. Of interest, Mezrich and co-workers demonstrated that kynurenine mediated Tregs generation takes place via AhR activation[68]. Immunosuppressive properties of IDO have been well defined in maternal-fetal acceptance, tumor immunity, autoimmunity and chronic infections[76]. Figure 1.5 shows IDO mediated tryptophan degradation and effect on T cells[77].
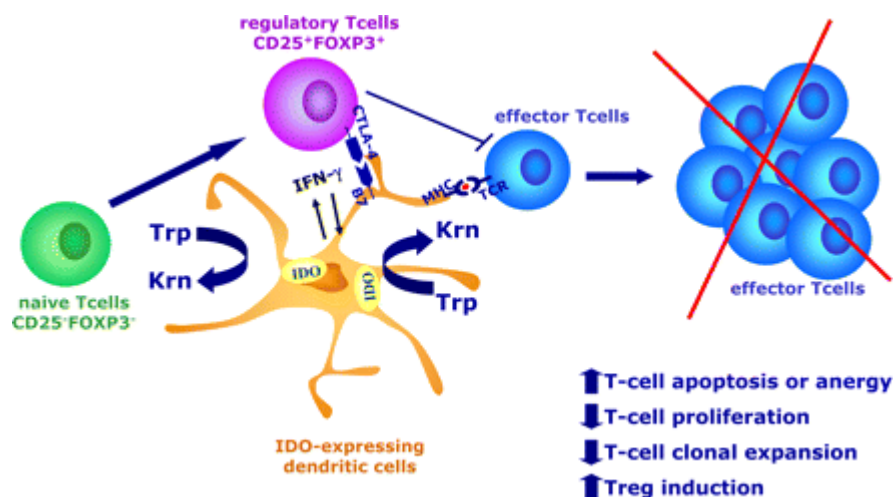
Figure 1.5: Tryptophan degradation by IDO
IDO induce tryptophan degradation which results in inhibition of T-cell proliferation, increase in T-cell apoptosis, and de novo formation of Tregs[77].

In the context of GvHD, experimental models have well established IDO as a critical regulator of GvHD. IDO knock-out mice showed increased colon GvHD and reduced survival after allogenic stem cell transplantation when compared to wild-type mice[74]. In a clinical context, GvHD patients tend to have increased IDO production which reflects a reactive release of immunosuppressive mediators in GvHD related inflammation, that is perhaps initiated to balance immune reactions[78]. IDO is well-known to induce peripheral tolerance by increasing regulatory T cells[79,80]. In terms of protective effect in GvHD, apart from Tregs and IDO positive cells, a new type of immune cell-innate lymphoid cells has gained substantial importance in the past few years.

1.5   Innate lymphoid cells (ILC) in GvHD

ILCs are a recently identified family of mononuclear hematopoietic cells that preserve epithelial integrity and tissue immunity throughout the body [81]. These cells are derived from Common Lymphoid Progenitor (CLP) and combines innate and adaptive modes of function [82]. With recent advances in understanding the development and proliferation of ILCs, they are classified into 3 groups. ILCs group 1, ILCs group 2 and ILCs group 3.

The group 1 ILCs comprises cells that produce type 1 cytokines like IFN-y [83] and aredependent on transcription factor T-bet for development . Initially, conventional (c) NK cells were classified in group 1 ILC since they express T-bet and produce significant amount of IFN-y. However, cNK cells turn out to differ from other group 1 ILC subset as they are developmentally dependent on Eomesodermin (Eomes, a T box transcription factor related to T-bet) but not on T-bet [84].

Innate lymphoid cells that predominantly produce type 2 cytokines are termed as group 2 ILCs or ILC2s [85]. ILC2s produce very high amount of IL-5 and IL-13, and also IL-9, IL-4 and GM-CSF[86,87]. These cytokines are vital for mucus production from goblet cells, eosinophils induction, muscle contraction, mastocytosis [88,89] and ILC2 produced amphiregulin is crucial for tissue repair[90]. ILC2s are developmentally dependent on the transcription factors retinoic acid receptor-related orphan receptor-a (RORa) [91] and GATA- binding protein 3 (GATA3) [92].

Group 3 ILCs are defined by the expression of transcription factor RORγT (*RORC*) for their development and expression of NK cell activating receptor NKp46 but are distinct from NK cells[93-95]. ILC3s are able to produce cytokines IL-17A and /or IL-22 [85]. ILC3s are divided into Lymphoid Tissue inducer (LTi) cells that expresses IL-17 and IL-22, natural cytotoxicity receptor (NCR) positive IL-22 producing ILC3s and NCR negative IL-17 producing ILC3s [83].

ILC3s has gained substantial focus ever since the discovery that IL-22 producing ILC3s are indispensable for mucosal immunity[95,96]. In particular, ILC3s are the major source of IL-22 cytokine that are protective to epithelial cells in the intestine [97]. These cell types are activated directly by bacterial metabolites via aryl hydrocarbon receptor (AhR) or indirectly through myeloid cells mediated cytokine IL-23 [98]. Studies of ILC3s on human gut are highly missing due to the lack of specific marker for ILCs, however, mice experiments have revealed that ILC3s play a crucial role in gut immunity by directly inducing epithelial cell proliferation, promoting epithelial cell mediated production of anti-inflammatory cytokines and antimicrobial peptides like Reg3a, preventing dissemination of commensal bacteria, and suppressing microbiota-specific pro-inflammatory CD4$^+$ T cell responses [99]. Figure 1.6 shows the development of innate lymphoid cells[100]
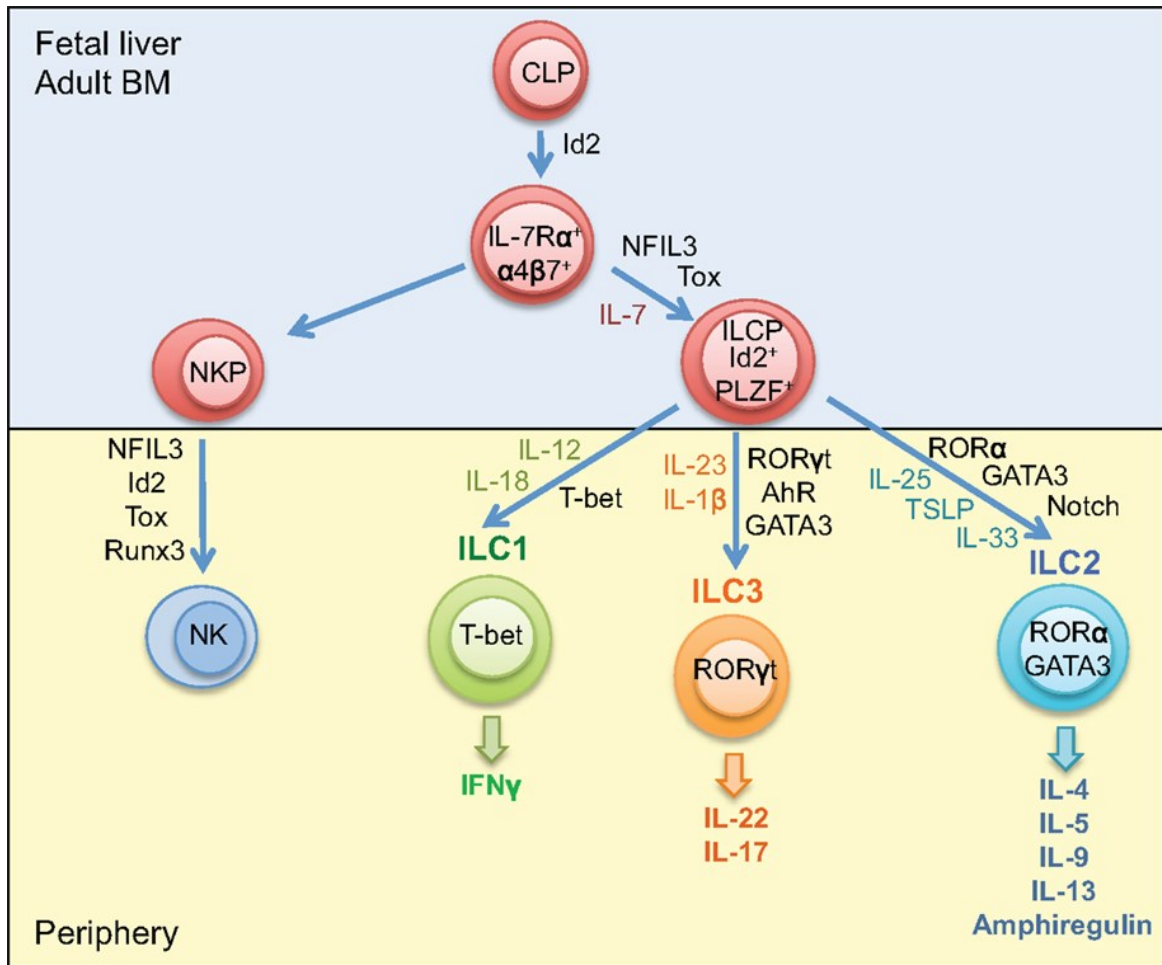
Figure 1.6: Development of Innate Lymphoid Cells.
In fetal liver or in adult bone marrow, ILCs differentiate from common lymphoid progenitor (CLP) in presence of transcription factor Id2. NK cell precursor gives rise to innate NK cells and ILC precursor gives rise to T-bet dependent ILC1s, GATA-3 dependent ILC2s and RORyt dependent ILC3s[100].

1.6   IL-17 in GvHD

Ubiquitously known as Th-17 cell cytokine, IL-17 is a pro-inflammatory cytokine known to mediate protection again extracellular pathogens, and promotes inflammatory pathology in autoimmune disease [101]. The inflammatory properties of IL-17 have gained a substantial importance in development of GvHD in recent years[102-104]. IL-17 production is regulated by transcription factor RORγT [105], an orphan nuclear receptor that drives the differentiation of Th17 cells.

Although IL-17 is defined as Th-17 cytokine, Th-17 pathway is inadequate to explain the early IL-17 mediated immunity that have crucial roles during stress

responses and host defense especially when the IL-17 mediated immune pathway is induced within hours in response to epithelial cell injury or activation of pattern recognition receptors (PRRs)[106-108], and this short time is not enough for the development of Th-17 cells. Therefore it is possible that the innate source of IL-17 exists and perhaps these cells in parts mediate regulation instead of inflammation. Furthermore, the inflammatory role of IL-17 in development of GvHD has been now challenged since the discovery of innate lymphoid cells [83]. In brief, table 1.2 presents an overview of some IL-17 producing cells [109].

Table 1.3: Innate IL-17 producing cells

Cell type	Inducing signal (ligand–receptor)	Main effector cytokines	Location or effector site	Functions	Transcript-ion factors
CD3⁺CD27⁻ γδ T cell	IL-23–IL-23R; IL-1–IL-1R; RAE1 or MICA–NKG2D; β-glucan–dectin 1; bacterial product–TLR	IL-17	Gut and skin	Surveillance; rapid host defence; maintenance of barrier function	RORγt, RUNX1, AHR and IRF4?
CD1d⁺CD3⁺NK1.1⁻ iNKT cell	IL-23–IL-23R; glycolipid–CD1d	IL-17	Liver, lung and skin	Surveillance; rapid host defence	RORγt
CD3⁻NKp46⁺ cell	IL-23–IL-23R; RAE1 or MICA–NKG2D; IL-15–IL-15R	IL-22 (IL-17 in humans)	Gut and skin	Production of pro-inflammatory mediators	RORγt, AHR, IRF4 and ID2
CD3⁻ CD4⁺KIT⁺THY1⁺ LTi-like cell	IL-23–IL-23; IL-7–IL-7R; bacterial product–TLR	IL-22 and IL-17	Lamina propria and spleen	Surveillance; lymphoid aggregate formation?	RORγt, ID2, AHR and STAT3
THY1⁺SCA1⁺CD3⁻ CD4⁻KIT⁻cell	IL-23–IL-23R; IL-7–IL-7R	IL-17, IL-22 and IFNγ	Lamina propria	Immune surveillance	RORγt and T-bet (AHR⁻)
Paneth cell	TNF–TNFR; bacterial product–NOD2	IL-17	Intestinal crypts	Surveillance; amplification of immune response	Not known
GR1⁺CD11b⁺ cell	Bacterial product–TLR	IL-17	Lung and kidney	Host defence	Not known

1.7 Microbial metabolites in GvHD

Human gastro-intestinal tract harbors trillions of microbes that are fundamental for well-being of their host. These microbes are necessary to educate and discipline the human immune system. The diversity and complexity of the gut microbiota can be evaluated by using 16S ribosomal RNA (rRNA) sequencing [110] technology. By now it is not surprising to see that the alteration of microbiome is

associated with cutaneous problems, gastric associated diseases, colorectal cancer, inflammatory bowel disease, liver complications, obesity, rheumatoid arthritis, and many more in the queue [111]. In the context of allogenic stem cell transplantation, 16S rRNA sequencing revealed the major microbiome shift in the course of ASCT [112]. Interestingly, there was huge predominance of Enterococcus species in patient with GvHD compared to non-GvHD patients [112]. Surprisingly, authors also shed light on the decrease of microbial metabolite indoxyl sulfate which occurred as a consequence of loss of bacterial diversity [112]. A more recent study proposed the loss of bacterial diversity and the decrease in urinary indoxyl sulfate in ASCT patients was associated with higher transplant related mortalityand poor survival [113]. , detection of higher indoxyl sulfate in urine of patients was associated with presence of clostridia species [113]. Collectively these finding suggests that the balanced microbial population and thereof, the bacterial metabolites may be important for immune mediated complications like GvHD.

Other bacterial metabolites like butyrate, a short chain fatty acid that is produced by bacteria as a result of dietary fiber degradation, has been implicated in maintaining integrity of intestinal epithelial cell and reduces the severity of GvHD [36]. Among several short chain fatty acid receptors, butyrate receptor GPR109a is known to be involved in butyrate mediate suppression of inflammation[114]. GPR109a signaling promotes anti-inflammatory properties in myeloid cells thereby generating regulatory T cells, promotes IL-18 production by epithelial cell which collectively suppress inflammation and promotes immune regulation[114]. Moreover, bacterial metabolite indole has also been shown to strengthen epithelial barrier and reduce mucosal inflammation[115,116]. Due to immense importance of balanced microbial diversity, it has been suggested that prebiotics, probiotics and post biotics approach could benefit the patients while sparring antibiotic approach [37]. Figure 1.8 shows the diagrammatic representation of possible clinical intervention of gut microbiota [37]
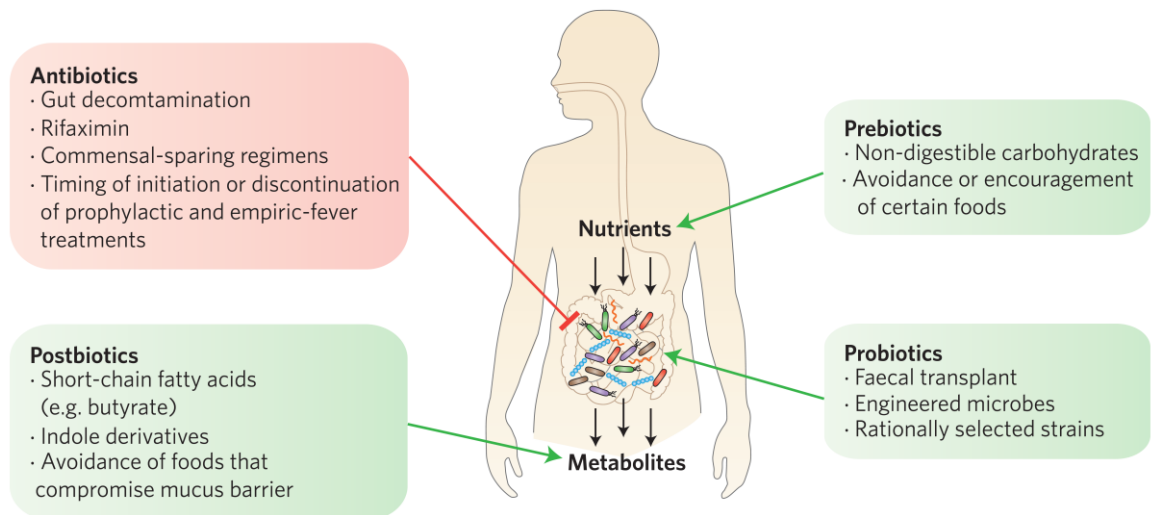
Figure 1.7: Clinical intervention of gut microbiota
Green box shows approaches to maintain healthy and balanced gut microbiome. Red box shows factors to destroy and alter microbiome[37].

1.8 Conclusion

Despite of broad understanding, a major issue in treatment of especially aGvHD is that most approaches are started too late, when major changes have already severely damaged the target tissue. Therefore, biomarkers allowing early identification of patients at high risk are needed. A handful of biomarkers have been discovered which might be used to guide treatment in the future [117].

The pathophysiology of aGvHD seems to be much more complex than our understanding due to the rising fact that bacterial diversity and bacterial metabolites plays crucial role in immune balance. Almost 1.5 million of bacterial metabolites are believed to be present in human immune system, effectively regulating both immune reaction and immune tolerance, ultimately deciding the fate of immune homeostasis. It is now of crucial importance to better understand the role of commensals in human health and therefor perhaps modulating bacteria and bacterial metabolites could be established as an alternative safe approach in future to improve the quality of life of GvHD patients.

Finally, practice of stem cell transplantation differs from countries, and within a same country, it differs from transplantation institutes. Approaches aiming at standardization of diagnosis and treatment are urgently needed and addressed by several consensus projects[118,119].

2 Research Objectives

Graft versus host disease (GvHD) accounts for significant morbidity and mortality after allogenic stem cell transplantation (ASCT). Early diagnosis of the disease provides clinicians a better strategy for treatment of patients to improve the quality of life after ASCT. Histological evaluation of apoptotic changes in the biopsies of affected organs, especially skin and gastrointestinal (GI) tract is so far the gold standard for the diagnosis of GvHD. Apoptosis of target organs are largely mediated by donor immune cells that infiltrates to skin and GI tract. The overall aim of this study was to analyze immune cell infiltrates and biomarkers during acute GI GvHD.

The specific aims of this dissertation were

1) to assess immunoregulation in intestinal biopsies of patients after allogeneic SCT in relation to presence of GvHD and outcome by two different approaches. First, $CD4^+$ and $CD8^+$ T cell infiltrates in GI tract of patients after ASCT were quantified using single antibody immunohistochemistry (IHC). In order to analyze functional changes at tissue level, Foxp3, IDO and IL-17 was accessed with IHC. Further characterizations of cellular source of $Foxp3^+$ and $IL-17^+$ cell were performed by double immunofluorescence. In a second approach, PCR was performed to analyze *FOXP3*, *IDO* and *RORC* at transcriptional level in order to confirm results obtained by protein expression.

2) to assess whether tissue markers of the GI tract can be used as biomarkers in patients. In addition to the described analyses, a panel of carefully selected messenger RNAs was analyzed in GI tract of transplanted patients in collaboration with Medical University Göttingen to identify possible new biomarkers of GvHD and outcome.

3) to characterize the functional role of the bacterial metabolite indoxyl sulfate with respect to immunoregulation in cultured dendritic cells in order to highlight the functional importance of bacterial metabolites.

3 Materials

3.1 Equipments

Autoclave	Technomara, Fernwald, Germany
Bioanalyzer 2100	Agilent Technologies, Böblingen, Germany
CASY Cell Counter	Innovatis/Roche, Basel, Switzerland
Centrifuge Sigma 2	Sartorius, Göttingen, Germany
Electrophoresis equipment	Biometra, Göttingen, Germany
ELISA plate reader	MWG Biotech, Ebersberg, Germany
EVOS Cell Imaging System	Life Technologies, Carlsbad, CA, USA
FACS Calibur flow cytometer	BD Biosciences, Franklin Lakes, NJ, USA
Forceps	Aesculap, Tuttlingen, Germany
Fluidigm	Fluidigm, South San Francisco, CA, USA
Heat sealer	Eppendorf, Hamburg, Germany
Hemocytometer	Marienfeld, Lauda-Königshofen, Germany
Incubators	Heraeus, Hanau, Germany
Laminar Flow Cabinet Clean Air	Telstar, Woerden, The Netherlands
Microscopes	Zeiss, Jena, Germany
Multipipettor Multipette plus	Eppendorf, Hamburg, Germany
NanoDrop 1000	Thermo Fisher Scientific, Schwerte, Germany
PCR Thermocycler PTC-200	MJ-Research/Biometra, Oldendorf, Germany
pH Meter	Knick, Berlin, Germany
Pipetboy	Integra Biosciences, Fernwald, Germany
Pipettes	Gilson, Milddleton, WI, USA
Pipettes	Eppendorf, Hamburg, Germany
Power supplies	Biometra, Göttingen, Germany

Realplex Mastercycler epGradient	Eppendorf, Hamburg, Germany
Rocking plattform HS250	IKA Labortechnik, Staufen, Germany
Sonifier 250	Branson, Danbury, CT, USA
TissueFAXS	TissueGnostics GmBH, Vienna, Austria
TissueLyser	Qiagen, Hilden, Germany
Vortexer	Scientific Industries Ink., Bohemia, NY, USA
Water purification system	Millipore, Eschborn, Germany
Waterbath	Julabo, Seelstadt, Germany
Western blot chamber	Biometra, Göttingen, Germany

3.2   Consumables

Cell culture flasks	Costar, Cambridge, MA, USA
Cell culture plates	BD, Franklin Lakes, NJ, USA
Cell scrapers	Sarstedt, Nümbrecht, Germany
Combitips for Eppendorf multipette	Eppendorf, Hamburg, Germany
Cryo tubes	Corning, Corning, NY, USA
Heat sealing film	Eppendorf, Hamburg, Germany
Hyperfilm^{TM} ECL	GE Healthcare, Chalfont St Giles, UK
Immobilon-P PVDF membrane	Millipore, Schwalbach, Germany
Micro test tubes (0.5 ml, 1.5 ml, 2 ml)	Eppendorf, Hamburg, Germany
Micropore filters	Sartorius, Göttingen, Germany
Microtiter plates (6, 12, 24, 96 wells)	Costar, Cambridge, MA, USA
Microtiter plates for ELISA	Costar, Cambridge, MA, USA
PCR plate Twin.tec 96 well	Eppendorf, Hamburg, Germany
Petri dish	Falcon, Heidelberg, Germany
Pipette tips	Eppendorf, Hamburg, Germany
Plastic pipettes	Costar, Cambridge, MA, USA
Polystyrene test tubes	Falcon, Heidelberg, Germany
Syringe Filters, sterile	Sartorius, Göttingen, Germany
Syringes and needles	Becton Dickinson, Heidelberg, Germany
Tubes (5 ml, 15 ml, 50 ml, 225 ml)	Falcon, Heidelberg, Germany

Whatman® Chromatography Paper   Sigma-Aldrich, St. Louis, MO, USA

3.3 Media, buffers and solutions

2-Mercaptoethanol	Gibco/Life Technologies, Carlsbad, CA, USA
Acrylamide	Carl Roth, Karlsruhe, Germany
APS	Merck Millipore, Billerica, MA, USA
Aqua	Braun
Bovine serum albumin	Sigma-Aldrich, St. Louis, MO, USA
CasyTON	Roche, Basel, Switzerland
DMSO	Sigma-Aldrich, St. Louis, MO, USA
FACS clean	BD Biosciences, Franklin Lakes, NJ, USA
FACS flow	BD Biosciences, Franklin Lakes, NJ, USA
FACS rinse	BD Biosciences, Franklin Lakes, NJ, USA
Fetal calf serum	Gibco/Life Technologies, Carlsbad, CA, USA
Hydrogen peroxide	Merck, Darmstadt, Germany
HCl	Carl Roth, Karlsruhe, Germany
Isopropanol	Braun
L-Alanyl-L-Glutamine	Merck Millipore, Billerica, MA, USA
Methanol	Thermo Fisher Scientific, Waltham, MA, USA
Mounting media for immunohistochemistry	Thermo Fisher Scientific, Waltham, MA, USA
Nuclease-free water	Gibco/Life Technologies, Carlsbad, CA, USA
PBS	Sigma-Aldrich, St. Louis, MO, USA

RPMI 1640	Gibco/Life Technologies, Carlsbad, CA, USA
TEMED	Sigma-Aldrich, St. Louis, MO, USA
Triton X100	Sigma-Aldrich, St. Louis, MO, USA
Tween 20	Sigma-Aldrich, St. Louis, MO, USA
Trypsin-EDTA	PAN Biotech, Aidenbach, Germany

3.4   Chemicals

All chemicals were purchased from Sigma-Aldrich (Taufkirchen, Germany) or Merck Millipore (Darmstadt, Germany) unless otherwise mentioned.

3.5   Enzymes, kits, and reagents for molecular biology

Agilent RNA 6000 Nano Kit	Agilent Technologies, Santa Clara, CA, USA
Amersham^{TM} ECL^{TM} Prime Western Blotting Detection Reagent	GE Healthcare, Chalfont St. Giles, UK
Aportinin	Roche, Mannheim, Germany
Bio-Rad protein assay	Bio-Rad, Munich, Germany
dNTPs	Roche diagnostics, Mannheim, Germany
Ethidium bromide	Sigma-Aldrich, St. Louis, MO, USA
Foxp3 transcription factor staining buffer set	eBioscience, San Diego, CA, USA
GM-CSF	Berlex, Seattle, USA
LPS	Enzo Life Sciences, Farmingdale, NY,

	USA
Human interleukin 4 (IL-4)	Promokine, Heidelberg, Germany
M-MLV Reverse Transcriptase	Promega, Madison, WI, USA
p-Coumaric acid	Sigma-Aldrich, St. Louis, MO, USA
Pepstatin	Roche, Mannheim, Germany
Proteinase K	Roche, Mannheim, Germany
QIAshredder™	Qiagen, Hilden, Germany
QuantiFast SYBR® green PCR Kit	Qiagen, Hilden, Germany
Random Decamers	Ambion/Life Technologies, Carlsbad, CA,USA
RNA*later*™	Qiagen, Hilden, Germany
RNase-free DNase Set	Qiagen, Hilden, Germany
RNeasy Mini Kit	Qiagen, Hilden, Germany
SDS	Sigma-Aldrich, St. Louis, MO, USA

3.6 Antibiotics

Penicillin and streptomycin for primary cell culture were purchased from Gibco Life Technologies, Carlsbad, California, United States of America.

3.7 Molecular weight standards

For Western Blot bands, Kaleidoscope Prestained Standard from BioRad (Munich, Germany) was used as molecular weight standard for proteins.

3.8 Oligonucleotides for qRT-PCR

Unmodified, HPLC-purified oligonucleotides were designed using UCSC genome browser and Perl primer software. Primer sequences were purchased from Eurofins MWG Operon (Ebersberg, Germany).

3.9 PCR Primers

3.9.1 Primers for RT-qPCR

Genes	Primer sequence
18S rRNA	Sense: ACC-GAT-TGG-ATG-GTT-TAG-TGA-G Antisense: CCT-ACG-GAA-ACC-TTG-TTA-CGA-C
BATF	Sense: GACAAGAGAGCCCAGAGGTG Antisense: TTCTGTGTCTGCCTCTGTCG
DEFA5	Sense: AGACAACCAGGACCTTGCTATCTC Antisense: GGTTCGGCAATAGCAGGTGG
DEFB4	Sense: AGTGAGAAGCGAATTTGAATTGGACAG Antisense: TGTATTCTTGGCTGCGACATTTCTTCC
EGR2	Sense: CACGTCCGGTGACCATCTTCCC Antisense: CCAGTCATGTCAATGTTGATCATGCC
FOXP3	Sense: GAAACAGCACATTCCCAGAGTTC Antisense: ATGGCCCAGCGGATGAG
GPR109A	Sense: GCGTTGGGACTGGAAGTTTG Antisense: GCGGTTCATAGCCAACATGA
IDO1	Sense: GGTCATGGAGATGTCCGTAAGGT Antisense: CCAGTTTCTTGGAGAGTTGGCAG
RORC	Sense: GCAGCGCTCCAACATCTTCTC Antisense: GCACACCGTTCCCACATCTC

3.9.2 Primers for Fluidigm microarray (digital qPCR)

Genes	Sequences
GAPDH	Sense: TTCGACAGTCAGCCGCATC Antisense: GCCCAATACGACCAAATCCGT
AHR	Sense: GGTTGTGATGCCAAAGGAAGAA Antisense: CGGATATGGGACTCGGCAC
BATF	Sense: GTGTGAGAGCCCGGAAGATT Antisense: ATCAGATGAGTCCTGTTTGCCA

CAMP	Sense: GGTCCTCGGATGCTAACCTCT Antisense: TTCACCAGCCCGTCCTTCTTG
CYP24A1	Sense: TGTGCATTGGTCGCCGATTA Antisense: CAAATACCACCATCTGAGGCG
CYP27A1	Sense: GTGCATTGGTCGCCGATTAG Antisense: CAAATACCACCATCTGAGGCG
CYP27B1	Sense: ACGCTCTCTTGGGCTCTGTA Antisense: CACAGGGTACAGTCTTAGCACTT
CYP2R1	Sense: CCAGGTGTACGGAGAGATCTT Antisense: TCAACCCATCCTCGGCCATA
DEFA5	Sense: AGACAACCAGGACCTTGCTATCTC Antisense: GGTTCGGCAATAGCAGGTGG
DEFB4A	Sense: AGTGAGAAGCGAATTTGAATTGGACAG Antisense: TGTATTCTTGGCTGCGACATTTCTTCC
EBI3	Sense: AGAGCACATCATCAAGCCCG Antisense: AGCTCCCTGACGCTTGTAAC
FOXP3	Sense: GAA-ACA-GCA-CAT-TCC-CAG-AGT-TC Antisense: ATG-GCC-CAG-CGG-ATG-AG
GATA3	Sense: CTCTTCGCTACCCAGGTGAC Antisense: GGTTGTAAAAAGGGGCGACG
GC	Sense: GGCTACCACTTTTACATGGTCA Antisense: TCATAATCCCGGCCTCTCTCT
GPR109A	Sense: GCCCAACCTCTCCTTAAATAACC Antisense: GGAAACCTTAGGCCGAGTCC
IDO1	Sense: AGCCCCTGACTTATGAGAACA Antisense: AGCTATTTCCAACAGCGCCT
IL10	Sense: TGCTGGAGGACTTTAAGGGT Antisense: CGCCTTGATGTCTGGGTCTT
IL12A	Sense: ACCTCTTTTATGATGGCCCTGTG Antisense: CAGCTCATCAATAACTGCCAGC
IL12B	Sense: TTCATCAGGGACATCATCAAACCT Antisense: AGTACTCCAGGTGTCAGGGT
IL17	Sense: CCTCATTGGTGTCACTGCTAC Antisense: GGGGGAAGTTCTTGTCCTCAG
Il22	Sense: TATCACCAACCGCACCTTCA Antisense: GCGCTCACTCATACTGACTCC
IL23	Sense: CCCAAGGACTCAGGGACAACAG Antisense: AGTAGGGAGGCATGAAGCTGG
IL33	Sense: ACAGACTCCTCCGAACACAG Antisense: CTTTGGCCTTCTGTTGGGATTTTC
PXR	Sense: AACTTACCACCAAGCAGTCCAA Antisense: GGACCTCCGACTTCCTCATC

REG3a	Sense: ATCCGCTGTCCCAAAGGCTC Antisense: AGCACAGACACCAGGTTTCCAG
RORC	Sense: GCAGCGCTCCAACATCTTCTC Antisense: GCACACCGTTCCCACATCTC
TBET	Sense: GGCGTCCAACAATGTGACCCA Antisense: TCTGGCTCTCCGTCGTTCAC
TNF	Sense: CTTTGGAGTGATCGGCCCC Antisense: GCTTGAGGGTTTGCTACAACA
VDR	Sense: GGCTACCACTTTTACATGGTCA Antisense: TCATAATCCCGGCCTCTCTCT

.

3.10 Antibodies

3.10.1 Antibodies for Immunohistochemistry and Immunofluorescence

Antibodies	Species	Dilution used in experiment	Stock concentration	Provider
Foxp3	Mouse monoclonal	1:50	0.5 mg/ml	eBioscience, CA, USA
IDO clone 1F8.2	Mouse monoclonal	1:250	100 μg	Millipore, Billerica, MA, USA
IL-17	Goat polyclonal	1:25	0.2 mg/ml	R&D
CD3 clone SP7	Rabbit monoclonal	1:50	N/A	Thermo Scientific
CD4 clone SP35	Rabbit monoclonal	direct	2.5 μg/ml	Ventana
CD8 clone Sp57	Rabbit monoclonal	1:2	2.5 μg/ml	Ventana
CD117	Rabbit polyclonal	1:400	11.7 g/L	Dako, Glostrup, Denmark
CD127	Rabbit polyclonal	1:150	0.82 mg/ml	Abcam, Cambridge, UK
CD127	Mouse monoclonal		0.5 mg/ml	Novus
Myeloperoxidase	Rabbit	1:500	3.3 g/L	Dako, Glostrup, Denmark

polyclonal				

Secondary antibodies

Fluorescein	Species	Dilution used in experiment	Stock	Provider
AF 488 (A11029)	Goat anti mouse	1:75	2 mg/ml	Invitrogen, Carlsbad, CA, USA
AF 488 (A21467)	Chicken anti goat	1:75	2 mg/ml	Invitrogen, Carlsbad, CA, USA
AF 546 (A10040)	Donkey anti rabbit	1:75	2 mg/ml	Invitrogen, Carlsbad, CA, USA
AF 594 (A21201)	Chicken anti mouse	1:150	2 mg/ml	Invitrogen, Carlsbad, CA, USA
AF 594 (A11012)	Goat anti rabbit	1:150	2 mg/ml	Invitrogen, Carlsbad, CA, USA
AF 594 (A21442)	Chicken anti rabbit	1:150	2 mg/ml	Invitrogen, Carlsbad, CA, USA
AF 647 (A21443)	Chicken anti rabbit	1:75	2 mg/ml	Invitrogen, Carlsbad, CA, USA

3.10.2 Antibodies for Flow cytometry

All the antibodies used for flow cytometry were raised in mouse against human unless mentioned.

Specificity	Isotype	Fluorochrome	Clone	Manufacturer
CD1a	Mouse IgG1	PE	SFCI19Thy1A8	Beckman Coulter, CA, USA
CD80	Mouse IgG1	APC	2D10	Biolegend, CA, USA
CD83	Mouse IgG1	PE-Cy7	HB15e	eBioscience, CA, USA
CD86	Mouse IgG1	FITC	2331(FUN-1)	BD, Franklin Lakes, NJ, USA
HLA-DR	Mouse IgG2a	FITC	B8.12.2	Beckman Coulter, CA, USA

CD4	Mouse IgG1	PE	RPA-T4	BD, Franklin Lakes, NJ, USA
CD8	Mouse IgG1	FITC	SK1	BD, Franklin Lakes, NJ, USA
CD25	Mouse IgG1	PE-Cy7	M-A251	BD, Franklin Lakes, NJ, USA
CD62L	Mouse IgG1	APC	DREG-56	BD, Franklin Lakes, NJ, USA
Foxp3	Rat IgG2a	APC	PCH101	eBioscience, CA, USA
Annexin		FITC		BD, Franklin Lakes, NJ, USA
7-AAD		APC		BD, Franklin Lakes, NJ, USA

3.10.3 Antibodies for Elisa

Capture, standard, and detection antibodies for Elisa were purchased from R&D, MN, USA

3.10.4 Antibodies for Western Blot

Antibodies	Species	Dilution	Molecular weight	Provider
iKBß	Rabbit	1:1000	45 kDa	Santa Cruz Biotechnology, Dallas, TX, USA
Phosphor AKT	Rabbit	1:1000	60 kDa	Cell Signaling Technology, Danvers, MA, USA
ß-Actin	Rabbit	1:2000	42 kDa	Sigma-Aldrich, St. Louis, MO, USA
Rabbit-HRP	Goat	1:2500		Dako, Glostrup, Denmark

3.11 Databases and Softwares

The following databases and software tools were used to design experiments and process data, respectively. If no version is stated, the detailed information can be found in the corresponding methods chapters.

AxioVision Rel 4.8	http://carl-zeiss-axiovision-rel.software.informer.com/4.8/
EndNote X7	Thomson Reuters, New York, NY, USA
FlowJo v9.5.3	FlowJo,LLC, Ashland, OR, USA
Fluidigm real time PCR analysis	https://www.fluidigm.com/software
GeneRunner version 3.05	http://www.generunner.com
GraphPad Prism 5.02	GraphPad Software, La Jolla, CA, USA
ImageLab v4.0	Bio-Rad, Munich, Germany
Microsoft Excel	Microsoft Deutschland GmbH
PerlPrimer version 1.1.14	http://perlprimer.sourceforge.net/
PubMed	http://www.ncbi.nlm.nih.gov/entrez
SPSS 21.0	http://www-01.ibm.com/software/de/analytics/spss/
USCS Genome Browser	http://www.genome.ucsc.edu

4 Methods

4.1 Patient samples collection

4.1.1 Ethics and consent

All the patients who underwent allogenic stem cell transplantation consented for the intestinal biopsies. Consent was taken prospectively by trained personnel. The project was approved by University Hospital Regensburg Ethics Committee **(approval number: 09/059, Analyze der intestinalen GvHD Immundysregulkation bei der GvHD).** All the investigation was conducted in accordance with the Helsinki Declaration.

4.1.2 Clinical and Histological Information

The overall clinical acute GvHD grade was diagnosed by clinicians according to NIH consensus. Histopathological grades were assessed by pathologist using standard criteria [120,121].

4.1.3 Patient characteristics

A total of 268 patients who were transplanted between July 2005 and November 2014 were enrolled in this study. Serial biopsies were obtained from patients after allogenic stem cell transplantation either as a regular routine follow-up or when the potential GvHD was suspected. Following table lists the patient characteristics.

Age at Tx (yr)	Mean= 50.3
	SE= 12.6
	Median= 53.5
	Range= 16-71

Gender	Male: n=172 patients
	Female: n= 96 patients
Donor type	Haploidentical: n= 5
	Siblings: n= 69
	Unrelated donor: n= 194
Match	Identical: n= 213
	Haplo: n= 5
	Single or multiple allele/antigen mismatch: n= 50
Conditioning	Standard: n= 37
	Reduced intensity: n= 231
Stem cell source	Double cord: n= 3
	Bone marrow: n= 16
	PBSC: n= 249
Mean CD34/kg	5.47 +/- 1.6 CD34/kg
Immunosuppressive prophylaxis	CyA/MMF: n=55
	Post transplant Cyclo/Tacro/MMF: n=3
	CsA/MTX: n=210
	Unrelated donors: All additional serotherapy with ATG d-3—1
Underlying disease stage	Early: n=63
	Intermediate: n=97
	Advanced: n=109
Diagnosis	AML: n= 144
	ALL: n= 29
	MDS: n= 22
	Myeloma: n=19
	Myeloproliferative neoplasia: n=19
	Lymphoma and Hodgkin´s disease: n=30
	Aplastic anemia n=5

GvHD after SCT	None: n= 88
	Grade 1-2: n= 116
	Grade 3-4: n= 64

4.2 Immunohistochemistry and Immunofluorescence

More than seven decades ago, Coons and co-workers demonstrated for the first time fluorescence technique to detect corresponding antigens in frozen tissue sections[122,123]. However, only since early 1990s has this method (widely accepted as immunohistochemistry) being applied in surgical pathology. Immunohistochemistry (IHC) is a method for localizing specific antigens in tissues or cells based on antigen-antibody recognition and is used to exploit the specificity provided by the binding of an antibody with its antigen at a light-microscopy level[124]. IHC allows the identification of cells with expression of specific surface markers in tissue. It also allows the assessment of the distribution and localization of specific cells in their surroundings and their relationship to other cells. Additionally, this method offers the possibility to observe the localization of specific molecules in the cells themselves.

4.2.1 Sample collection and storage

University Hospital Regensburg ethical review board approved the use of patient biopsies. All patients gave written informed consent in accordance with the Declaration of Helsinki. Gut biopsies were retrieved from ASCT patients by means of colonoscopy by trained physicians. Tissue biopsies were fixed in 4% formalin for 24 h and embedded in paraffin. Sections of approximately 2–3 µm thickness were cut from tissue blocks and stained with hematoxylin and eosin in accordance with the standard protocols. Histopathological analysis was performed without knowledge of the clinical data. Common histopathological features of GVHD, such as apoptosis of epithelium, loss of crypts and cellular infiltrates for neutrophils, eosinophils and lymphocytes in general, were assessed

separately for the epithelial area and the lamina propria. (Biopsies storage and handling took place in Institute of Pathology, University Hospital Regensburg)

4.2.2   Immunohistochemistry

Formalin fixed paraffin embedded (FFPE) biopsies were cut 2-3 µm thick, picked up on SuperFrost® Plus microscope slides. Slides were incubated at 80°C for 30 minutes (this allows proper attachment of tissue section to the slides) to melt the paraffin and transferred to Xylol to dissolve the paraffin followed by descending alcohol line as follows:

Step	Length
Xylol	5-10 min
Xylol	5-10 min
100 % Ethanol	3-5 min
100 % Ethanol	3-5 min
96 % Ethanol	3-5 min
96 % Ethanol	3-5 min
70 % Ethanol	3-5 min
Distill water	

Antigen retrieval was performed with citrate buffer (pH 7.2) for 32 minutes in microwave (300 Watts). Citrate buffer is widely known to break formalin cross links and unmask the antigens. Slides were fixed to the cover plates where biopsy section was sandwiched between the slide and the cover plate and were loaded into the cassette base. Sections were washed twice with 1x wash buffer (Dako, S300685-2), blocked with hydrogen peroxide (Dako, S2023) for 5 minutes to block endogenous peroxidase. Sections were then incubated with primary antibody prepared in antibody diluent (Dako, S2022) for 1 hour at room temperature (RT) with following antibodies: CD4, CD8, Foxp3, IL-17, IDO. Detail antibody information is provided in table 3.10.1. Secondary antibodies were used from Dako against the respective species. DAB substrate (Dako, K3468) was added for 10 minutes. Slides were gently taken out of cover plates. Cover plates were transferred to 0.3% sodium hypochlorite solution for cleaning. Slides were

the placed in hemalam for one minute and washed with warm tap water. Sections were placed in descending alcohol line as follows:

Step	Length
70 % Ethanol	3-5 min
96 % Ethanol	3-5 min
96 % Ethanol	3-5 min
100 % Ethanol	3-5 min
100 % Ethanol	3-5 min
Xylol	5-10 min
Xylol	5-10 min

Finally, biopsy sections were sealed with entellan (Merck, 1079610500) to finish the immunostaining bench work. Biopsies were manually analyzed at 400X magnification Zeiss Axioskop 40 microscope using semi quantitative scoring system. CD4, CD8 and IDO positive cell were analyzed in semi quantitative fashion. For Foxp3^{+} and IL-17^{+} cells, positive cells were counted in high power field (HPF). An HPF is defined as the 40X objective with the field diameter of 0.31mm^2. 4-10 HPF were analyzed depending on the size of biopsies. Semi quantitative scoring and HPF analysis was kindly performed by Senior Pathologist Dr. Elisabeth Huber.

4.2.2.1 Preparation of citrate buffer

Solution A: 2.1 g Citric acid monohydrate ($C_6H_8O_7$-H_2O, Merck,1002440500) in 100 ml Millipore H_2O (Storage at 4°C)

Solution B: 29.41 g trisodium citrate dehydrate ($C_6H_5Na_3O_7$-2H_2O, Merck, 1064480500) in 1 l Millipore H_2O (Storage at 4°C)

Preparation: 1 ml Solution A + 49 ml Solution B fill to 500 ml with Millipore H_2O. Set pH to 7.2. (Storage at RT)

4.2.2.2 Preparation of 1x wash buffer

Working solution: 1: 10 dilution from concentrated 10X solution.

100ml washing buffer 10x + 900ml Millipore H_2O

4.2.2.3   Preparation of DAB substrate

1 part DAB chromagen+49 parts DAB substrate diluent

980µl DAB-Substrate + 20µl DAB-Chromogen, 100 µl per samples

4.2.2.4   Preparation of 0,3% Sodium hypochlorite-Solution

3 litre Solution: 200ml 4%-4,5% sodium hypochlorite + 2800ml distilled water

Cleaning of cover plates: Cover plates were placed for 2 days in sodium hypochlorite, washed with distilled water and cleansed object slide surface with soap and sponge. Cover plates were then rinsed with distilled water and left to dry. Cleaning solution was stored in airtight box and changed every 6 months.

4.2.3   Double Immunofluorescence

FFPE biopsies were cut 4-5 µM thick. They were incubated at 80°C for 30 minutes followed by immersing in Xylol twice for 10 minutes each following descending alcohol line as explained in paragraph 4.2.2. Sections were washed twice with PBS and blocked with 20% Bovine Serum Albumin (BSA) for 20 min at RT. Sections were washed twice with PBS. Double immunofluorescence staining was performed for Foxp3/CD4, Foxp3/CD8, IL-17/CD3, IL-17/CD4 and IL-17/CD117. Primary antibodies diluted in 1% BSA were applied to sections for 45 min at RT. Detailed information on primary antibodies is provided in table 3.10.1. Sections were washed twice with PBS. Primary antibodies were covalently linked to Alexa Flour 488 (dilution 1:75) or Alexa Flour 594 (dilution 1:150) for 30 minutes at RT followed by two times washing with PBS. Detailed information on secondary antibodies is provided in table 3.10.1. Sections were counterstained with DAPI, washed twice with PBS and sealed with mounting media. Cells were manually counted at 400X magnification using Zeiss microscope.

4.3   Quantitative Real-Time PCR

Discovered by Kary Mullis in 1983 and awarded a Noble Prize in 1993 for his discovery, Polymerase Chain Reaction (PCR) is a method where a nucleic acid sequence can be exponentially amplified *in vitro.* PCR is one of the most powerful

technologies in molecular biology. With this technique, specific sequences within a DNA or cDNA template can be copied or 'amplified', many thousands to million-fold using sequences specific oligonucleotides, heat stable DNA polymerase, and thermal cycling. PCR amplifies DNA exponentially, doubling the number of target molecules with each amplification cycle.

4.3.1   Biopsies collection and storage

Intestinal biopsies were collected after giving informed consent to patients who underwent allogenic stem cell transplantation in University Hospital Regensburg. Biopsies were transferred to 500 µl RNA later (Quiagen) and immediately stored at 4°C and were further stored at -20 °C. RNA was extracted when required.

4.3.2   RNA extraction

Before RNA extraction, tissues were centrifuged at 4000 rpm for 5 minutes and were transferred to 700 µl RLT buffer supplemented with 1% ß-mercaptoethanol. Tissues were then sonicated for five seconds, 3-5 times, till the complete homogenization was ensured. Tissues were filtered through QIAshredder column by centrifugation at RT for 3 min at 13000xg before proceeding to RNA extraction. Total RNA was extracted from intestinal biopsies using the RNeasy Mini Kit (QIAGEN) according to manufacturer's recommendation. To remove potential DNA contaminations, on-column DNA digestion with the RNase-free DNase Set (Qiagen) was implemented according to the protocol. RNA concentration was measured with ND-1000 Nano Drop Spectrophotometer. RNA integrity and quality was controlled using Agilent Bioanalyzer as per manufacturer's instructions. RNA was stored at -80 °C for further use.

4.3.3   Reverse Transcription PCR (RT-qPCR)

Total RNA was reverse transcribed into complementary DNA (cDNA) using Moloney murine leukemia virus reverse transcriptase (M-MLV RT) enzyme. Random decamers were used to prime cDNA synthesis. The volume of 1 µg of total RNA was adjusted to 13 µl with nuclease-free ddH2O and mixed with 1 µl

Random Decamers (Promega) and 1 µl dNTPs (10 mM) on ice. Secondary structures of RNA were dissolved by 5 min incubation in Thermocycler at 65 °C followed by immediate incubation ice for 1 min. After mixing with 4 µl M-MLV Buffer (5x;Promega), samples were incubated at 42 °C for 2 min. Reverse transcription started upon addition of 1 µl RT enzyme (50 min, 42 °C) and was stopped by heat inactivation of the enzyme (15 min, 70 °C). cDNA samples are stable at -20 °C.

4.3.4   Quantitative Real-Time PCR (qPCR)

Reverse transcribed cDNA products were analyzed on a Mastercycler Ep Realplex using the QuantiFast SYBR Green PCR Kit. Primer sequences were purchased from Eurofins MWG Operon, Ebersberg, Germany except when other companies are mentioned. *18S* was used as reference gene for all the gene of interest. PCR reaction was carried out in 96 well plate format adapted to the Eppendorf Realplex Mastercycler EpGradient S system. The amount of amplified DNA relative to reference gene*18S* rRNA was measured through the emission of light by SYBR green dye after each extension step. Melting curve was monitored to determine the specificity of amplification product.

The reaction component and cycling protocol for RT-qPCR are listed below:

Table 4.1: RT-qPCR reaction composition

Components	Concentration	Volume
SYBR Green mix (2x)		5 µl
Nuclease-free ddH2O		3 µl
Template DNA	1000 ng	1 µl
Primer_sense	10 µM	0.5 µl
Primer_antisense	10 µM	0.5 µl
Final Volume		10 µl

Table 4.2: Cycling protocol for RT-qPCR

Cycle step	Temperature	Time consumed	Number of cycles
Initial denaturation	95°C	5 min	1x
Denaturation	95°C	8 sec	45x
Annealing and Extension	58°C	20 sec	
Final denaturation	95°C	15 sec	1x
Final extension	60°C	15 sec	
Melting Curve	60-95°C	10 min	1x
Cooling	4°C	Hold	

4.4 Fluidigm Array

(These experiments were performed in Medical University of Göttingen and German Primate Centre, Göttingen, in October 2015 under Celleurope Secondment Scheme)

Fluidigm array is a digital PCR that assists in quantification of expressed genes, like a RT-qPCR. It can run up to 9,216 reactions simultaneously where one can test 96 cDNA samples against 96 assays. The flexibility of fluidigm allows to design own reaction depending on one's needs, letting run the samples in duplicates for higher accuracy.

The individual reactions are carried out in a microarray chip, and are depicted on a computer as single squares forming a heat map; the color gradient is representative of the copy number of the DNA. The results are easy to interpret, visualize and to perform analysis on.

This technique reduces pipetting errors, since the experiment is carried out in just few hours, consisting of a number of qPCR plates, and a lot more pipetting. In addition, a very small amount of cDNA is required for each reaction, which is very beneficial in instances where there are small amount of samples available, i.e. in the cases of human GvHD tissues. Figure 4.1 demonstrates a typical Integrated Fluid Circuit (IFC) Fluidigm plate with 96*96 dynamic array showing samples inlets and assay inlets.
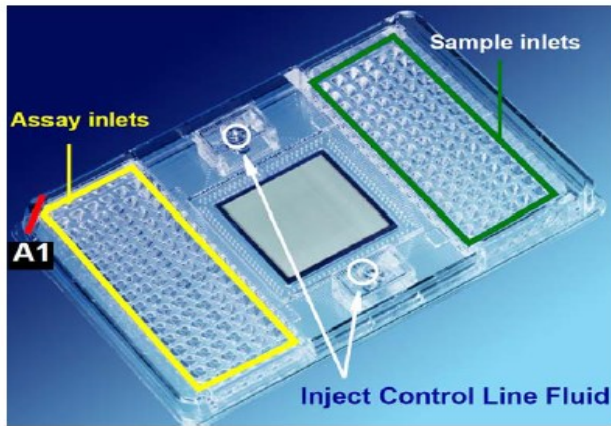
Figure 4.1: 96*96 Dynamic Array IFC sample and assay inlets

4.4.1 RNA isolation and cDNA synthesis

RNA isolation and cDNA synthesis was performed in University Hospital Regensburg as described in section 4.3.2-4.3.3. Instead of 1000 ng RNA, only 200 ng of RNA was synthesized to cDNA. The samples were parceled to Medical University of Göttingen in dry ice. Samples were received by corresponding collaborators within 24 hours and were safely stored untill further experiments were executed.

4.4.2 Pre-amplification

All the primers were obtained from Eurofins in a lyophilized state. Forward and reverse primers were reconstituted with nuclease free water to the concentration of 100µM. Equal volume of primers (5 µl each) was mixed to form a primer pair. Primer pairs were diluted to 500 nM (1:200 dilutions) using 1X DNA suspension buffer as shown in Table 4.3. So formed mixture is termed as Specific Target Amplification (STA) Primer Mix. This 10X STA Primer Mix was stored at 4 $^\circ$C for short term use and at -20 $^\circ$C for long term use. Experiment was performed for 48 primer pairs in 96 samples at a time. For pre-amplification, STA reaction solution was prepared with TaqMan PreAmp Master Mix, 500 nM of pooled STA Primer Mix, DNA suspension buffer and cDNA as listed in Table 4.4.

Table 4.3: Preparation of 500 nM (10X) pooled STA Primer Mix

Component	48 Primer Pairs
1 µl each primer pair (100 µM each)	48 µl
1X DNA Suspension Buffer	152 µl
Total	200 µl

Table 4.4: STA Reaction solution

Component	Volume/reaction (µl)	96 samples with overage (µl)
TaqMan PreAmp Master Mix (Applied Biosystem PN 4391128)	2.5	260
500 nM pooled STA Primer Mix	0.5	52
DNA suspension Buffer	0.75	78
cDNA	1.25	
Total	5.0	390

In a 96 well plate, 3.75 µl of STA pre mix (pre amp master mix, STA primer mix and DNA suspension buffer) was pipetted as shown in table 2.5.2. To each well 1.25µl of individual cDNA was added. At this point, the final concentration of STA mix was 50 nM. Plate was sealed using plate sealer and transferred to thermocycler for pre-amplification. 14 cycles were preamplified with the following thermal protocol: 95 ^{o}C for 10 min (reaction activation phase), 95 ^{o}C for 15 sec, 60 ^{o}C for 4 min (amplification phase, 14 cycles), and 4 ^{o}C forever.

In order to remove unincorporated primers in the preamplified samples, cleanup procedure was performed with Exonuclease I (E. coli derived enzyme). Exonuclease I was diluted to 4 Units/µl as shown in Table 4.5.

Table 4.5: Exonuclease I Reaction solution

Component	Per 5 µl samples (µl)	96 Samples with Overage (µl)
Water	1.4	166
Exonuclease I Reaction Buffer	0.2	24
Exonuclease I at 20 Units/µl	0.4	48
Total Volume	2.0	240

2 µl of Exo I at 4 Units/µl was added to each 5 µl STA reaction, vortexed, centrifuged and placed in a thermal cycler with the following programmer: 37 ^{o}C for 30 minutes (Digestion phase), 80 ^{o}C for 15 minutes (Inactivation phase) and 4 ^{o}C for reaction termination. The final products were diluted 5-fold by adding 18 µl DNA suspension buffer, making a total cDNA volume of 25 µl. The cDNA was stored at -20 °C till further use.

4.4.3   Digital qPCR with Fluidigm

Table 4.6: Preparing Sample Pre-Mix and Samples for Gene Expression using Fluidigm Dynamic Arrays

Component	Volume per inlet (µl)	Volume per inlet with overage (µl)
2X SsoFast EvaGreen Supermix with Low ROX	2.5 µl	3 µl
20X DNA Binding Dye Sample Loading Reagent	0.25 µl	0.3 µl
PreAmp and Exo I- treated sample	2.25 µl	2.7 µl
Total Volume	5 µl	

3.3 µl of the Pre-Mix for each sample was aliquoted and mixed with 2.7 µl of the PreAmp and Exo I- treated cDNA on a 96 well plate. The plate was centrifuged and kept ready to be loaded onto the chip.

Table 4.7: Preparing the Assay Mix

Component	Volume per inlet (µl)	Volume per inlet with overage (µl)
2X Assay Loading Reagent	2.5 µl	3 µl
1X DNA Suspension Buffer	2.05 µl	2.46 µl
100 µM each primer pair	0.45 µl	0.54 µl
Total Volume	5 µl	

5.46 µl of the Assay Mix was aliquoted and mixed with 0.54 µl of each 100 µM primer pair mix, to make a total volume of 5 µl. The plate was centrifuged and kept ready to be loaded onto the chip.

Priming and Loading the Dynamic Array IFC

To prime the Dynamic Array chip prior to use, a control line fluid was injected into each accumulator on opposite sides of the chip. The blue protective film was removed from the bottom of the chip, and the chip was placed in an IFC Controller (MX for the 48.48 Dynamic Array or the HX for the 96.96 Dynamic Array) to be primed for the experiment. Following priming, 5 µl of each assay was loaded onto the left side of the chip, and 5 µl of each sample was loaded into the respective inlets on the right side of the chip. The Array was then returned to the respective IFC Controller to Mix the samples and assays onto the chip. The chip

was then run using the BioMark Gene Expression Data Collection software, following the given parameters for the 96.96 dynamic arrays.

Table 4.8: Priming and Loading the Dynamic Array IFC

Condition	Temperature (°C)	Time (s)	Biomark HD Ramp Rate (°C)	Biomark Ramp Rate (°C/s)
Thermal Mix	70	2400	5.5	2
	60	30	5.5	2
Hot Start	95	60	5.5	2
PCR*	96	5	5.5	2
	60	20	5.5	2
Melting Curve	60	3	1	1
	60-95		1°C/3s	1°C/3s

*40 cycles

Genes that were analyzed by Fluidigm is given in material section

4.5 Cell Culture

4.5.1 Isolation of Monocytes

Peripheral blood mononuclear cells (PB-MNCs) were separated by leukapheresis of healthy donors [125], followed by density gradient centrifugation over Ficoll/Hypaque [126]. Monocytes were then isolated from MNCs by counter current centrifugal elutriation [127]. Elutriation was performed in a J6M-E centrifuge equipped with a JE 5.0 elutriation rotor and a 50 ml flow chamber (Beckman, Munich, Germany). After sterilizing the system with 6% H_2O_2 for 20 min, the system was washed with PBS. Following calibration at 2500 rpm and 4°C with Hanks BSS, MNCs were loaded at a flow rate of 52 ml/min. Fractions were collected and the flow through rate was sequentially increased according to Table 4.9. Monocytes are the largest cells within MNCs and are thus mainly obtained in the last fraction. Monocyte yield were donor dependent, typically between 10-20% of total MNCs. Usually the purity of monocytes were 85-95%. Yield and purity varied slightly, depending on the donor.

Table 4.9: Elutriation parameter and cell types

Fraction	Volume (ml)	Flow rate (ml/min)	Main cells isolated
Ia	1000	52	Platelets
Ib	1000	57	
IIa	1000	64	B- and T- lymphocytes. NK cells
IIb	500	74	
IIc	400	82	

IId	400	92	
III	800	130	Monocytes

4.5.2   Freezing and thawing of cells

Freezing media consisted of 80% dimethyl-sulfoxide (DMSO) and 20% fetal calf serum (FCS). Cells were harvested and suspended in ice-cold RPMI 1640 and 1 ml of cell suspension was added to 1 ml ice-cold freezing media in cryo-vials, properly closed and inverted twice to mix. To allow gradual freezing at a rate of -1°C/min, the vials were placed in Styrofoam containers or isopropanol-filled cryo-containers (Nalgene) and frozen at –80°C for 24 h. For long-term storage, the samples were then transferred to liquid nitrogen (-196°C).To recover frozen cells, the cell suspension was thawed in a room temperature at 25°C. To dilute the toxic DMSO, the suspension was transferred to 10-25 ml serum-containing media as soon as thawed and the cells were spun down (7 min, 300xg, 4°C) and resuspended in fresh media

4.5.3   Dendritic cell culture

Immature monocyte-derived dendritic cells (DCs) were generated by culturing 0.67×10^6/ml elutriated monocytes in RPMI media supplemented with Glutamine, Penicillin/Streptomycin and 10% FCS. For monocytes to differentiate into immature DCs, 20 U/ml recombinant human IL-4 and 280 IU/ml GM-CSF was added as described earlier [128]. Cells were incubated for 5 days at 37 °C with 5% carbon dioxide and 95% relative humidity. On day 5, immature DCs were treated with 100 ng/ml Lipopolysaccharide (LPS) without or with varying concentration of Indoxyl 3-Sulfate (I3S) (Sigma Aldrich). Cells were further incubated for 48 hours. I3S was added directly to monocytes as well on day 0 when mentioned. On day 7, mature DCs were analyzed for cell viability and surface markers expression with flow cytometer and the cytokines in the supernatant was analyzed by ELISA.

4.5.4   Mixed Leukocyte Reaction

When leukocytes from two unrelated individuals are cultured together, they begin to proliferate and the phenomenon is termed as mixed leukocyte reaction (MLR). First described in 1964, Mixed Leukocyte Reaction (MLR) could be useful as an indicator of compatibility between siblings prior to organ transplantation to assess the risk of rejection of the transplant[129]. Indeed, later on it could be shown that the observed proliferation of the T lymphocytes is a response to the "allogenicity" of the two leukocyte populations and that an MLR is absent if the mixed leukocyte culture (MLC) is carried out between syngeneic populations which express the same MHC alleles. In a syngeneic MLC, the proliferative response depends on the presence of both non-self-antigens and antigen presenting cells like dendritic cells in the leukocyte populations. In an allogeneic setting, the MHC incompatibility alone is sufficient to trigger T cell proliferation, the magnitude of the reaction being solely dependent on the costimulatory capacity of the antigen presenting cells.

For MLR, ten thousand monocyte derived LPS stimulated mature DCs (with and without Indoxyl-3 sulfate) were co-cultured with hundred thousand lymphocytes (fraction IIa isolated by elutriation). Cells were cultured in 96 well plates with the final volume of 200 µl (100µl DCs+100 µl lymphocytes) in each well. The RPMI 1640 media was supplemented with 5% filtered AB serum. Figure 4.2 depicts the diagrammatic experimental settings for MLR. DC donor and lymphocyte donor were chosen different to ensure allogenic reaction. Cells were incubated at 37 $^\circ$C with 5% carbon dioxide and 95% relative humidity. On day 5, supernatant was collected from each condition from last 4 wells. On day 6, cells were counted and FACS was performed.

Plate Layout for Mixed Lymphocyte Reaction. Shaded area represents each well.

		1	2	3	4	5	6	7	8	9	10	11	12
Lymphocytes alone	A												
Lym+(DCs+LPS)	B												
Lym+(DC+LPS+1µM IS)	C												

Lym+(DC+LPS+10µM IS)   D

Lym+(DC+LPS+100µM IS)   E

F

G

H

Figure 4.2: Plate Layout for Mixed Lymphocyte Reaction

4.6   Fluorescence Activated Cell Sorting

Multicellular organisms have identical DNA but varying amount of protein. Fluorescence activated cell sorting (FACS) is a flow cytometry based method that detect both intra- and extracellular protein of interest in/on the cells and sort them accordingly. Different proteins on a same cell can be marked with antibodies conjugated to different fluorochromes.

The process begins with a population of single cells suspended in a medium, injected into a stable stream that forces cells to travel one by one in a laminar flow fashion. Cells pass through the beam of laser light. Scattered light and fluorescence emission provide information about the particle's properties. Light scattered in forward direction provides information about size of cells and side scatter measures granularity of cells.

Based on the excitation and emission wavelength of fluorochrome conjugated to cells, varying protein expression by cells can be measured. Also, using this fluorochrome labelled antibodies; different population of cells can be sorted and collected.

To access the protein expression, 0.5 million of monocyte derived LPS-stimulated DCs   (see section 4.6.3) were collected on day 7 of the culture. Cells were washed twice with 1 ml FACS buffer. Cells were then stained with surface markers: CD1a, CD80, CD83, CD86 and HLA-DR along with the respective isotype control. Cells were incubated at 4 $^{\circ}$C for 30 minutes. Cells were washed thrice with FACS buffer and resuspended in 300 µl FACS buffer. Flow cytometric measurement was performed on a BD FACS Calibur.

For lymphocytes, cells were incubated with CD4, CD8, CD25 and CD62L with their respective isotypes. For Foxp3, intracellular nuclear staining was performed according to the manufacturer's instructions. Cells were incubated with fixation/permeabilization solution for 45 min at 4 ^{o}C. Cells were then washed thrice with permeabilization buffer. Foxp3 staining was performed for 30 min at 4 ^{o}C. Cells were washed twice with permeabilization buffer and once with normal FACS buffer. Cells were resuspended in 300 µl FACS buffer and subjected to flow cytometry analysis.

Composition of
 FACS buffer: 5 ml of 60mg/ml Immunoglobulin + 5 ml of 10% sodium azide + 500 ml PBS
Fixation/Permeabilization solution: 1 part of Fix/Perm concentrate+4 part of Fix/Perm diluent
Permeabilization buffer: 1 part of 10X buffer + 9 parts of distill water

4.7   Enzyme Linked Immunosorbent Assay (ELISA)

Supernatant from cell cultures were collected (day 7 for dendritic cells and day 5 for lymphocytes) and were stored at -20 ^{o}C. Indirect or sandwich ELISA was performed to detect the cytokines released into cell culture medium. ELISA was performed according to manufacturer's recommendation. The optical density of each well was immediately determined with a microplate reader set to 450 nm wavelength.

4.8   Protein Analysis

4.8.1   Protein Isolation

For protein isolation, monocytes were isolated as described in section 4.5.1 and were cultured to immature DCs as described in section 4.5.3. Immature DCs were transferred to 6-well plates, stimulated with/without LPS and with/without Indoxyl

3-sulfate for 5 min, 30 min and 60 min. After respective stimulation, plates were transferred to ice, cells were transferred to 15 ml falcon tube (on ice), centrifuged at 1300 rpm for 7 minutes at 4 ^{o}C. Possible remaining cells in the 6-well plates were obtained by washing the wells with cold PBS for 3 times. 500 µl of freshly prepared pre-equilibration buffer (Buffer B) which contain Cytoplasmic Extraction Buffer (CEB) (also called Buffer A in this setting) was added to falcon tube containing stimulated DCs whereas 500 µl of buffer was added to 6-well plates to obtain any remaining cells in the plate. Cells were incubated in buffer for 4 min on ice and collected. Lysates was centrifuged and the supernatant was carefully discarded. Subsequently, 60 µl of freshly prepared lysis buffer (Buffer C) was added to the cell pellets and incubated for 10 min on ice. 60 µl of SDS buffer was added to the cell lysate and transferred to 95 ^{o}C heater for 10 min to denature the secondary protein structure. The obtained protein lysates were aliquoted in three Eppendorf tubes, 40 µl each, and stored at -80 ^{o}C for long term storage.

Required Buffers and solutions

Buffer A

Table 4.10: Protein isolation Buffer A

Reagents	Final concentration	Final volume
Tris/HCl (pH 7,9	10mM	1 ml
KCl	60mM	447 mg
EDTA	1 mM	37 mg
Distill Water		100 ml

Buffer B

Table 4.11: Protein isolation Buffer B

Reagents	Stock concentration	Final concentration	Final volume
EDTA	500 mM	1.5 mM	3 µl
Dithiothreitol	100 mM	1 mM	10 µl
EGTA	200 mM	1 mM	5 µl
ß- Glycerophosphate	1 M	50 mM	50 µl
Sodium fluoride	1 M	50 Mm	50 µl
Sodium pyrophosphate	250 mM	25 Mm	100 µl
Sodium orthovanadate	200 mM	1 mM	5 µl
Leupeptin	1 mg/ml	2 µg/ml	2 µl
Pepstatin A	1 mg/ml	2 µg/ml	2 µl
Aprotinine	2 mg/ml	2 µg/ml	1 µl
Buffer A			772 µl
Final volume			1000 µl

Buffer C

Table 4.12: Protein isolation Buffer C

Reagents	Stock concentration	Final concentration	Final volume
Nonidet P40	10%	0.4%	40 µl
Chymostatin	20 mg/ml	100 µg/ml	5 µl
Bestatin	5 mg/ml	10 µg/ml	2 µl
E64	3 mg/ml	3 µg/ml	1 µl
1,10-Phenanthrolin	0.1mg/ml	1 mM	1 µl
Buffer B			951 µl
Total end volume			1000 µl

Table 4.13: Preparation of SDS sample buffer (2X)

Reagents	Final concentration	Final volume
Glycerine	20 %	10 ml
Tris buffer (pH 6.8)	125 mM	5 ml
Ssdium dodecyl sulfate	4 %	2 g
2-Mercaptoethanol	10 %	5 ml
Bromophenol Blue	0.02 %	10 mg

4.8.2 SDS-Polyacrylamide-Gel Electrophoresis

Protein samples obtained from section 4.8.1 were separated using discontinuous gel system which is composed of stacking gel and separating gel mainly consisting acrylamide (AA). Separating gel of 10% and stacking gel of 5% were prepared freshly as mentioned in Table 4.14. In order to achieve complete polymerization, ammonimum persulfate (APS) was added that acts as a free radical initiators and N, N, N', N'-tetramethylenedianime (TEMED) was added to catalyze the gel polymerization as mentioned in Table 4.15.

Table 4.14: SDS-PAGE stock solutions

Gel stock solution	Seperating gel	Stacking gel
Final AA concentration	10%	5%
Stacking gel buffer	-	25 ml
Separating gel buffer	25 ml	-
SDS (10%)	1 ml	1 ml
Acrylamide (AA) (30%)	33 ml	16,7 ml
Millipore water	Adjust to 100 ml	

Table 4.15: SDS-PAGE gel mix solutions

	Separating gel	Stacking gel
Separating gel stock solution	6 ml	-
Stacking gel stock solution	-	2.5 ml
TEMED	6 µl	2.5 µl
APS (10%)	30 µl	20 µl

Two clean glass plates were held together congruent to each other by means of rubber seal in between glass plates to ensure leakage free space between the glasses. 6 ml of separating gel was casted in the glass plates, with isopropanol on top for quick polymerization. Once the separating gel polymerized, isopropanol was poured off and rinsed with distill water and let the glass dry. Stacking gel was poured over separating gel and the 10 well combs were gently inserted in the stacking gel avoiding air bubbles formation. Once the gel was polymerized, gel was mounted in the electrophoresis tank that was filled with 1X Laemmli buffer. The rubber seal was gently removed from between the plates; comb was gently taken out without damaging the gel. 10-20 µl of protein from section 4.8.1 was loaded into the separate wells, along with 5 µl of "Kaleidoscope precision plus protein standard" in a separate well. The gel was run with 80 volts for the first 20 minutes till the sample start running into the stacking gel. Voltage was increased to 100 volts for 30 min until the proteins reached the surface of separating gel. Next, the voltage was increase to 120 volts for almost 100-140 minutes and the separation of bands was continuously monitored until the desired proteins were resolved through the separating gel according to their size [130,131].

Table 4.16: Required buffers and solutions for SDS gel preparation

Solutions	Final concentration	Weight	Constituents
Separating gel buffer	1.5 M	90.83 g	Tris/HCl pH 8.8
	Add Millipore water to 500 ml		
Stacking gel buffer	0.5 M	30 g	Tris/HCl pH 6.8
	Add Millipore water to 500 ml		
Sodium dodecyl sulfate	10%	10 g	SDS
	Add Millipore water to 100 ml		
Ammonium persulfate	10%	1 g	APS
	Add Millipore water to 10 ml and store aliquots at -20°C		
Laemmli buffer (5X)	40 mM	15 g	Tris
	0.95 M	21 g	Glycine
	0.5%	15 g	SDS
	Add Millipore water to 3 liters, store at RT		

4.8.3   Western Blot analysis and Immunostaining

Proteins separated by SDS-PAGE were electrophoretically blotted onto the PVDF (Polyvinyl difluoride) membrane using a three-buffer semi-dry system and then visualized using specific antibodies immunostaining and the ECL detection kit.

To transfer the proteins from the gel to the membrane, PVDF membrane was cut into the size of gel. Membrane was first soaked in 70% isopropanol and transferred to anode buffer B. Meanwhile, three pieces of whatman filter paper, cut in the size of membrane, were soaked in anode buffer A, and placed on the electrophoresis chamber. Three more whatman papers were soaked in anode buffer B, placed on top of first three papers. Air bubbles were gently removed from the papers. With the help of forceps, membrane was placed over the filter paper. SDS gel was carefully removed from glass plate, immersed in buffer B for 10 s and placed on top of the membrane. Another 3 sheets of whatman soaked in buffer C were laid on top of the gel, followed by the cathode. Protein transfer took place 11 volts for 1 hour at RT.

Table 4.17: Required buffers and materials for transferring protein for immunodetection

Buffer A (Anode)	36.3 g (300 mM)	Tris (pH 10.4)
	200 ml (20%)	Methanol
	Add Millipore water to 1000 ml	
Buffer B (Anode)	3.03 g (25mM)	Tris (pH 10.4)
	200 ml (20%)	Methanol
	Add Millipore to 1 liter	
Buffer C (Cathode)	5.2 g (4mM)	ε-amino-n-caproic acid pH 7.6
	200 ml (20%)	Methanol
	Add Millipore water to 1 liter	
Polyvinyl difluoride membrane	Cut to a size of SDS gel	

PVDF membrane onto which proteins were blotted was washed 3 times, 10 min each in wash buffer (1X TBS + 0.1% Tween 20) and blocked with 5% milk (5 g milk dissolved in wash buffer and filtered) for 1 hour at RT.   Membrane was washed once again 3 times, 10 min each with wash buffer, incubated with primary antibody (diluted in 5% milk) overnight at 4 ^{o}C. Next day, membrane was washed three times, incubated with horseradish peroxidase (HRP)-conjugated secondary antibody (diluted with 5% milk) for 1 hr. at RT. For detection of the protein bands,

membrane was washed 3x10 min followed by swirling in 5 ml ECL reagent (+ 1.5 µl of 30% hydrogen peroxide) for 2 minutes. Blots were exposed to high performance chemiluminiscence film for 5-300 seconds depending on the signal intensity.

All the protein of interest were always normalized to the reference gene, beta-actin. For this, previous antibody was stripped off. For this, membrane was washed 3x10 min followed by stripping off the old signal with Reblot solution (1:10 diuluted) for 15 min at RT. Membrane was washed 3x10 min and preceded with blocking, washing, primary and secondary antibody procedure. Stripping was performed every time when more than one antibody was to be bound on the same membrane and these antibodies are isolated from the same species.

Images were processed, analyzed and graphed using Image Lab software.

4.9   Statistical Analysis

SPSS was used for patient data analysis. Data was analyzed for normal distribution. Normally distributed data were analyzed by student t test for two groups and one way anova for more than two groups. Non normally distributed data were analyzed by Mann Whitney test for two groups and Kruskal Wallis test for more than two groups. Correlations were depicted with Pearson correlation test for normally distribued data and Spearman correlation for non normal data. Experiments involving healthy volunteers were analyzed with graphpad prism. Non parametric one way anova was performed to calculate statistical significance.

For the entire experiments, graph represents mean and standard error of mean (s.e.m). Null hypothesis (no difference between two or more groups) was assumed for all the graphs. p values less than 0.05 between two or more groups was considered to reject null hypothesis thus being statistically significant.

Data transformation or normalization was not performed throughout the experiment thus all the results are the representation of raw data.

5 Results

5.1 Analysis of immune cell infiltrates during acute gastro-intestinal (GI) graft-versus-host disease (GvHD).

5.1.1 Analysis of CD4^{+} cell infiltrates and CD8^{+} cell infiltrates during acute GI-GvHD

GvHD is described by the activation of donor T cells in the recipient's hematopoietic system [1]. CD4^{+} T cells and CD8^{+} T cells play an essential role in GvHD as they represents the T lymphocytes of immune system. CD4^{+} T cells and CD8^{+} T cells were analyzed in the gut biopsies of patients after ASCT. Formalin fixed paraffin embedded (FFPE) gut biopsies were stained with a monoclonal anti-CD4 antibody (undiluted) and a monoclonal anti-CD8 antibody (1:2 dilution). Positive cells were analyzed in Zeiss Axioscope 40 microscope. Since T cells represents the majority of immune cell infiltrates, counting CD4^{+} and CD8^{+} T cells manually was not feasible. Therefore the biopsies were scored in a semi quantitative fashion [132] (this was done in close collaboration with Dr. Elisabeth Huber , Institute of Pathology, University Hospital Regensburg). Scored values were collected and analyzed using SPSS. Patients were divided into three groups: i) with no GvHD, ii) mild GvHD as grade 1, and iii) moderate to severe GvHD as grade 2-4. Upon analysis, the number of infiltrating CD4^{+} T cells showed increasing trend in gut biopsies of the patients who were diagnosed with grade 1 GvHD. Patients who were diagnosed with grade 2-4 GvHD did not show any difference in CD4^{+} T cell infiltrates when compared to non GvHD controls, they rather had less CD4^{+} T cells infiltration when compared to grade 1 GvHD as shown in Figure 5.1(A). On the contrary CD8^{+} T cells were significantly increased along with the exacerbation of GvHD as shown in Figure 5.1(B) suggesting that CD8^{+} T cell mediated inflammation occurs during the course of GvHD.
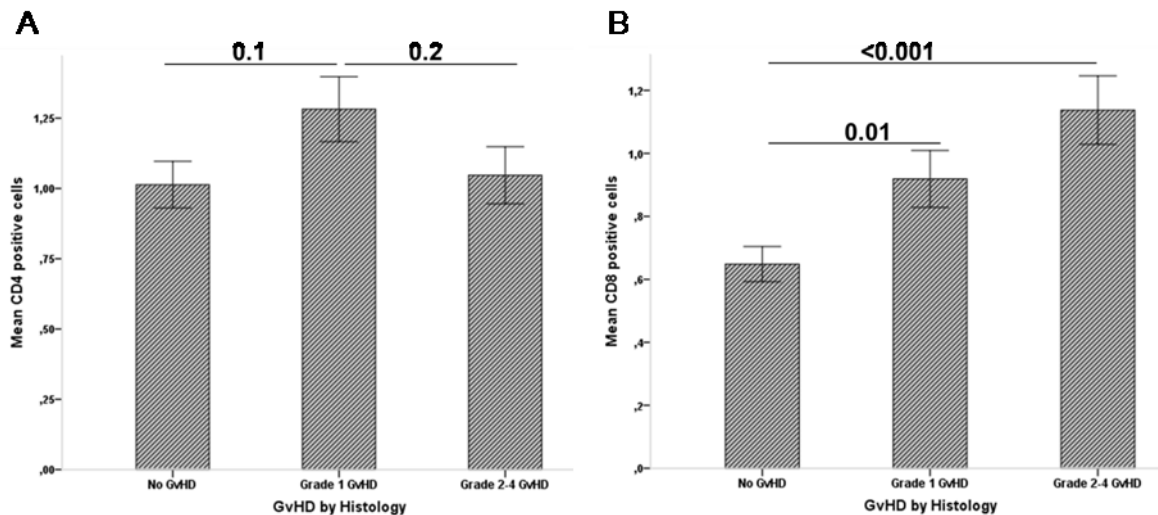
Figure 5.1: Infiltration of CD4$^+$ T cells and CD8$^+$ T cells in gut during acute GI-GvHD
A. Infiltration of CD4$^+$ T cells shows increasing trend during grade 1 GvHD which declines during grade 2-4 GvHD to the level of non GvHD patients. N=199 (No GvHD=81; Grade 1=64; Grade 2-4=54). B. CD8$^+$ T cell infiltrates significantly increases in grade 1 GvHD and even stronger in grade 2-4 GvHD when compared to non GvHD controls. N=197 (No GvHD=81; Grade 1=61; Grade 2-4=55). The distribution of CD4$^+$ and CD8$^+$ T cells were non-normal therefore non-parametric Kruskal-Wallis test was performed to calculate p values. Bar represents mean ± s.e.m.

Next, the numbers of infiltrating CD4$^+$ T cells were correlated with infiltration of CD8$^+$ T cells, absence of crypts and apoptosis of epithelial cells in gut biopsies. CD8$^+$ T cells were also correlated with crypt loss and epithelial apoptosis.

As shown in Table 5.1, CD4$^+$ T cell infiltrates highly correlated with the numbers of infiltrating CD8$^+$ T cells confirming the fact that CD4$^+$ T cells are necessary for the maintenance of CD8$^+$ T cells[133,134]. CD4$^+$ T cells did not correlate with crypt loss but were associated with apoptosis of epithelial cells in the gut which could be attributed to different CD4 subsets like Th1, Th2 and Th17 cell type leading to CD8$^+$ T cell activation. CD8$^+$ T cells highly correlated with CD4$^+$ T cell infiltrates loss of crypts and epithelial apoptosis, thus supporting the fact that increased infiltrations of cytotoxic T cells destroy crypts and epithelia and hence exacerbates GvHD (Figure 5.1 B). Furthermore, Kaplan-meier estimates revealed that patients with greater degree of epithelial apoptosis has significantly higher frequency of TRM when compared to the patients with lesser epithelial apoptosis confirming that apoptosis is the diagnostic hallmark of GvHD.

Table 5.1: Correlation table of CD4$^+$ and CD8$^+$ infiltrates with crypt loss and epithelial apoptosis in the gut of ASCT patients
Nonparametric Spearman's correlation was used to determine the correlation coefficient and significance between each group.

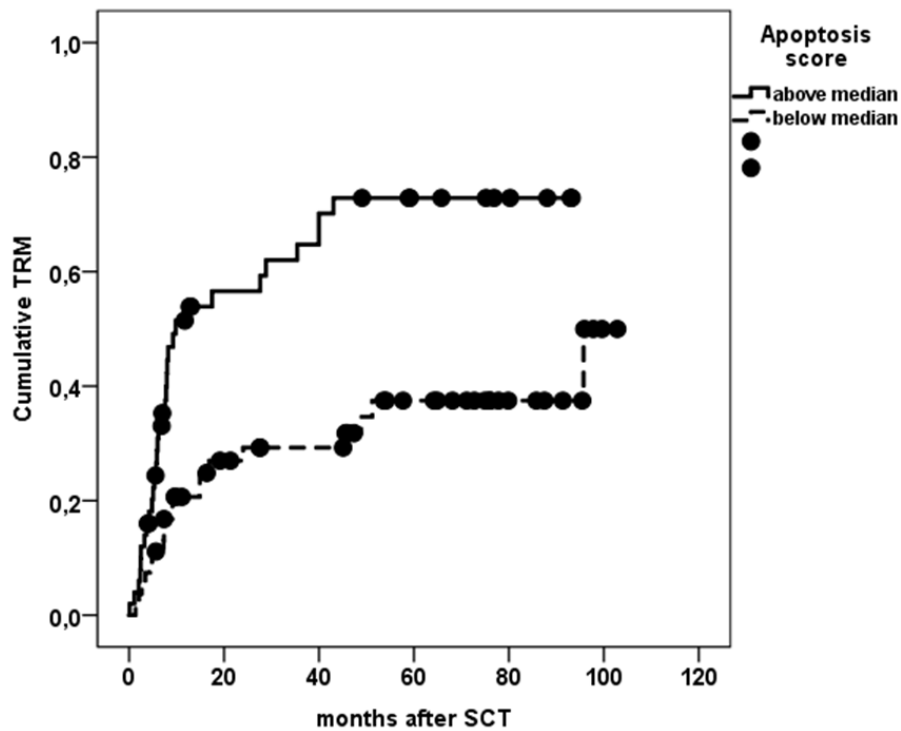|		CD4$^+$ cells	CD8$^+$ cells	Crypt loss	Epithelial apoptosis
CD4$^+$ cells	Correlation coefficient		0.329	-0.06	0.145
	Number of patients		197	200	200
	P value		**<0.001**	0.35	**0.04**
CD8$^+$ cells	Correlation coefficient	0.329		0.31	0.225
	Number of patients	197		198	198
	P value	**<0.001**		**0.001**	**<0.001**

Figure 5.2: Survival curve in relation to epithelial apoptosis.
Cumulative TRM significantly increases (p log rank= 0.001) in patients with greater degree of epithelial apoptosis when compared with patients with less epithelial apoptosis. N= 109 patients.

5.1.2 Foxp3$^+$ cells increase during acute GI-GvHD and are produced by CD4$^+$ cells and/or CD8$^+$ cells

Single antibody immunohistochemistry for Foxp3 was performed on 199 gut biopsies as explained in method section 4.2.2. Foxp3$^+$ cells were determined by the strong nuclear staining with the morphology that resembles lymphocytes. Manual counting of Foxp3$^+$ cells in gut biopsies revealed that these cells significantly increases in the patients suffering from severe acute GI-GvHD when compared to non GvHD patients as shown in Figure 5.3(A), which is a controversial finding to the existing belief that Tregs are diminishing during GvHD[135]. Grade 1 GvHD patients also depicted increasing trend of Foxp3$^+$ T cell infiltrates compared to non GvHD patients. To confirm the upregulation of Tregs during GvHD, *FOXP3* mRNA was analyzed by RT-qPCR as described in method section 4.3. This analysis revealed that *FOXP3* expression significantly increases during severe acute GI-GvHD when compared to non GvHD controls. Upregulation of *FOXP3* mRNA expression between non GvHD patients and grade 1 GvHD patients; and between grade 1 vs grade 2-4 patients were also nearly significant (0.07 and 0.06 respectively) as shown in Figure 5.3(B). Taken together, a significant increase of Tregs during GvHD suggests a previously unrecognized immunoregulatory loop that might have been induced due to pronounced inflammatory reaction mediated by effector T cells.

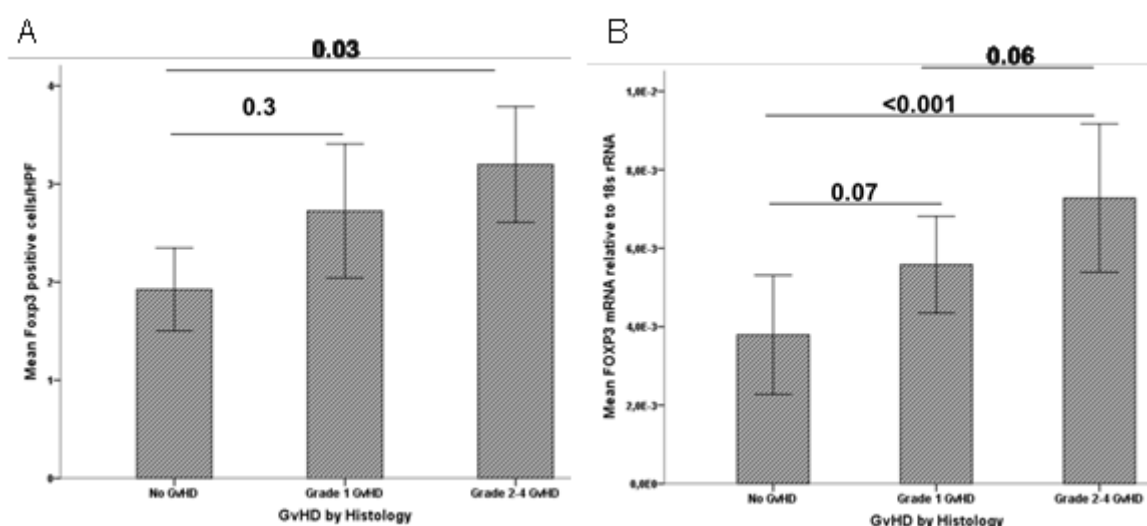**Figure 5.3: Infiltration of Foxp3$^+$ cells and expression of FOXP3 mRNA in GI tract during acute GI-GvHD.**
A. Foxp3$^+$ cells significantly upregulates during moderate-severe GI-GvHD compared to non GvHD patients. N=199 (No GvHD=80; Grade 1=64; Grade 2-

4=55). B. *FOXP3* mRNA significantly upregulates during moderate-severe GvHD when compared to non GvHD controls. N=314 (No GvHD=147; Grade 1=94; Grade 2-4=73). Data were non-normally distributed therefore non-parametric Kruskal-Wallis test was performed to calculate p values. Bar represents mean ± s.e.m.

In order to verify these results obtained in analyzing *FOXP3* expression on mRNA level, the correlation with Foxp3 protein expression was analyzed for 88 gut biopsies. The result demonstrated that Foxp3 protein expression highly correlates with *FOXP3* mRNA expression as shown in Table 5.2.

Table 5.2: Correlation table of Foxp3$^+$ cell infiltrates and FOXP3 mRNA in the gut of ASCT patients.
Nonparametric Spearman's correlation was used to determine the correlation coefficient and significance between protein and mRNA expression.

	FOXP3 mRNA
Foxp3$^+$ infiltrates	
Correlation coefficient	0.686
Significance	< 0.001
No. of patients	88

.

Subsequent interest was to explain the possible cellular source of Foxp3$^+$ cells for which single and double immunofluorescence techniques were established.

Single staining for Foxp3 expression was successfully established using anti-Foxp3 antibody as shown in Figure 5.4 B. As indicated by withe arrow, positive cells were determined nuclear Foxp3 staining. The specificity of antibody was determined by using negative control as shown in Figure 5.4 A. Likewise, single staining using an anti- CD4 antibody was established as shown in Figure 5.5.

Figure 5.5 A is a negative control where only secondary antibody was used in absence of primary antibody. No positive signals were observed.

Figure 5.5 B is a positive control for anti-CD4 antibody where both primary and secondary antibodies were used. It can be seen that thymus tissue contains numerous CD4$^+$ T cells and therefore served as a positive control for CD4 signal in subsequent experiments.

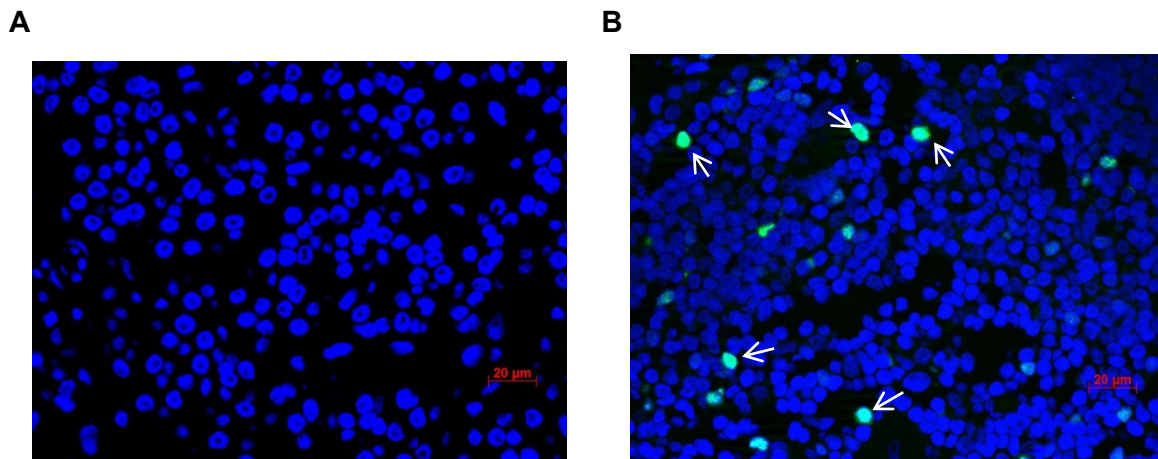A   B

Figure 5.4: Foxp3 staining in thymus tissue.
A. Negative control without primary antibody, only with secondary antibody. B.
Positive control with anti-Foxp3 primary antibody. Secondary antibody recognizes
the first antibody and is labelled with Alexa Flour 488. White arrows indicates
Foxp3$^+$ cells. Nuclei were counterstained with DAPI (blue). Images were taken at
400 times magnification. Scale bar represents 20 µm.

A   B
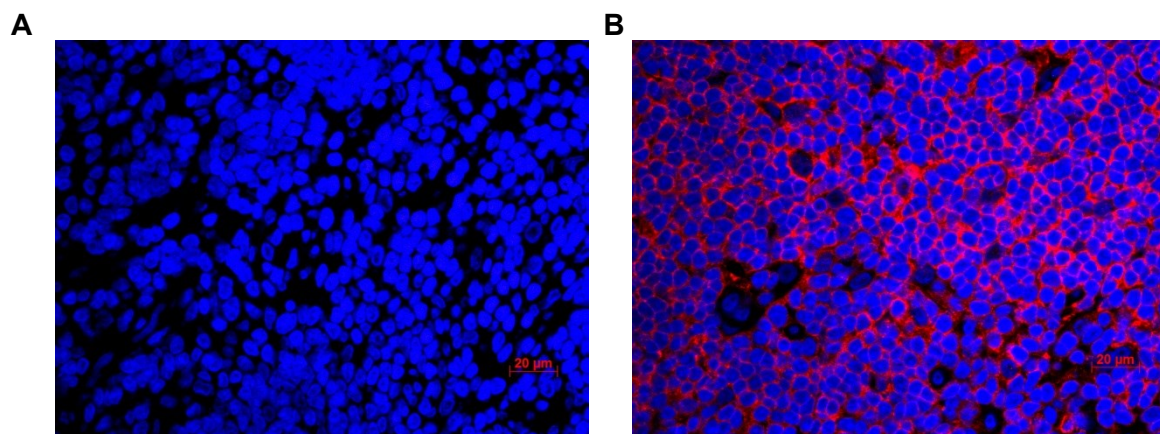
Figure 5.5: CD4 staining in the thymus tissue.
A. Negative control without primary antibody, only with secondary antibody. B.
Positive control with anti-CD4 primary antibody. Secondary antibody recognizes
the first antibody and is labelled with Alexa Flour 594. Numerous CD4$^+$ cells are
seen in red. Nuclei were counterstained with DAPI (blue). Images were taken at
400 times magnification. Scale bar represents 20 µm.

After the successful establishment of single stainings for Foxp3 and CD4, the
next step was to establish double staining. In order to establish the successful
double immunofluorescence method, thymus tissue was labelled with Foxp3 and
CD4 together. Primary antibodies that were raised in different species (Foxp3 in

mouse and CD4 in rabbit) were mixed together, thymus tissue was stained with primary antibodies followed by specific secondary antibodies. Image analysis was done by using an epifluorescence microscope. Pictures were taken at 400 times magnification with the desired filters. Figure 5.6 represents an exemplary double immunofluorescence.
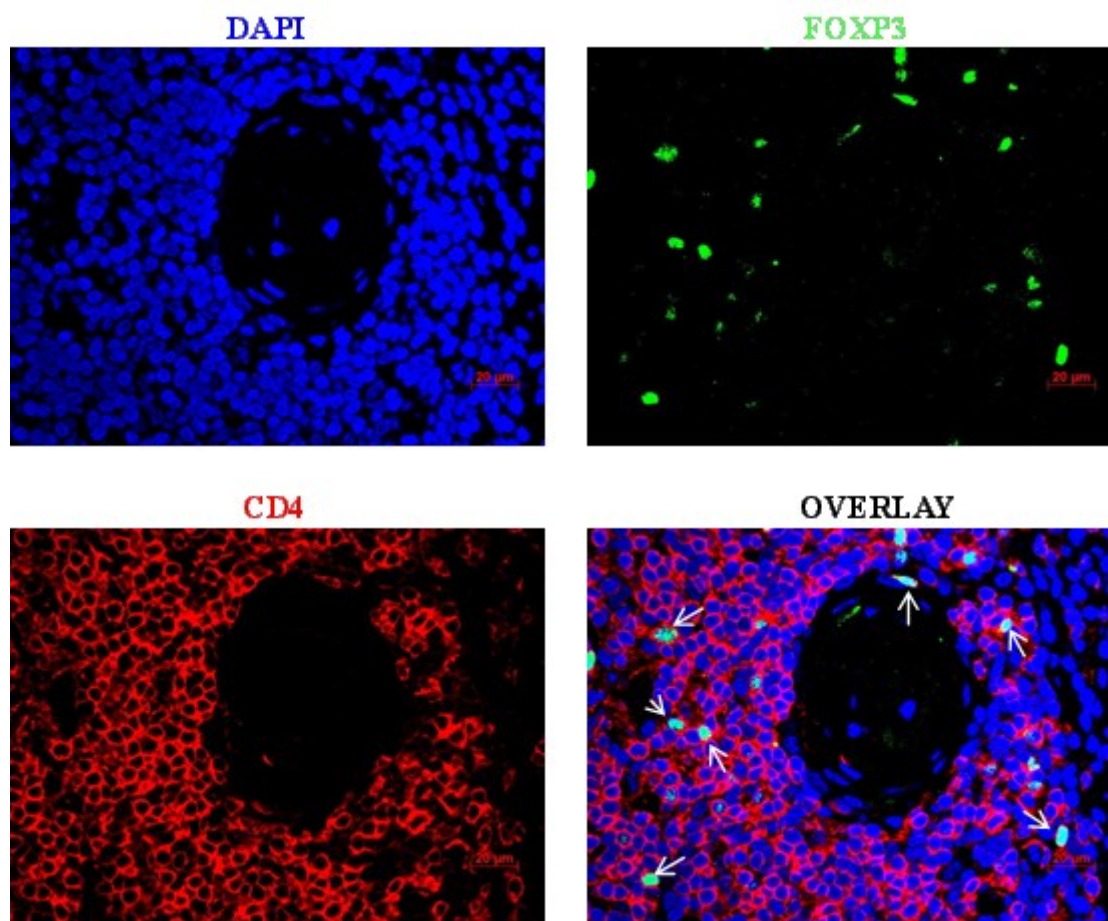
Figure 5.6: Foxp3$^+$CD4$^+$ double staining of thymus tissue.
Foxp3 signal corresponds to Alexa Flour 488 (green). CD4 signal corresponds to Alexa Flour 594 (red). Overlay is a merge of all channels where arrow indicates double positive cells. Nuclei were counterstained with DAPI (blue). Images were taken at 400 times magnification. Scale bar represents 20 μm.

Once the double fluorescence methodology was well established, the method was applied on colon biopsies of transplanted patients. Double immunofluorescence was performed with the combination of anti-Foxp3 and anti-CD4 antibodies in 22 transplanted colon biopsies. As shown in Figure 5.7, Foxp3$^+$ cells were positive for CD4 marker in ASCT patients. Foxp3 positive cells are well-known to express the CD4 marker as an indicator of CD4$^+$ T cells. Interestingly it was observed that there exist some Foxp3$^+$ cells which are

negative for CD4 marker as shown in Figure 5.8. Therefore double staining for Foxp3 and CD8 was performed to further characterize the Foxp3 positive, CD4 negative cell population.

Figure 5.7: Foxp3$^+$CD4$^+$ double staining of colon tissue of GvHD patient.
Foxp3 signal corresponds to Alexa Flour 488 (green) shown by green arrow. CD4 signal corresponds to Alexa Flour 594 (red) shown by red arrow. Overlay is a merge of all channels where white arrow indicates double positive cells. Nuclei were counterstained with DAPI (blue). Images were taken at 400 times magnification. Scale bar represents 20 μm.
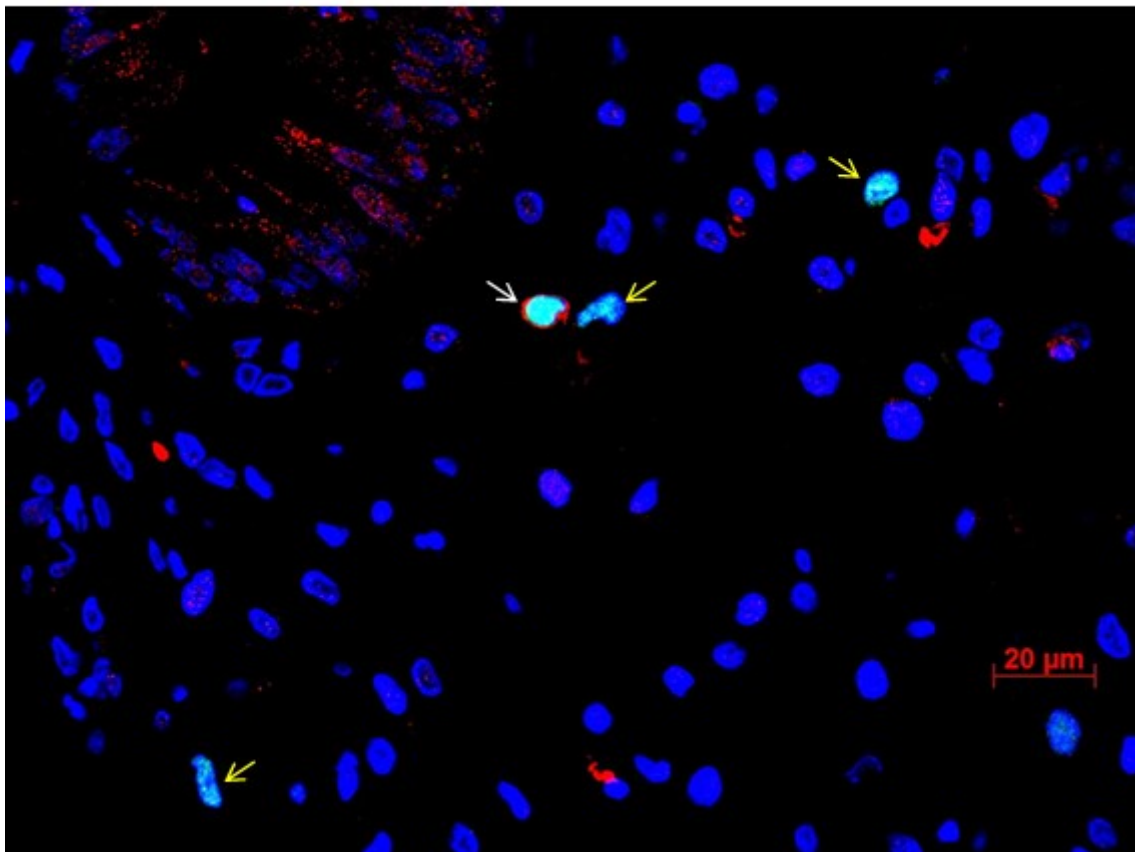
Figure 5.8: Foxp3$^+$CD4$^+$ double staining of colon tissue of GvHD patient.
Foxp3 signal corresponds to Alexa Flour 488 (green). CD4 signal corresponds to Alexa Flour 594 (red). Image is a merge of three channels where white arrow indicates double positive cell. Yellow arrow indicates CD4$^-$Foxp3$^+$ cells. Nuclei were counterstained with DAPI (blue). Image was taken at 400 times magnification. Scale bar represents 20 µm.

Anti-CD8 staining was established in similar way to the anti-CD4 staining. Double staining was performed for Foxp3+CD8 on 22 colon biopsies of ASCT patients. Surprisingly CD8$^+$ Foxp3$^+$ cells were observed in the colon of GvHD patients as shown in Figure 5.9. Therefore it was evident that not only CD4$^+$ T cell but also CD8$^+$ T cells are involved in Foxp3 expression. These results suggest the involvement of at least two different subsets of regulatory T cells in GvHD that might be involved in dampening the inflammatory reaction and establishing immune homeostasis in the course of GvHD.
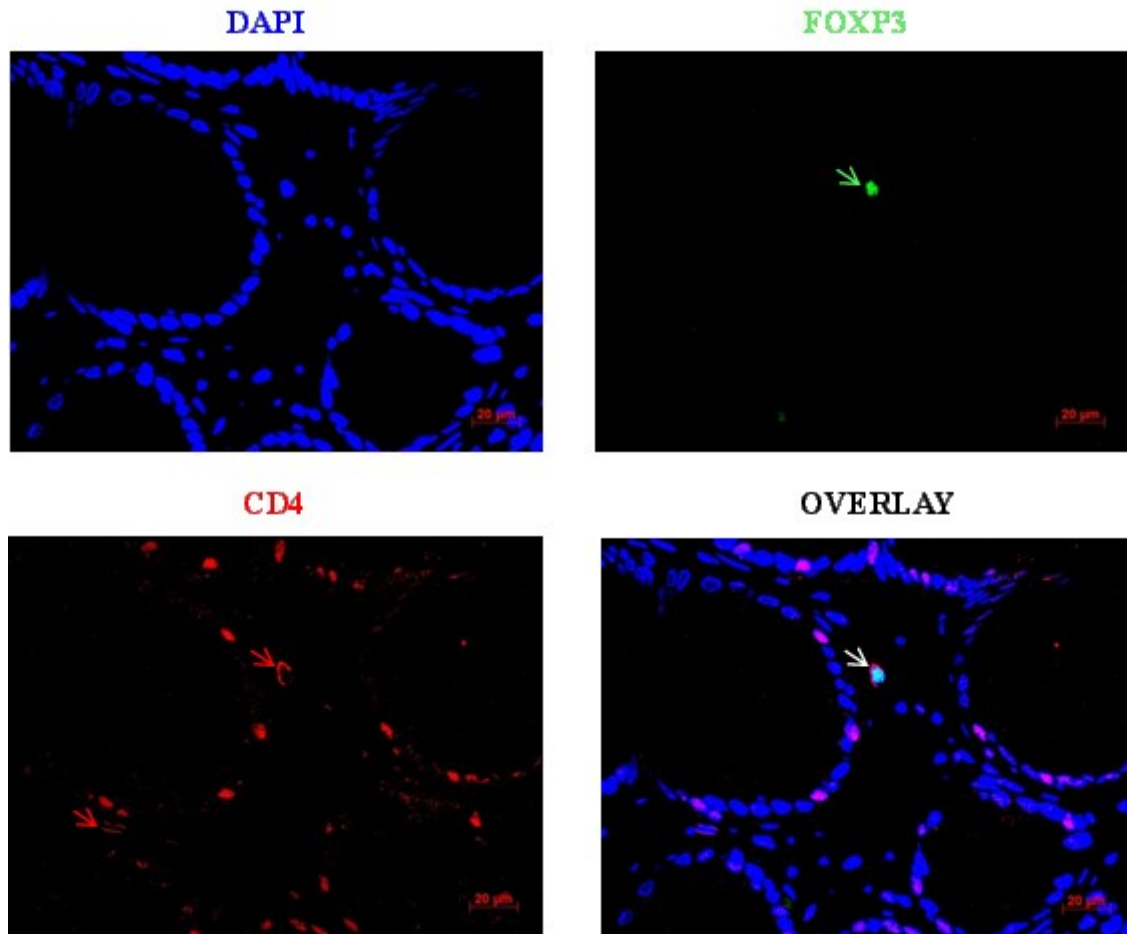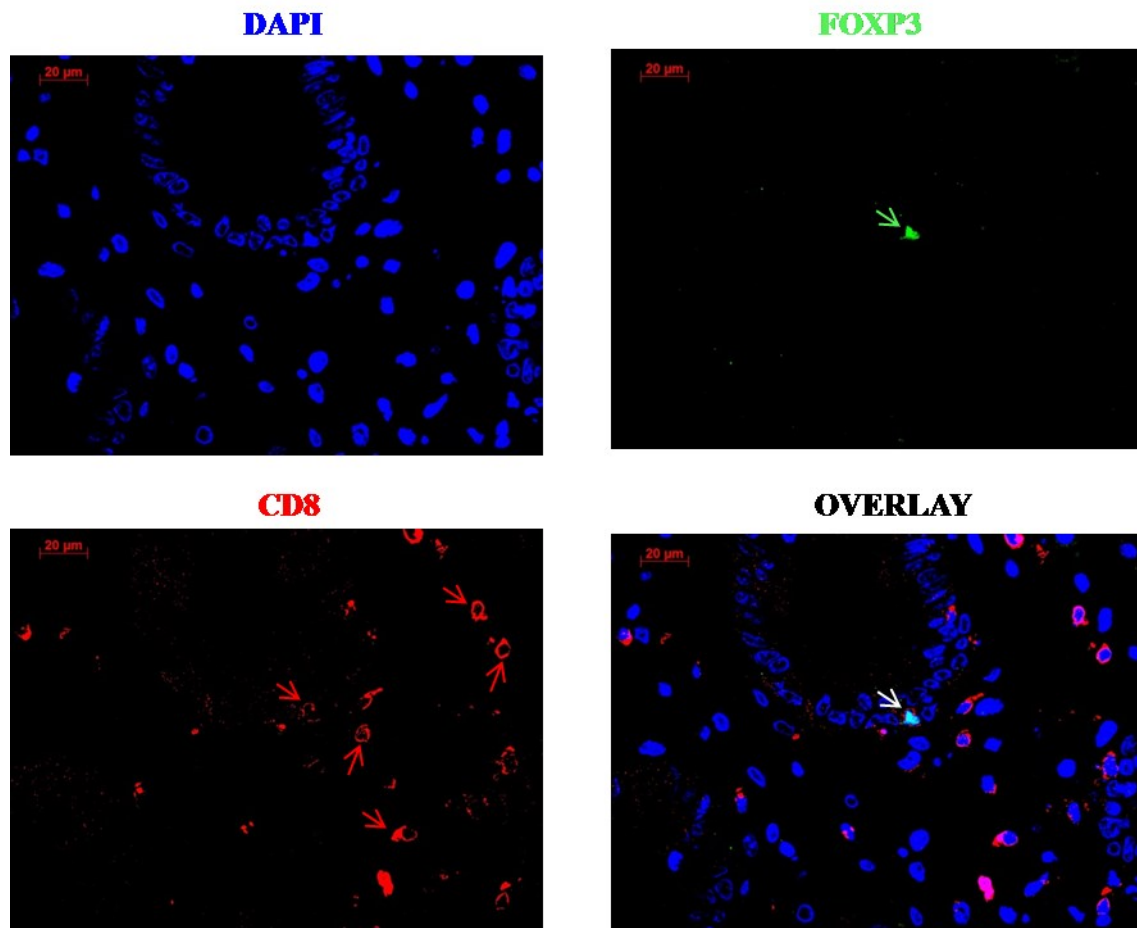
Figure 5.9: Foxp3⁺CD8⁺ double staining of colon tissue of GvHD patient.
Foxp3 signal corresponds to Alexa Flour 488 (green) shown by green arrow. CD8 signal corresponds to Alexa Flour 594 (red) shown by red arrow. Overlay is a merge of all channels where white arrow indicates double positive cells. Nuclei were counterstained with DAPI (blue). Images were taken at 400 times magnification. Scale bar represents 20 μm.

After realizing the existence of two types of Foxp3⁺ cells i.e. CD4⁺ and CD8⁺ Foxp3⁺ cells, the number of double positive cell per high power field was determined. Both sets of double positive cells (CD4+Foxp3 and CD8+Foxp3) were manually counted per high power field. Depending on the size of biopsies, 4-10 high power fields were analyzed. As shown in Figure 5.10 (A) CD4⁺ Foxp3⁺ cells were significantly upregulated in patients with Grade 1 GvHD when compared to non GvHD patients. Grade 2-4 GvHD patients exhibited upregulating trend as compared to non GvHD patients. Of note, CD8⁺ Foxp3⁺ cells seemed to upreulated only in grade 2-4 GvHD patients as shown in Figure 5.10 (B). The importance of CD8⁺ Foxp3⁺ cells in GvHD mediated protection has been well documented in experimental model [136] but so far no evidence exists in clinical

data. It can be suspected that these CD8$^+$Foxp3$^+$ cells are induced in later phase of GvHD possibly to counterbalance the extreme immune mediated inflammation.
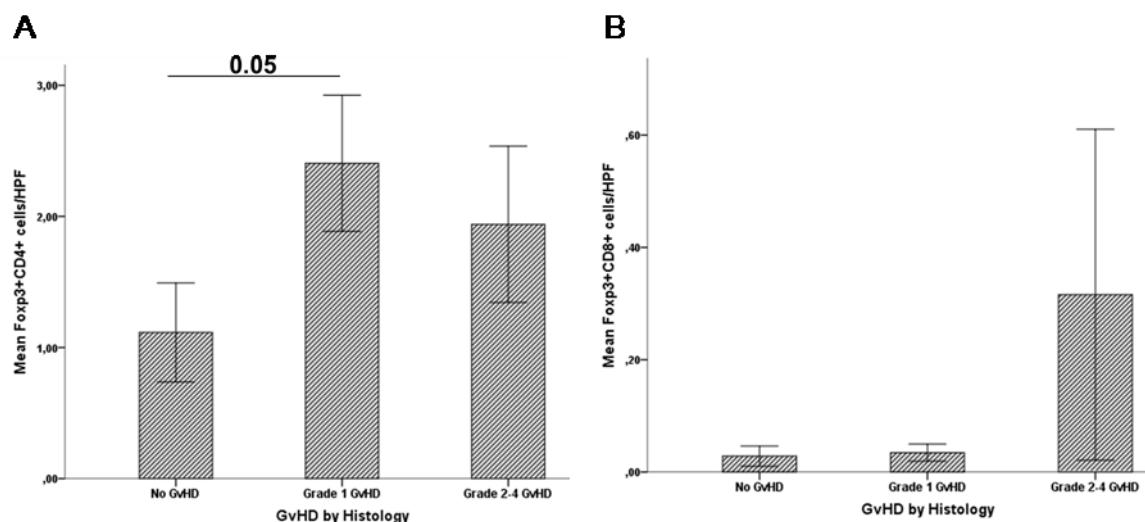
Figure 5.10: Quantification of CD4$^+$Foxp3$^+$ cells and CD8$^+$Foxp3$^+$ cells by double immunofluorescence.
A. Number of Foxp3$^+$ cells/HPF that are produced by CD4$^+$ T cells. Double positive cells significantly increases in patients during grade 1 GvHD and has increasing trend in grade 2-4 GvHD. B. Number of Foxp3$^+$ cells/HPF that are produced by CD8$^+$ T cells. There is a trend of strong upregulation in the patients in Grade 2-4 GvHD. N=22 patients. Non-parametric Kruskal-Wallis test was performed to calculate p value. Bar represents mean ± s.e.m.

5.1.3   IDO$^+$ cells increase during acute-GI-GvHD and correlates with Foxp3 expression

Indoleamine 2,3-dioxygenase (IDO) is an intracellular enzyme that degrades the essential amino acid tryptophan [137]. IDO suppresses T-cell responses and promotes immune tolerance. Its immunosuppressive properties have been implicated in mammalian pregnancy, tumor resistance, chronic infection, autoimmunity and allergic inflammation[138]. Single antibody immunohistochemistry was performed on 193 gut biopsies to analyze IDO expression after allogenic stem cell transplantation. Unbiased semi quantitative scoring was performed on stained biopsies (by Dr. Elisabeth Huber in co-operation with department of

pathology). IDO$^+$ cells significantly increased in patients showing the symptoms of low, medium or high grade GvHD when compared to GvHD free patients as shown in Figure 5.11(A). Furthmore, *IDO* mRNA was analyzed by RT-qPCR in 190 samples. Upregulation of IDO expression during GvHD at protein level was further supported by increased expression of *IDO* mRNA at transcriptional level as shown in Figure 5.11(B). In addition, correlation was calculated for IDO protein and mRNA expression as shown in Table 5.3 and was observed that gene and protein expression highly correlates with each other. Moreover, expression of IDO was correlated with Foxp3 protein and *FOXP3* mRNA expression. It was interesting to note that IDO protein highly correlates with Foxp3 protein and *FOXP3* mRNA expression (table 5.4). *IDO1* mRNA as well highly correlated with Foxp3 protein and *FOXP3* mRNA expression. These findings reveal the existence of strong immunoregulatory loop between IDO expression and Foxp3 expression in response to GvHD-mediated inflammation in ASCT patients. To our surprise, neutrophil infiltrates were also found to be significantly correlated with IDO and Foxp3 expression both at protein and mRNA level. This raises the hypothesis that myeloid derived suppressor cells are invoved in immunoregulation during GvHD. As myeloid derived suppressor cells are dependent on an intact and diverse microbiome, it will be of interest to assess the interaction of microbiota disruption with intestinal immunoregulation in the future. An intact microbiome might help to compensate inflammation by allowing induction of regulatory mechansims.

Figure 5.11: Infiltration of IDO$^+$ cells and expression of IDO1 mRNA in GI tract during acute GI-GvHD.
A. IDO$^+$ cells significantly upregulates during GvHD compared to non GvHD controls. N=193 (No GvHD=80; Grade 1=60; Grade 2-4=53). B. IDO1 mRNA significantly upregulates during severe GvHD when compared to non GvHD controls. N=190 (No GvHD=100; Grade 1=52; Grade 2-4=38). Data were non-normally distributed therefore non-parametric Kruskal-Wallis test was performed to calculate p values. Bar represents mean ± s.e.m.

Table 5.3: Correlation table of IDO with Foxp3 (protein and mRNA) infiltrates and neutrophil infiltrates.
Nonparametric Spearman's correlation was used to determine the correlation coefficient and significance between protein and mRNA expression. Lp=lamina propria

		IDO protein	IDO1 mRNA	Foxp3 protein	FOXP3 mRNA	Neutrophils in Lp
IDO protein	Correlation coefficient	1	0.275	0.381	0.425	0.486
	Number of patients	194	75	193	87	194
	P value		**0.01**	**<0.001**	**<0.001**	**<0.001**
IDO1	Correlation coefficient	0.275	1	0.476	0.221	0.525

mRNA	Number of patients	75	191	75	189	77
	P value	0.01		**<0.001**	**0.002**	**<0.001**
Neutrophils in Lp	Correlation coefficient	0.486	0.525	0.456	0.567	1
	Number of patients	194	77	200	90	206
	P value	<0.001	<0.001	**<0.001**	**<0.001**	

5.1.4 IL-17^{+} cells decrease during acute GI-GvHD and are produced by non-T cells

IL-17 cytokine is long known to be hallmark of Th17 cell type while only recently researchers revealed that the majority of IL-17 released during an inflammatory response is produced by innate immune cells [109]. To analyze the cellular expression of IL-17^{+} cells after ASCT, immunohistochemistry was performed on 197 gut samples after ASCT. It was observed that IL-17 significantly downregulates as GvHD exacerbates (Figure 5.12 A). To further confirm the downregulation of IL-17 in ASCT patients, the transcription factor for IL-17, *RORC* was analyzed at mRNA level using RT-qPCR on 197 transplanted biopsies. In parallel to protein expression, *RORC* mRNA expression was also downregulated with the severity of GvHD (Figure 5.12 B) supporting the hypothesis that these IL-17^{+} cells could be protective rather than inflammatory in the context of ASCT and that the loss of these protective cells could contribute to potential GvHD.
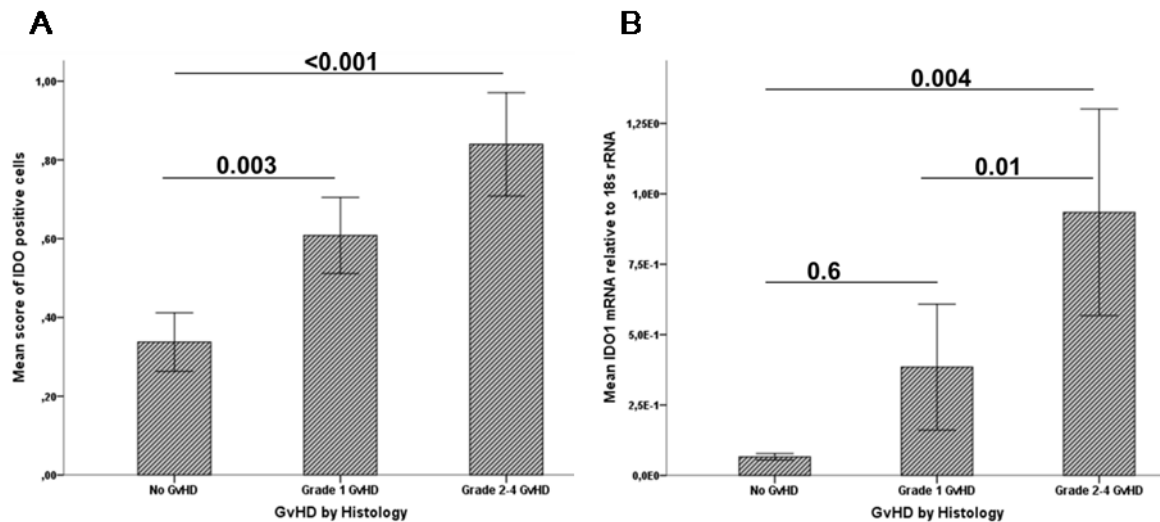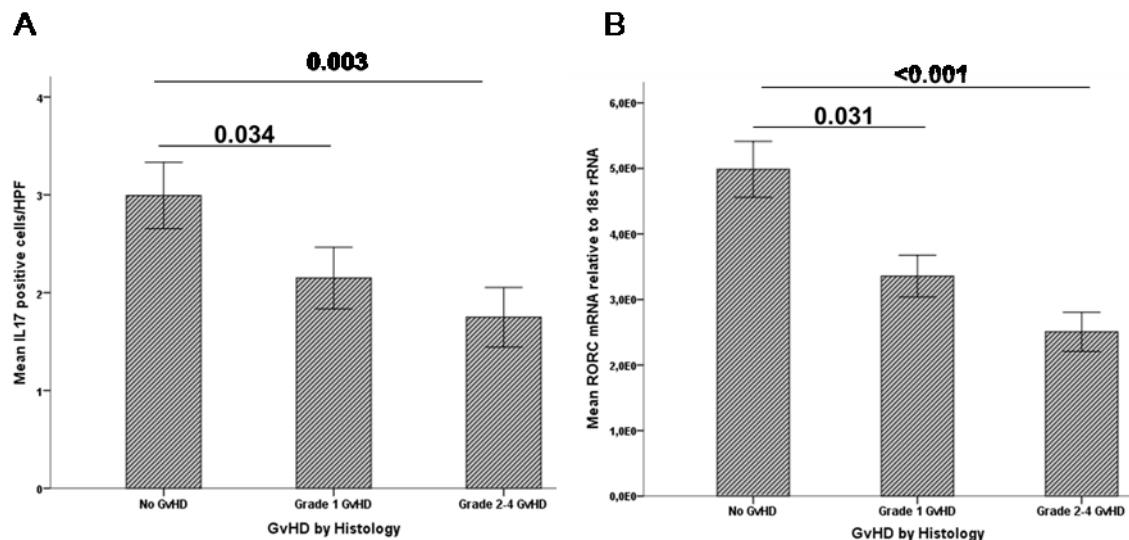
Figure 5.12: Infiltration of IL-17⁺ cells and expression of *RORC* mRNA in GI tract during acute GI-GvHD.
A. IL-17⁺ cells significantly downregulates during GvHD compared to non GvHD controls. N=197 (No GvHD=79; Grade 1=63; Grade 2-4=55). B. *RORC* mRNA significantly downregulates during severe GvHD when compared to non GvHD controls. N=197 (No GvHD=100; Grade 1=57; Grade 2-4=40). Data were non-normally distributed therefore non-parametric Kruskal-Wallis test was performed to calculate p values. Bar represents ± s.e.m.

The correlation between IL-17 protein and *RORC* mRNA was analyzed for 82 gut biopsies that were common samples for IHC and RT-qPCR. Significant correlation was observed between protein expression and gene expression when data were correlated in terms of GvHD grade 0,1 and 2-4 as shown in Figure 5.13 (A). The loss of IL-17 and *RORC* was analyzed in terms of transplant related mortality(TRM). 82 patients enrolled in the study showed that the loss of IL-17/*RORC* potentially leads to significantly higher TRM as shown in Figure 5.13 (B). Taken together, these results suggests that there is a potential loss of protective IL-17⁺ cells during GvHD which leads to higher transplant related mortality.

Figure 5.13: IL-17 protein correlates with *RORC* mRNA and Treatment Related Mortality (TRM) occurs more frequently in patients with low IL-17/*RORC* expression.
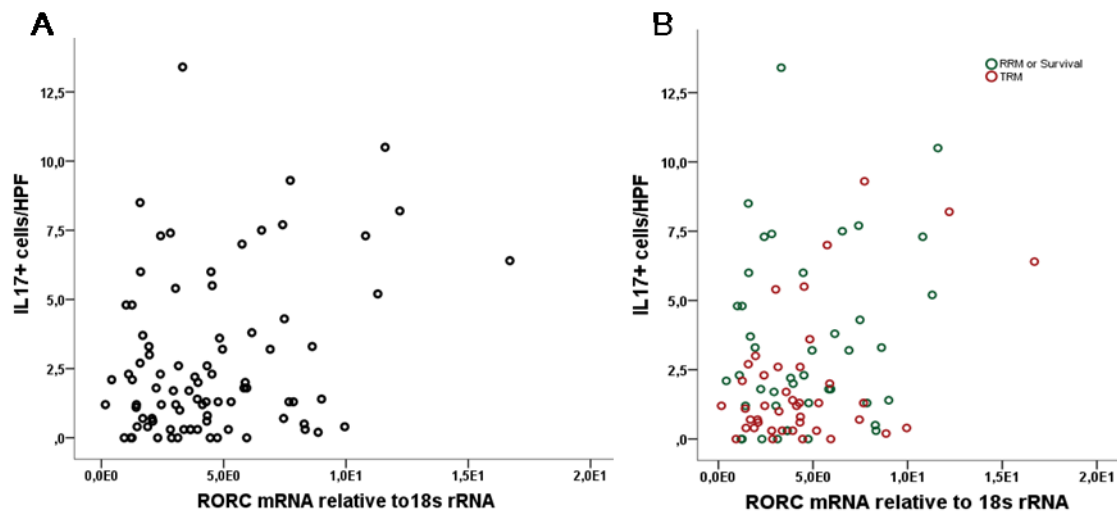A. Scatter plot diagram of IL-17 expression and *RORC* expression with the correlation coefficient of 0.224 and p value 0.04 when data were controlled for histological GvHD. N=82 patients. B. Green circles represent patients with Relapse Related Mortality (RRM) or survival. Red circles represent patients with Transplant related mortality(TRM). Patients with reduced IL-17/*RORC* expression exhibited frequent TRM with the correlation coefficient of 0.297 and p value 0.006 when data were controlled for TRM.

IL-17 is a typical marker for Th-17 cell types which are inflammatory subset of CD4^{+} T cells [139,140]. Along with the downregulation of IL-17 and the hypothesis that IL-17^{+} cells are protective, next, the cellular source of IL-17 was analyzed. Double immunofluorescence was established for IL-17 and CD4 to depict if these IL-17 cells are of Th-17 origin or not. For this, colon biopsies of Crohn's disease patients were utilized to establish single staining for IL-17 and CD4 individually as shown in Figure 5.14. Anti-CD4 antibody was used in undiluted state as mentioned before. The anti-IL-17 antibody was titrated in different dilution. Based on precise signal that can be well differentiated from background, dilution of 1:25 was chosen for the consecutive experiments. Due to the complexity of immunofluorescence for cytokines on paraffin biopsies, it was necessary to assure that the specific signal is being analyzed and that false signal, or background, or autofluorescence is being avoided. Therefore two individual analyzers (one analyzer being highly experienced pathologist) manually counted IL-17^{+} cells per high power filed on 39 colon biopsies in a blindfold fashion at 40X

magnification. As shown in Figure 5.15, two individual analyzers observed similar results. Total IL-17$^+$ cells were downregulated with an exacerbation of GvHD. The number of cells counted per high power field was also similar.
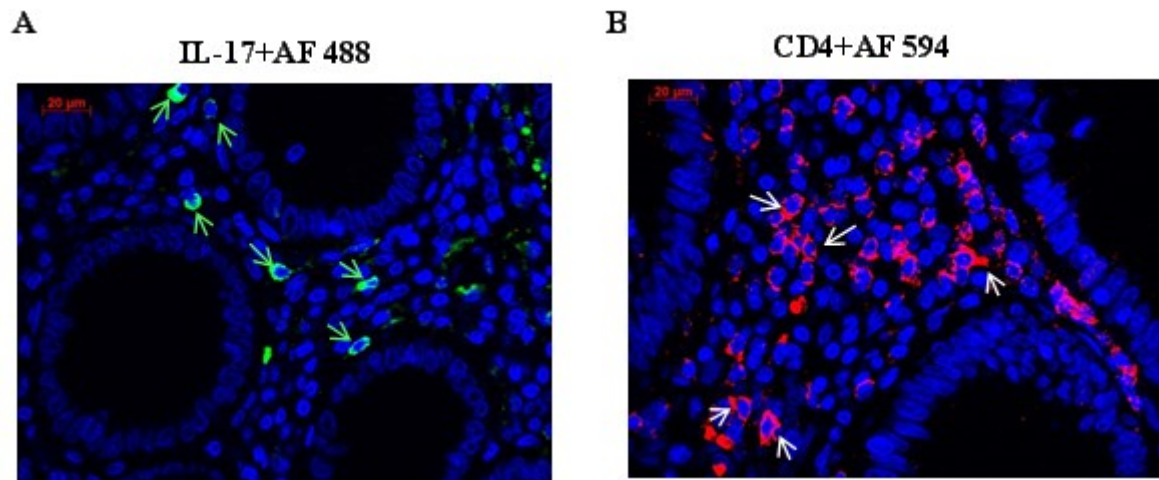
Figure 5.14: IL-17 and CD4 staining in colon tissue.
A. IL-17 signal corresponds to AF 488 shown by green arrows. B. CD4 signal corresponds to AF 594 shown by white arrows. Numerous CD4$^+$ cells are seen in red. Nuclei were counterstained with DAPI (blue). Images were taken at 400 times magnification. Scale bar represents 20 μm.
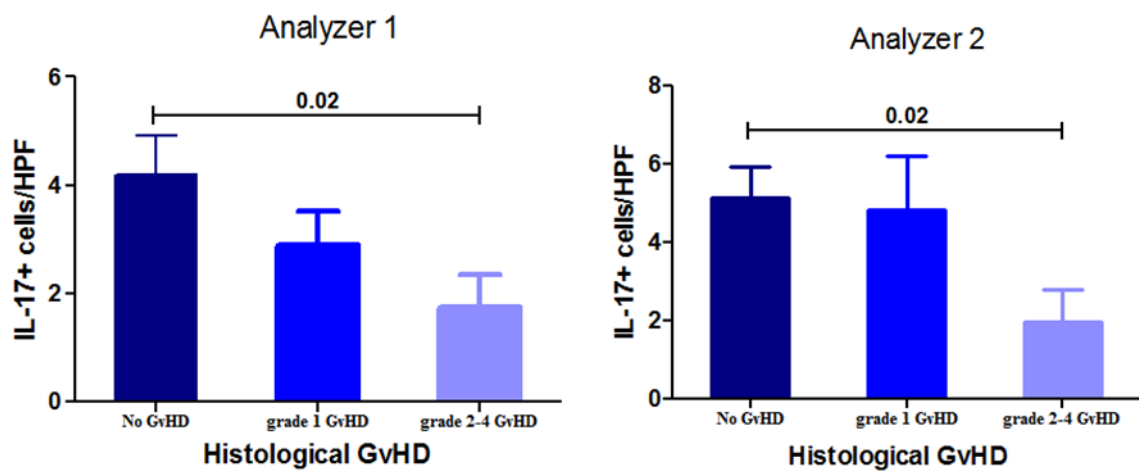
Figure 5.15: IL-17$^+$ cells analysis by two independent analyzers.
Two analyzer individually analyzed colon biopsies after ASCT. Both analyzers showed downregulation of IL-17$^+$ cells at the course of GvHD. Anti-IL-17 antibody was applied on biopsies followed by Alexa Flour 488 conjugated secondary antibody. IL-17$^+$ cells were manually counted per high power field by two analyzers with epifluorescence microscope in a blindfold fashion. Number of samples included in analyzes is 39 for analyzer 1 and 33 for analyzer 2. Data

were non-normally distributed therefore non-parametric Kruskal-Wallis test was performed to calculate p values. Bar represents mean + s.e.m.

After successful establishment of single immunofluorescence, and the confirmation that the protein of interest, IL-17 staining is trustworthy, double immunofluorescence was established as shown in Figure 5.16 where double positive cell (IL-17$^+$CD4$^+$) and IL-17 positive but CD4 negative cell can be seen.

.
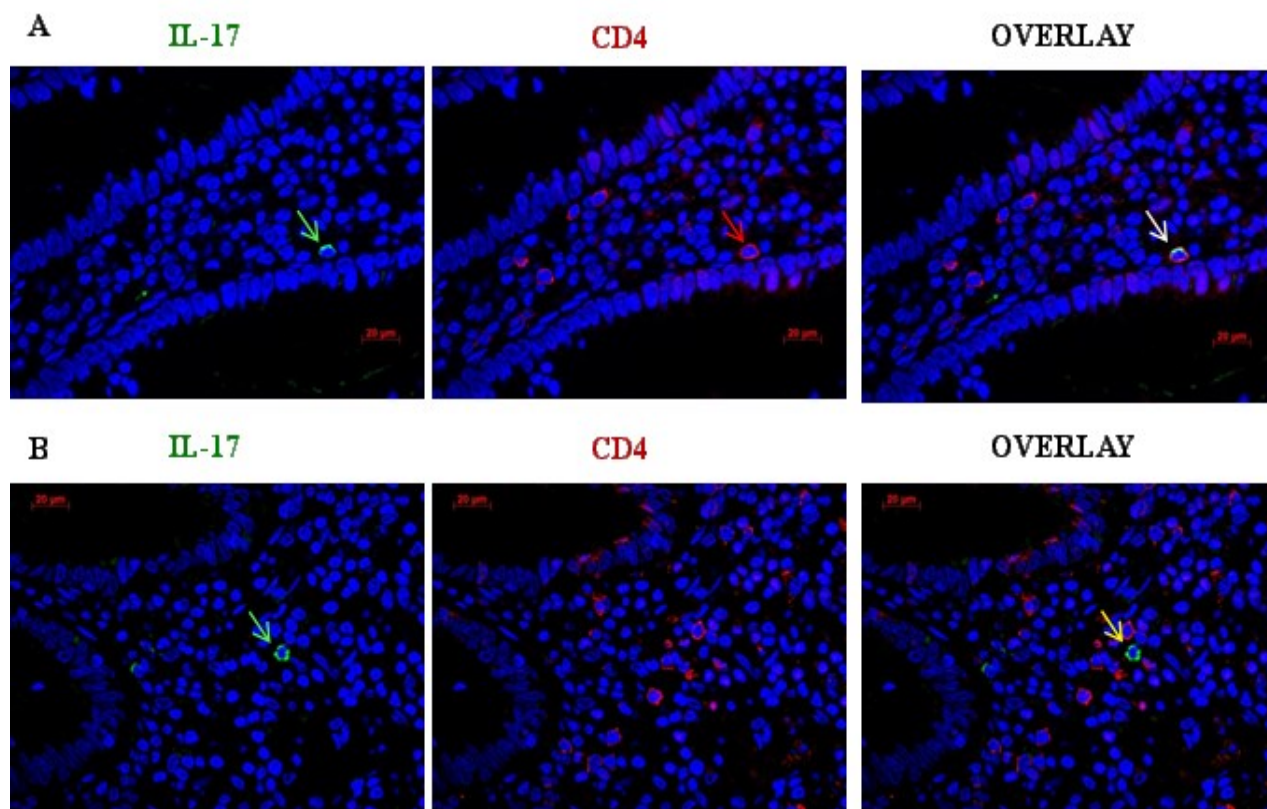
Figure 5.16: Establishment of IL-17$^+$CD4$^+$ double staining in colon biopsy of Crohn's disease patient.
A. Green arrow indicates IL-17$^+$ cell. Red arrow indicates CD4$^+$ cell. Several CD4$^+$ cells can be seen in lamina propria of colon. Overlay image shows double positive cell indicated by white arrow. B. Green arrow represents IL-17$^+$ cell. Several CD4$^+$ cells can be seen in lamina propria of colon. Overlay shows CD4$^-$ IL-17$^+$ cell indicated by yellow arrow. Nuclei were counterstained with DAPI (blue). Images were taken at 400 times magnification. Scale bar represents 20 μm.

Once the double immunofluorescence was well established, the technique was applied on colon biopsies of allogenic stem cell transplant patients. At 400 times magnification per high power field, we aimed to analyze and quantify double positive cells. Surprisingly, IL-17 signal did not colocalize with CD4 signal in all

the samples tested as shown in Figure 5.17 (A). To our knowledge this is the first report to reveal the existence of non CD4 IL-17+ cells in human gut biopsies therefore supporting the idea that non Th17 cells are able to produce IL-17. However, other T cells like gammadelta T cells and NKT cells are possibly a major source of IL-17. To further clarify the cellular source of IL-17, double immunofluorescence was performed for IL-17 and CD3 together. 39 transplanted colon biopsies were stained for IL-17 and CD3. Again, to our surprise, so far none of the IL-17 signal colocalized with CD3 expression so far tested as shown in Figure 5.17 (B) suggesting a new paradigm in the role of IL-17 in GvHD. We assume that these IL-17+ cells are of innate origin and are perhaps of protective nature in the context of GvHD related inflammation
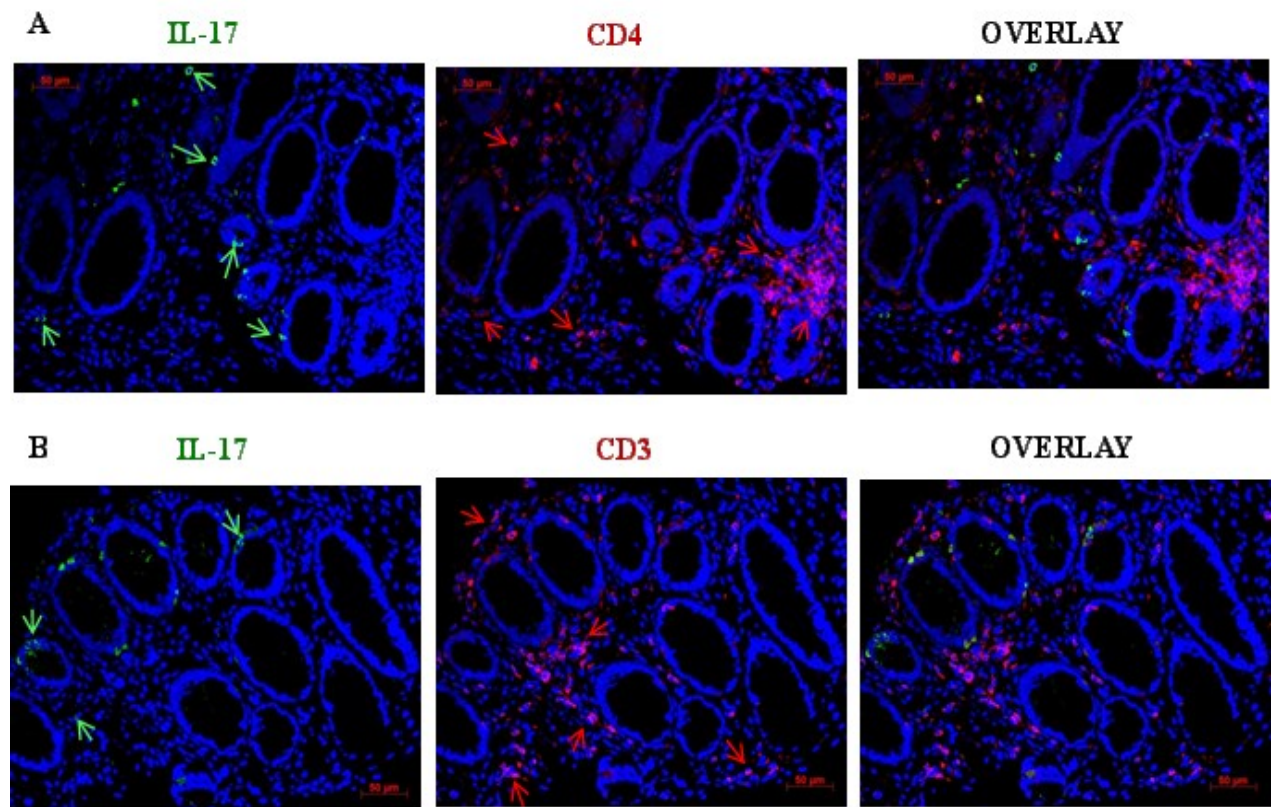
Figure 5.17: IL-17$^+$CD4$^+$ (A) and IL-17$^+$CD3$^+$ (B) double staining of colon tissue of ASCT patient.
A. Green arrow indicates IL-17$^+$ cells. Red arrow indicates CD4$^+$ cells. Several IL-17$^+$ and CD4$^+$ cells can be seen in crypts and lamina propria of colon. Overlay image shows that IL-17 signal do not colocalize with CD4 signal. B. Green arrow represents IL-17$^+$ cells. Red arrow indicates CD3$^+$ cells. Several IL-17$^+$ and CD3$^+$ cells can be seen in crypts and lamina propria of colon. Overlay shows IL-17 signal do not colocalize with CD3 signal. Nuclei were counterstained with DAPI (blue). Images were taken at 200 times magnification. Scale bar represents 50 μm.

To this point, we observed that IL-17 protein is of non T cell origin. To further clarify the cellular source of IL-17, double fluorescence was performed for anti-IL-17 together with the marker anti-CD117 (c-kit) which is expressed by innate lymphoid cell type 3 (ILC3s). Interestingly, IL-17$^+$ cells were found to be positive for CD117 as shown in Figure 5.18 (A) implicating the possible involvement of IL-17 producing ILC3s which are known to be protective cells in the course of inflammation. Consequently, it was also seen that there exist IL-17 positive but CD117 negative cells as shown by a yellow arrow in Figure 5.18 (B) suggesting that there exists perhaps, heterogeneity of IL-17 producing cells, of innate origin.
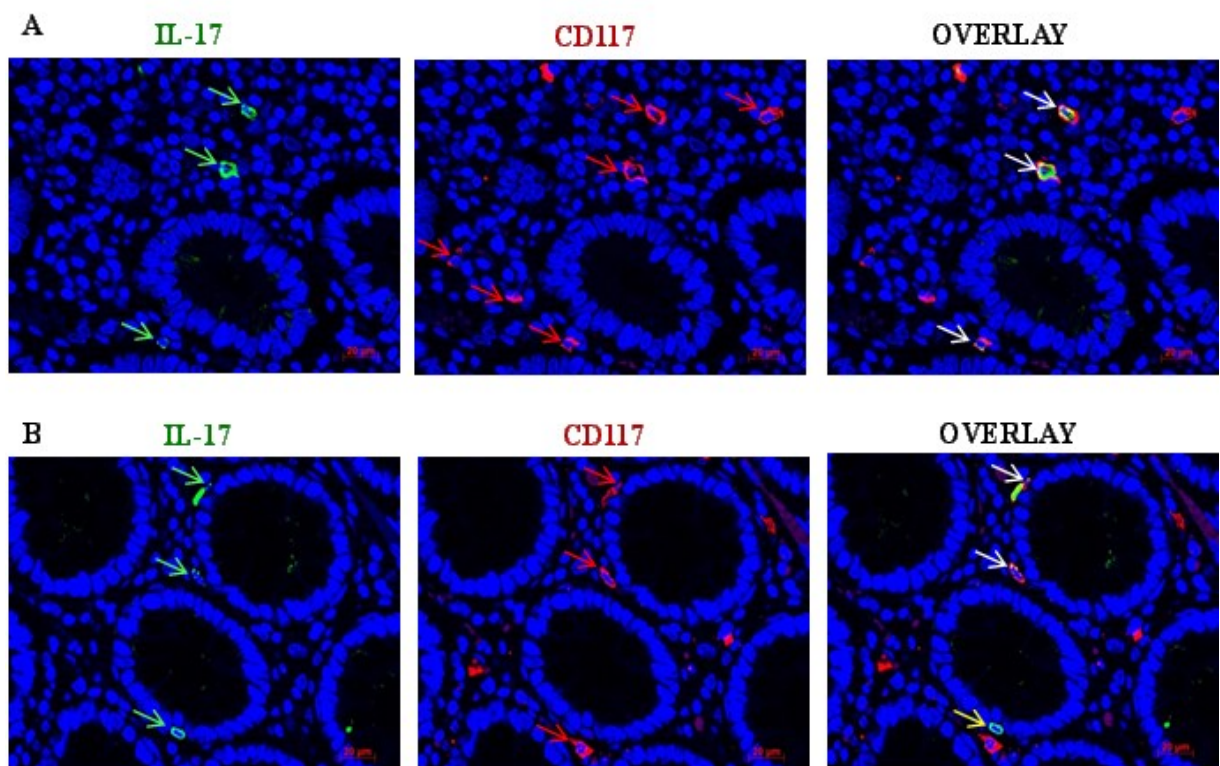
Figure 5.18: : IL-17$^+$CD117$^+$ double staining of colon tissue of ASCT patient. Green arrow indicates IL-17$^+$ cells. Red arrow indicates CD117$^+$ cells. Several IL-17$^+$ and CD117$^+$ cells can be seen in crypts and lamina propria of colon. Overlay image shows that IL-17 signal colocalizes with CD117 signal in A&B as indicated by white arrow while yellow arrow indicates CD117 negative IL-17$^+$ cell in image B. Nuclei were counterstained with DAPI (blue). Images were taken at 400 times magnification. Scale bar represents 20 μm.

5.2 Analysis of gene profiles during acute GI-GvHD (in collaboration with Medical University of Göttingen)

As a part of Celleuorpe collaborative scheme, a digital PCR called 'Fluidigm array' was performed in Medical University of Göttingen (UMG-GOE). 192 transplanted patients were chosen for the study. 200 ng of RNA was transcribed to cDNA as required by the Fluidigm array protocol and these samples used to profile the relevant genes during GvHD.

5.2.1 Gene expression by fluidigm array correlates with gene expression by qPCR

In the context of gastro-intestinal GvHD, there has always been scarcity of patient biopsies in transplant centres therefore the analyzes of gene profile is often not possible. Regensburg medical centre put an effort to collect patient's biopsies after transplantation and the availability of biopsies motivated us to implement mRNA analysis in a bigger scale. In collaboration with the Medical University of Göttingen, gene array was performed using Fluidigm microarray digital PCR. Based on previous findings, 28 relevant genes (as listed in materials section 3.9.2) were analyzed using digital PCR, among those seven genes that were already analyzed in University Medical Centre Regensburg were repeated to confirm the accuracy of digital PCR of Göttingen by conventional RT-qPCR of Regensburg.. Although it has been previously reported that both mRNA[141] and micro RNA[142] expressions are highly reproducible in digital PCR when compared to conventionally followed RT-qPCR, we aimed to confirm these results in transplanted biopsies. To further check the accuracy of digital PCR, different primer sequences were designed for three genes whereas the same primer sequences were used for rest of the four genes. It was observed that the expression of seven genes highly correlated between digital PCR and conventional RT-qPCR independent of the differences in primer sequences used as shown in Table 5.4. This correlation data suggests the accuracy and precision of digital PCR is highly comparable to conventional RT-qPCR.

Table 5.4: Correlation of gene expression by digital PCR and conventional qPCR.
Nonparametric Spearman's correlation was used to determine the correlation coefficient and significance between Fluidigm digital PCR and conventional qPCR mRNA expression.

Genes	No. of samples	Correlation coefficient	P value	Primer sequence
BATF	92	0.424	<0.001	Different
DEFα5	176	0.753	<0.001	Same
DEFβ4	176	0.143	0.05	Same
FOXP3	175	0.317	<0.001	Same
GPR109A	178	0.327	<0.001	Different
IDO	151	0.473	<0.001	Different
RORC	156	0.199	0.01	Same

Of note, GAPDH was used as reference gene for digital PCR since *18S* rRNA failed to show dissociation curve.

5.2.2   Differential gene expression during acute-GI-GvHD

As it became evident that the digital PCR correlates with conventional RT-qPCR, we aimed to analyze the gene expression in terms of GVHD and transplant related mortality. Due to the fact that samples are pre-amplified and GAPDH is used as reference gene, we choose only those samples that showed GAPDH expression within 15 cycles in the digital PCR. This restriction was chosen in order to make the analysis more precise.

Gene expression was analyzed into terms of GvHD vs no GvHD patients for the selected genes. Table 5.5 shows the list of genes with their p values for the gene of interest. Of 21 carefully selected genes, only three genes were found to be significantly altered in GvHD as indicated by bold p values in the table. These genes were further analyzed with respect to different grades of GvHD and transplant related mortality.

Table 5.5: Differential gene experssion during acute GI-GvHD.
Gene expression was analyzed for non GvHD (n=57) vs GvHD (n=61) patients. Mann-Whitney test was performed to determine the significance.

S.N	Genes analyzed	Alteration in GvHD	p value

1	*AHR*	Up	0.6
2	*CATH*	Up	0.5
3	*CYP24A1*	Up	0.1
4	*CYP27A1*	Down	**0.007**
5	*CYP27B1*	Up	0.1
6	*CYP2R1*	Down	0.4
7	*EBI3*	Up	0.08
8	*GATA3*	Up	0.2
9	*GC*	Down	0.8
10	*IL10*	Up	0.2
11	*IL12A*	Up	0.6
12	*IL12B*	Down	0.7
13	*IL17*	Up	0.4
14	*IL22*	Up	0.2
15	*IL23*	No change	0.9
16	*IL33*	Up	0.07
17	*PXR*	Down	**0.05**
18	*REG3A*	Up	0.1
19	*TBET*	Up	0.1
20	*TNF*	Down	0.4
21	*VDR*	Down	**0.007**

It was observed that *CYP27A1*, an enzyme involved in vitamin D synthesis, and *VDR* (vitamin D receptor) itself that recognizes the active vitamin D, is significantly downregulated during GvHD and the loss of the gene is associated with transplant related mortality as shown in Figure 5.19. Cyp27a1 is involved in first step of active vitamin D synthesis[143]. VDR binds to active form of vitamin D and is a well-defined immunomodulator that acts via NF-AT or NF-kB signaling pathways[144]. Significant loss of *VDR* at tissue level together with the loss of *CYP27A1* could partially attribute to the exacerbation of inflammation during GvHD.

Next, the correlation between *CYP27A1* and *VDR* was calculated. To our surprise we observed a strong correlation between *CYP27A1* and *VDR* expression with p value <0.001 and a correlation coefficient of 0.654 in 118 patients samples as shown in Figure 5.20 (A). When this correlation was further analyzed in terms of transplant related mortality (TRM), once again, loss of both *CYP27A1* and *VDR* was found to be strongly correlated with TRM with a p value <0.001 and a

correlation coefficient of 0.647 in 112 patients as shown in Figure 5.20 (B). Taken together these data strongly reveal a sequential loss of vitamin D metabolism and processing that could lead to altered immunoregualtion which subsequently leads to severe inflammation in GvHD. This result could also partially explain the previously reported fact that transplanted patients depict low level of vitamin D in the serum[145] that could possibly be accounted for the loss of *CYP27A1* and *VDR*.
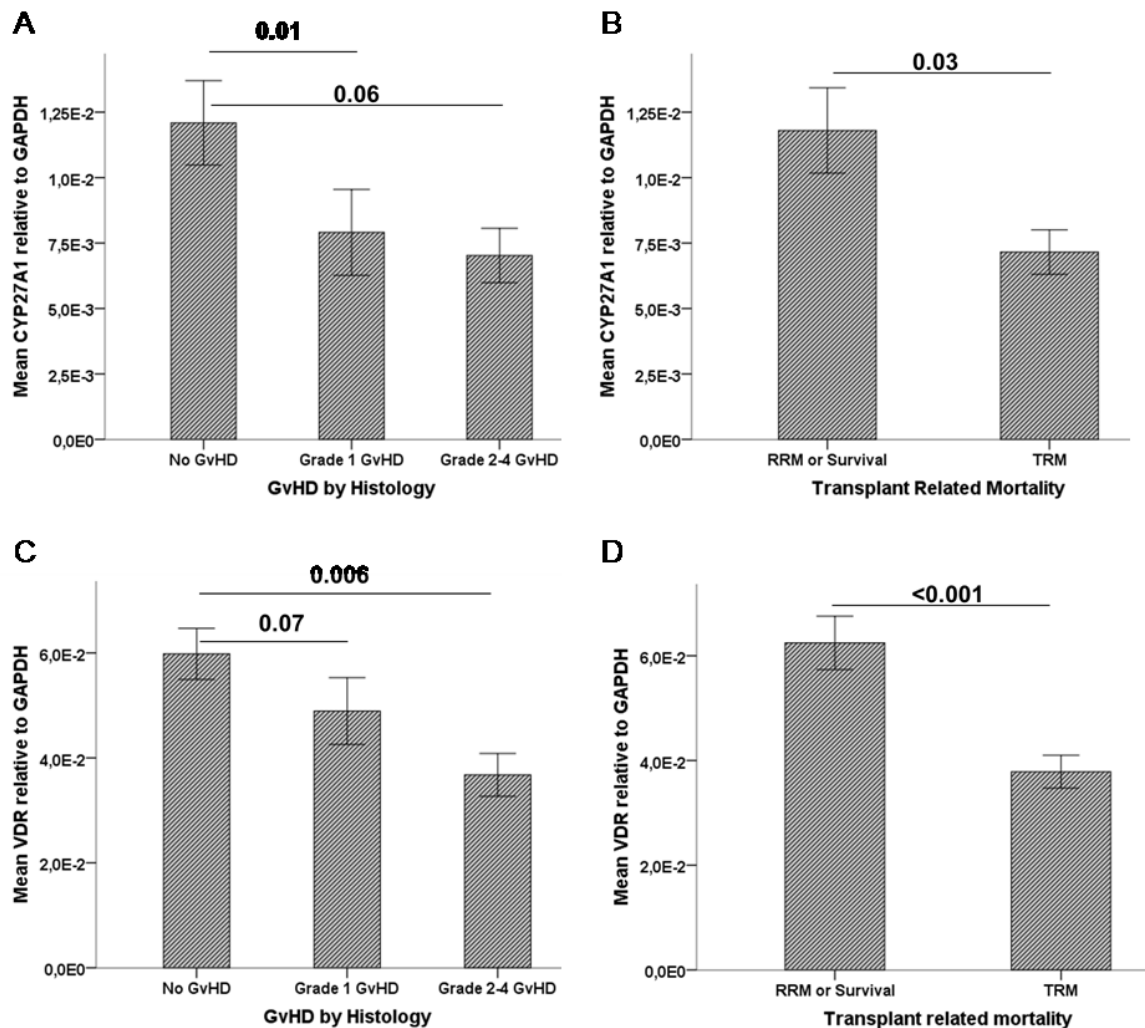
Figure 5.19: Alteration of *CYP27A1* and *VDR* gene expression during acute GI-GvHD.
A. *CYP27A1* significantly downregulates during aGI-GvHD when compared to non GvHD patients. C.There is significant loss of *VDR* mRNA during GI-GvHD when compared to non GvHD patients. N=118 (No GvHD=57 patients, Grade 1 GvHD=38 patients, Grade 2-4 GvHD=23 patients). B. Loss of *CYP27A1* is significantly associated with transplant related mortality. D. Loss of *VDR* is significantly associated with transplant related mortality. N= 115 (RRM=64 patients, TRM=51 patients).). Data were non-normally distributed therefore non-parametric Kruskal-Wallis and Mann-Whitney test was performed to calculate p

values. Bar represents ± s.e.m. RRM=Relapse Related Mortality; TRM=Transplant Related Mortality; *VDR*=Vitamin D Receptor.
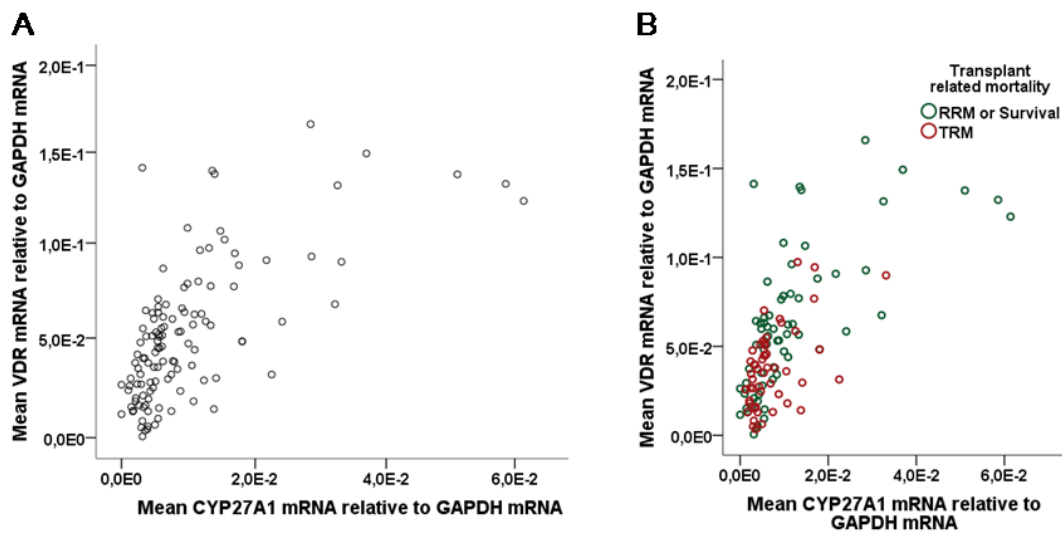
Figure 5.20: *CYP27A1* mRNA correlates with *VDR* mRNA and TRM occurs more frequently in patients with low *CYP27A1/VDR* expression.
A. Scatter plot diagram of *CYP27A1* mRNA and *VDR* mRNA with the correlation coefficient of 0.654 and p value <0.001. N=118 patients. B. Green circles represent patients with Relapse Related Mortality (RRM) or survival. Red circles represent patients with Transplant related mortality(TRM). Patients with reduced *CYP27A1/VDR* expression exhibited frequent TRM with the correlation coefficient of 0.647 and p value <0.001 when data were controlled for TRM. N=112 patients. Data were non-normally distributed therefore non-parametric Mann-Whitney test was performed to calculate p values. Data represents ± s.e.m.
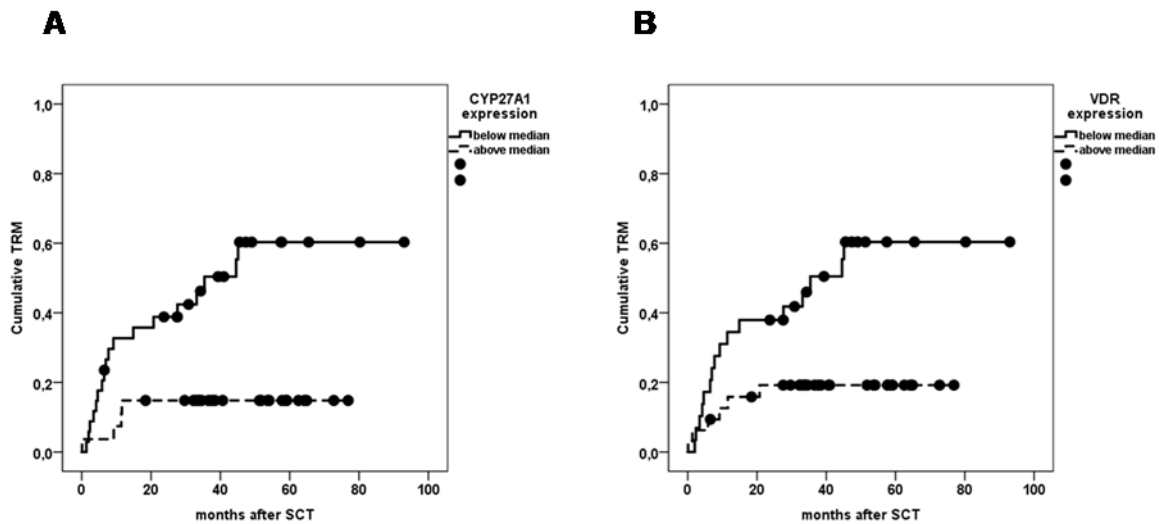
Figure 5.21: Survival curve in relation to median *CYP27A1* and *VDR* mRNA expression.
A: Cumulative TRM in patients with low expression of *CYP27A1* significantly increases (p log rank= 0.002) when compared with patients with high *CYP27A1* expression. B: Cumulative TRM in patients with low expression of *VDR* significantly increases (p log rank= 0.008) when compared with patients with high *VDR* expression. N= 63 patients.

Next, patients were further classified into either low or high *CYP27A1* and *VDR* based on their mRNA expression. Absolute median values of *CYP27A1* and *VDR* expression were calculated and the patients were divided into 'below median' and 'above median' group. Kaplan-Meier estimates for TRM are shown in Figure 5.21. Patients with less *CYP27A1* mRNA showed significantly higher frequency of TRM than the patients with more *CYP27A1* mRNA expression. Furthermore, a significant reduction of TRM was observed with a higher expression of *VDR* mRNA (p=0.001). These results collectively suggest that the vitamin D receptor along with the vitamin D related enzyme Cyp27a1 are lost during GvHD and that this possibly leads to a compromised immunosuppression.

Cyp27b1 is another vitamin D related enzyme that are involved in synthesis of active form of Vitamin D[146]. Although there was no difference in *CYP27B1* mRNA expression when compared in GvHD vs. no GvHD patients, this gene was found to be significantly altered when patients were divided into no GvHD, grade 1 GvHD and grade 2-4 GvHD groups. While *VDR* and *CYP27A1* were downregulated in GvHD, we found that *CYP27B1* significantly upregulates during acute GI-GVD and the mortality due to transplant occurs frequently in patients

with high expression of *CYP27B1* mRNA as shown in Figure 5.22. While the function of *CYP27B1* in GI tract is least studied, it has been previously documented that in skin, when microbial pathogens bypass the damaged epidermal barrier and are recognized by TLRs, *CYP27B1* is upregulated[147]. Furthermore, reports shows that *CYP27B1* increase in response to injury and TLR activation[148] suggesting the involvement of *CYP27B1* in inflammatory reactions. These findings may explain that *CYP27B1* expression in the GI tract is an indicator of inflammation which increases in GI-GvHD.

Figure 5.22: Alteration of *CYP27B1* gene expression during acute GI-GvHD.
A. CYP27B1 significantly upregulates during severe aGI-GvHD when compared to non GvHD or mild GvHD patients. N=118 (No GvHD=57 patients, Grade 1 GvHD=38 patients, Grade 2-4 GvHD=23 patients). B. Gain of CYP27B1 is significantly associated with transplant related mortality. N= 115 (RRM=64 patients, TRM=51 patients). Data were non-normally distributed therefore non-parametric Kruskal-Wallis and Mann-Whitney test was performed to calculate p values. Bar represents ± s.e.m. RRM=Relapse Related Mortality; TRM=Transplant Related Mortality.

In addition of Vitamin D related genes, there was one more gene that was significantly altered in aGI-GvHD: Pregnane Xenobiotic Receptor (*PXR*). PXR is a nuclear hormone receptor that senses xenobiotic compounds and metabolize these compounds to avoid immune mediated inflammation[149]. PXR is well-known receptor for Rifaximin. It has been shown that rifaximin activates PXR that leads to maintenance of intestinal immune homeostasis[149]. Inhibition of NF-kB pathway is well accepted mechanism of PXR mediated immune suppression[150].

In a cohort of 118 patients, *PXR* mRNA expression in the GI-tract of ASCT patients revealed a significant downregulation especially in patients who are severely affected by GvHD as shown in Figure 5.23 (A). This result partly explains the clinical fact that severe GvHD patients do not respond to rifaximin medication which could be due to the loss of responsive receptor. Furthermore, patients who died due to transplantation exhibited relatively low *PXR* expression which is nearly significant when compared to relapse related mortality (RRM) or surviving patients as shown in Figure 5.23 (B)
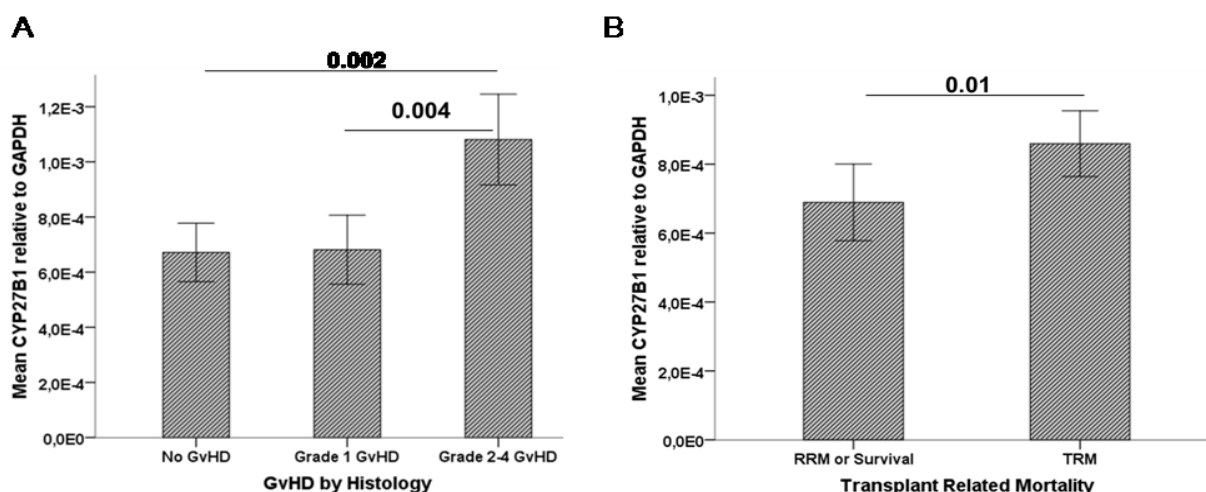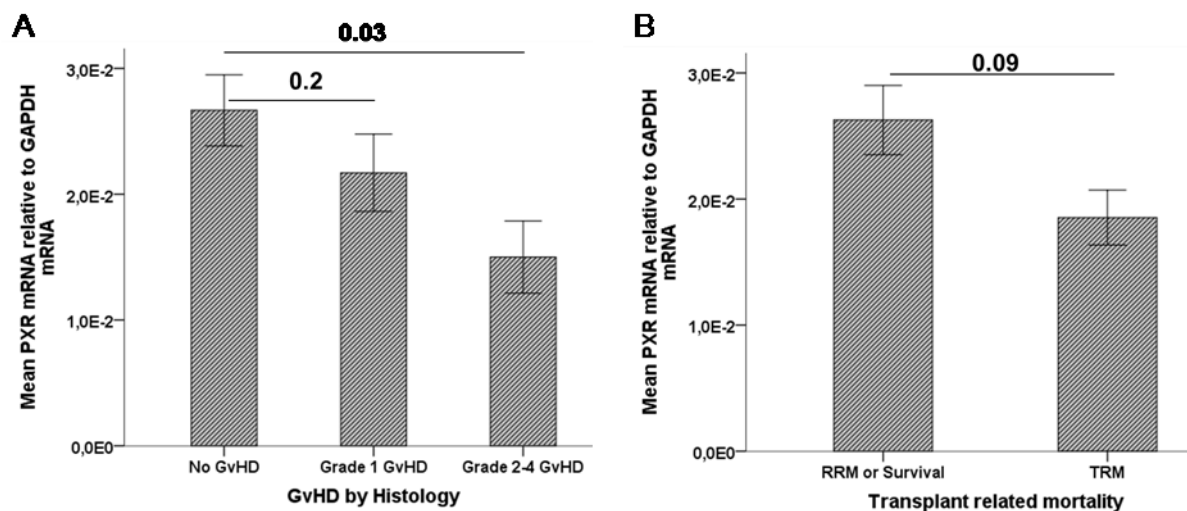

Figure 5.23: Alteration of *PXR* gene expression during acute GI-GvHD.
A. *PXR* significantly downregulates during severe aGI-GvHD when compared to non GvHD patients. N=118 (No GvHD=57 patients, Grade 1 GvHD=38 patients, Grade 2-4 GvHD=23 patients). B. Loss of *PXR* is associated with transplant related mortality and is nearly significant. N= 115 (RRM=64 patients, TRM=51 patients). Data were non-normally distributed therefore non-parametric Kruskal-Wallis or Mann-Whitney test was performed to calculate p values. Bar represents ± s.e.m. RRM=Relapse Related Mortality; TRM=Transplant Related Mortality

Next, we investigated the expression of *PXR* (rifaximin receptor) in relation to the type of gut decontamination regime used for transplanted patients. Patients were given either rifaximin (44 patients) or the combination of ciprofloxacin and metronidazole (74 patients). Although not significant, we observed an upregulation of *PXR* mRNA expression in patients treated with rifaximin when compared to patients treated with Cipro/metro as shown in Figure 5.24. This suggests a partial role of rifamixin in upregulating *PXR* at mRNA level. The reason why this upregulation is not significant can be attributed to several other factors such as loss of i) Paneth cells[151], ii) loss of protective IL-17, iii) alteration of vitamin D related gene, iv) overall loss of *PXR* itself.
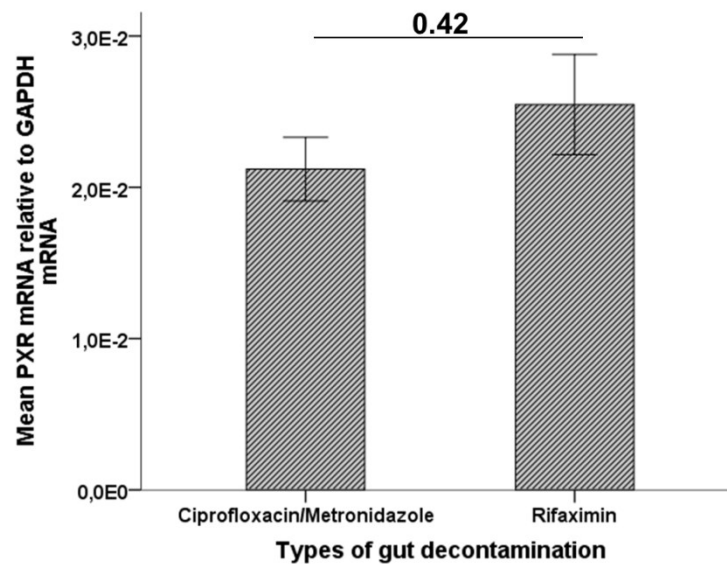
Figure 5.24: Alteration of *PXR* gene expression after transplantation in response to types of gut decontimation.
PXR mRNA depicts trend of upregulation when patients have rifaximin (44 patients) for gut decontamination compared to patients with ciprofloxacin/metronidazole (74 patients). N=118. Data were non-normally distributed therefore non- mean parametric Mann-Whitney test was performed to calculate p value. Bar represents ± s.e.m.

5.3 Immunomodulatory effects of bacterial metabolite Indoxyl 3-sulfate (I3S): implications for GvHD

Maintained bacterial diversity is crucial for balanced immune system and normal immune function. Bacterias act on immune and non-immune cells by producing bacterial metabolites. The interplay between microbiome and immune system have gained significant attention in recent years partially due to the fact that the immune related diseases were the consequences of loss of microbial diversity in gut[112,113,152]. As such, alteration of gut microbiome is associated with autoimmune diseases, obesity[153], cardiovascular disease[154], and inflammatory bowel disease[152].

Indole derivatives such as indole-3-carbinol (I3C) and indirubin-3'-oxime (IO) exhibit immunosuppressive and anti-inflammatory effect on bone marrow derived DCs in mice[155]. A recent study reported that the decrease in urinary Indoxyl 3-sulfate (I3S), an indole derivative, was associated with disrupted microbiome and poor outcome early after allogenic stem cell transplantation (ASCT) and that abundance of clostridia species such as Lachnospiraceae and Ruminococcaceae) were associated with high urinary I3S[113]. To analyze immunomodulatory effect of I3S, dendritic cells were cultured and treated with I3S as described in method section 4.5.3. Cell viability, DC surface marker and cytokine production, mRNA expression was analyzed. DCs were cocultured with allogenic T cells and thus cytokine production by T cells was followed.

5.3.1 I3S does not induce apoptosis in monocyte derived DCs

Since the effect of I3S has not yet been evaluated on human dendritic cells and the body of literatures have shown the cytotoxic effect of I3S, the extent of apoptosis and necrosis was initially examined in monocyte derived mature dendritic cells (mDCs). Immature DCs on day 5 were stimulated with LPS and simultaneously treated with varying concentration of I3S (1, 10,100, 500 and 1000 µM). There was no observable difference in apoptotic cells in any concentration of I3S when compared to untreated control mature DCs (Figure 5.25). Similar effect was observed when I3S was added to the cells on day 0 (data not shown). 1-10

µM of I3S is present in healthy individuals with normal kidney function. Since 100 µM and above I3S concentration represents physiologically toxic concentration for various other cell types including epithelial and endothelial cells, this study limited the I3S concentration up to 100µM.
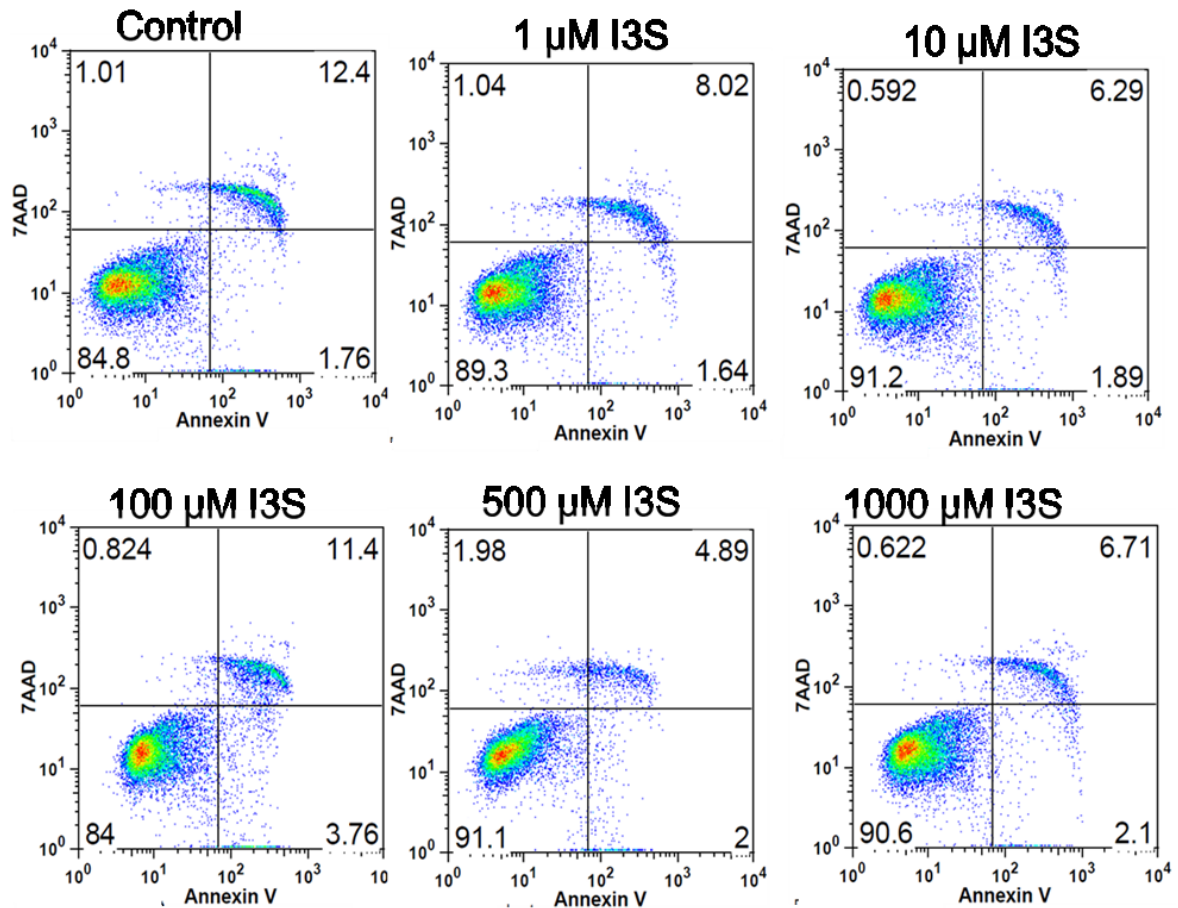
Figure 5.25: Apoptosis measurement of LPS stimulated mature DCs by Annexin V/7AAD staining.
Immature DCs were stimulated with 100 ng/ml LPS +/- I3S for 48 hours. Viability was determined by Annexin V/7-AAD staining Control DCs were not treated with I3S. Live cells (represented in lower left quadrant) remained unchanged in I3S treated DCs when compared to I3S untreated control DCs.

5.3.2   I3S does not alter survival of mature DCs

I3S did not seem to affect both survival and viability of mature DCs. Although at 10μM DC growth seems to slightly increase (Figure 5.26 A), it is however not significant and, in addition, the viability tends to remain unaltered independent of I3S concentration (Figure 5.26 B). Therefore the concentration of 1μM, 10μM and 100 μM were chosen for the subsequent experiments.
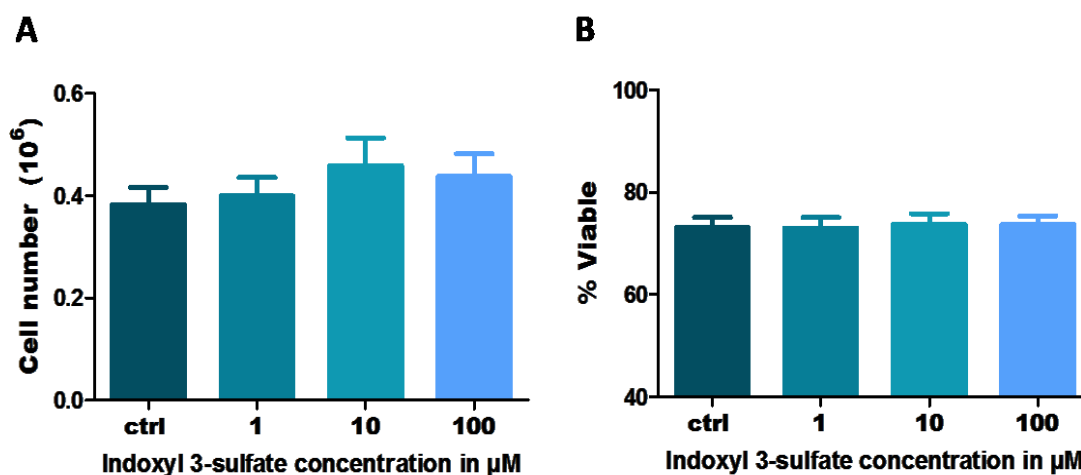
Figure 5.26: Effect of I3S on survival of human monocyte-derived mature DCs.
Immature DCs were stimulated with 100 ng/ml LPS +/- I3S for 48 hours. A. Cell counting was performed by means of a cell analyzer (CASY). B. Percentage of viable cells were determined by CASY. Bar represents mean + s.e.m of n=10 individual donors.

5.3.3   I3S alters LPS-induced changes in surface marker expression of mature DCs

DCs are crucial in stimulating T cell and mounting appropriate immune responses to pathogens and inflammation. The effects of I3S on expression of several surface markers that are responsible for T cell stimulation was examined (Figure 5.27). Due to the donor dependent variation in expression of protein, control DC was calculated as 100% expression of protein and I3S treated DCs were analyzed with respect to control. When I3S was added on day 5, and DCs were

exposed to I3S for 48 hours only, CD80 and CD86 were strongly downregulated while CD1a, CD83 and HLA-DR remained unaffected (Figure 5.27).
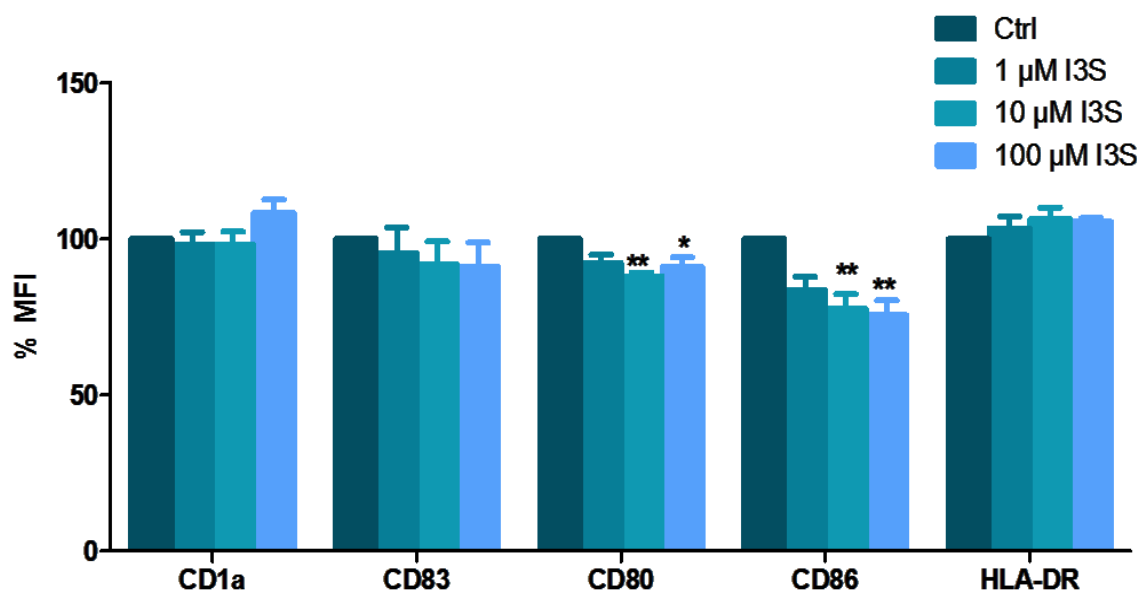
Figure 5.27: Impact of I3S on surface marker expression of human monocyte-derived DCs.
Graphical representation of CD1a, CD83, CD80, CD86 and HLA-DR expression on mDCs with or without I3S. Bars show the mean + s.e.m of n=8 individual donors for CD1a, CD83 and CD86 and n=7 individual donors for CD80 and HLA-DR. *$p < 0.05$, **$p < 0.01$, * show significant differences between control and treatment (Kruskal Wallis and post-hoc by Dunn's Multiple Comparison Test).

5.3.4   I3S alters LPS-induced pro-inflammatory and anti-inflammatory cytokines in monocyte derived mature DCs

The effects of I3S on pro-inflammatory and anti-inflammatory cytokine production following LPS activation in monocyte derived mDCs were assessed. 100 ng/ml LPS induced production of pro-inflammatory cytokines such as IL-12 and IL-6. Monocyte derived mDCs exposed to varying concentration of I3S and simultaneously stimulated with LPS produced lower levels of pro-inflammatory cytokines (Figure 5.28). IL-12 and IL-6 were significantly downregulated in presence of I3S, whereas an anti-inflammatory cytokine IL-10 was significantly upregulated (Figure 5.28). I3S treatment to DCs on day 0 gave similar results (data not shown). Taken together, these results suggest that bacterial metabolite I3S is able to suppress the inflammatory response of LPS-stimulated DCs by inhibiting the pro-inflammatory mediators thereby promoting an anti-inflammatory mediator.
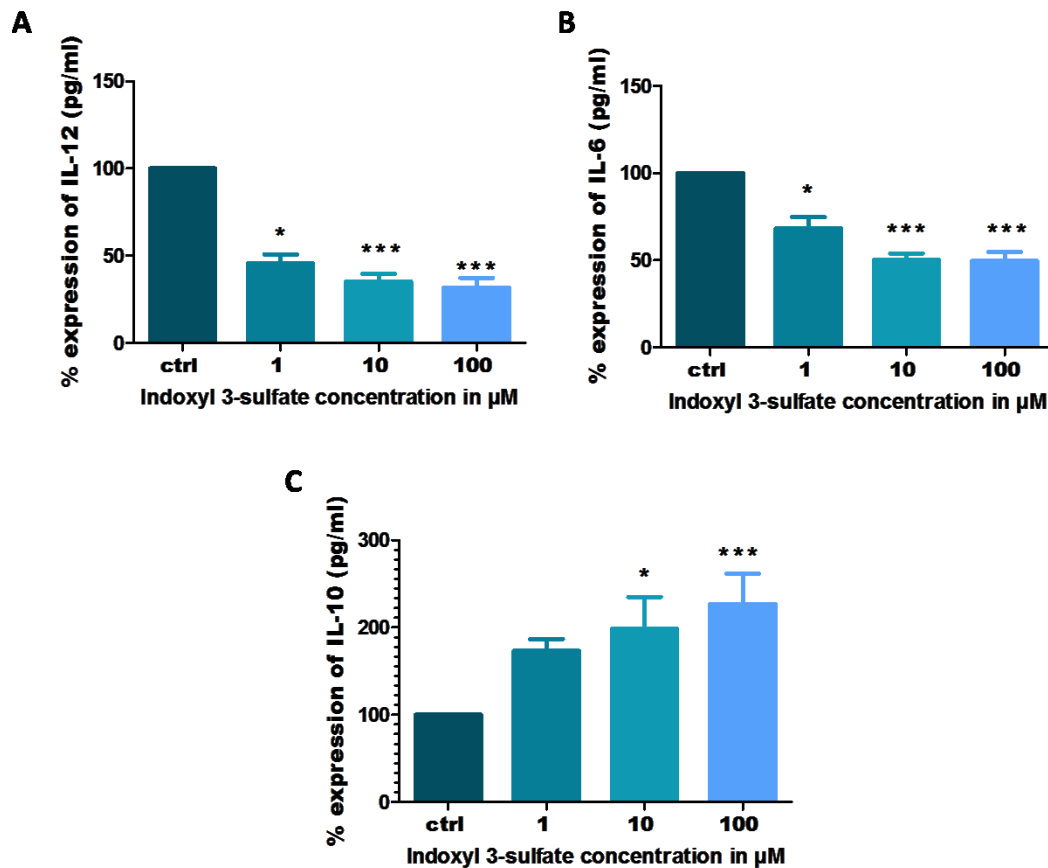
Figure 5.28: Downregulation of LPS-induced pro-inflammatory cytokines and upregulation of anti-inflammatory cytokine by I3S treated mature DCs. Cytokine release in the cell supernatant of mDCs was accessed by ELISA for IL-12 (A), IL-6 (B) and IL-10 (C). Results are representative of eight individual healthy donors with n=8. Bars show the mean + s.e.m of n=10 individual donors for A & B, and n=7 individual donors for C. . *p<0.05, ***p<0.001, * show significant differences between control and treatment (Kruskal Wallis and post-hoc by Dunn's Multiple Comparison Test).

5.3.5 I3S alters IL-12 pathway to mediate anti-inflammatory and immunoregulatory effect by mDCs

To analyze if the IL-12 alteration takes place at the transcriptional level or not, iDCs on day 5 were stimulated with LPS and treated with I3S for 4 hours. DCs were collected and RNA was extracted from the cells. Two step RT-qPCR was performed for *IL-12A, IL-12B* and *AHR* mRNA. Immature DCs which were not treated with either LPS or I3S did not express IL-12 gene. DCs stimulated with LPS expressed both *IL-12A* and *IL-12B*. In presence of I3S IL-12A and IL-12B showed strong trend of downregulation (Figure 5.29 A&B) which is in parallel with

reduction of IL-12 cytokine production. To our surprise, the receptor that binds to I3S, aryl hydrocarbon receptor (AhR), remained utterly unaltered (Figure 5.29 C) suggesting that the immunomodulation of DCs by I3S might not be attributed to AhR. In addition, ikB protein was analyzed by western blot. DCs were stimulated on day 5 with LPS and treated with I3S for five minutes. Phospho-protein was collected and ran through SDS-PAGE. Western blot showed that LPS unstimulated iDCs are able to express ikB and that the short term LPS stimulation downregulates ikBß expression as shown in Figure 5.30. When DCs were treated with I3S, ikB was partially restored with 10 µM I3S when compared to LPS stimulated iDCs (Figure 5.30). Taken together, these results suggest that the indole derivate Indoxyl 3-sulfate uses IL-12 pathway and NF-kB pathway to suppress inflammation.
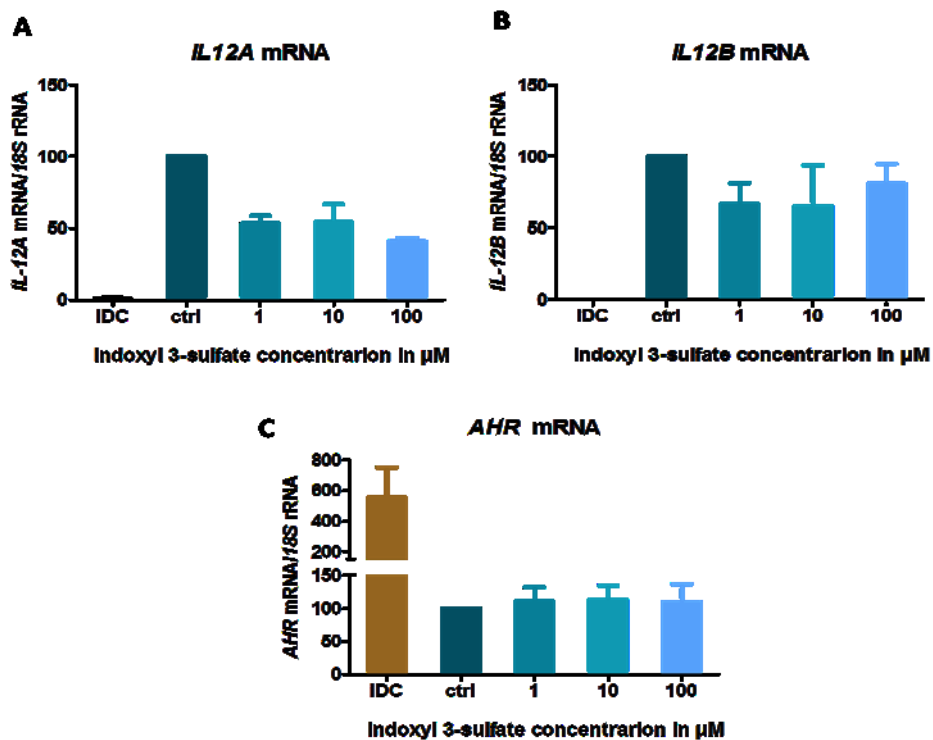
Figure 5.29: I3S mediates immunosuppression by altering IL-12 pathway but not AhR pathway.
Monocyte derived immature DCs on day 5 were stimulated with 100 ng/ml LPS and varying concentration of I3S for 4 hours. Cells were collected lysed and IL-12 trancription was evaluated by RT-qPCR for IL-12A (A), IL-12B (B) and AhR (C). mRNA expression was normalized to *18S* rRNA expression. Bar represents mean +s.e.m of n=3 individual donors.
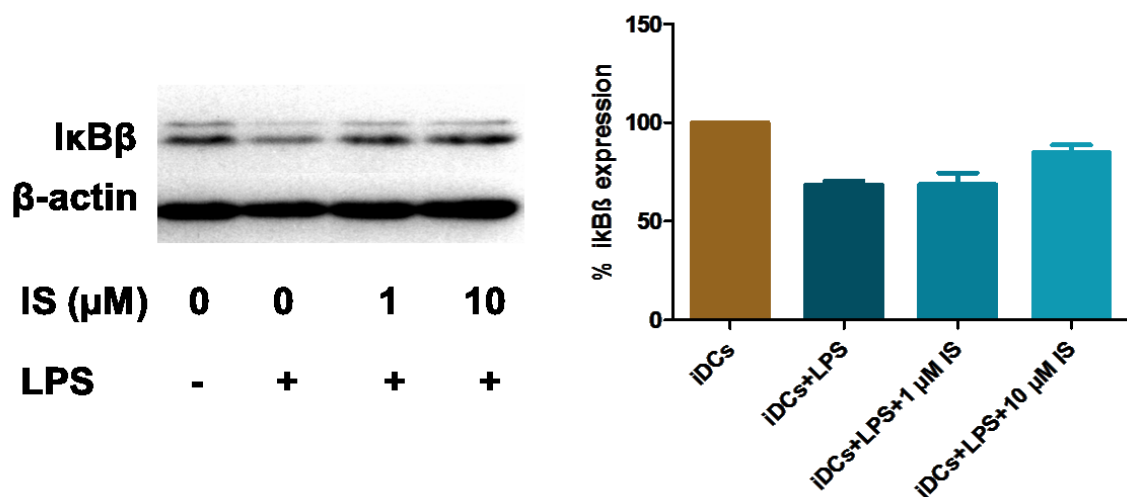
Figure 5.30: Effect of I3S on iKB expression.
Immature DCs were stimulated with LPS, treated with I3S for 5 minutes. Protein lysates were collected and western blot was performed to access expression of ikBß. Representative blot is shown on left and densitometric anaylsis is shown on right. Bars show the mean + s.e.m of n=3 individual donors.

5.3.6   I3S treated monocyte derived mDCs suppress the proliferation and cytokine production of antigen-specific T cells.

To investigate if the alteration of surface marker and cytokine production by DCs also alters T cell proliferation, DCs and T cells from different donors (to ensure allogenic reaction) were co-cultured in the ratio 1:10 in mixed lymphocyte reactions, T cell proliferation was monitored on day 6. DCs were previously treated with I3S on day 5. Lymphocytes did not proliferate in absence of DCs (Figure 5.31 A). When lymphocytes were grown with I3S treated DCs, lymphocytes proliferated less as compared to the lymphocytes that are grown with control DCs (only LPS stimulation, no I3S treatment) Figure 5.31 A). Cytokines produced by DC stimulated lymphocytes were assessed by ELISA. As shown in Figure 5.31 B, C&D, lymphocytes produced significantly lower amount of IFN-y and TNF while IL-10 showed trend of downregulation when stimulated with I3S treated DCs as compared to I3S untreated control DCs. Unstimulated lymphocytes were not able to produce cytokines (Figure 5.31 B, C& D). Similar results were obtained when lymphocytes were stimulated with DCs that were

previously treated with I3S on day 0 (data not shown). Taken together, these results suggest that I3S not only modulates dendritic cell function but also indirectly modulates the T cell function at cytokine level.
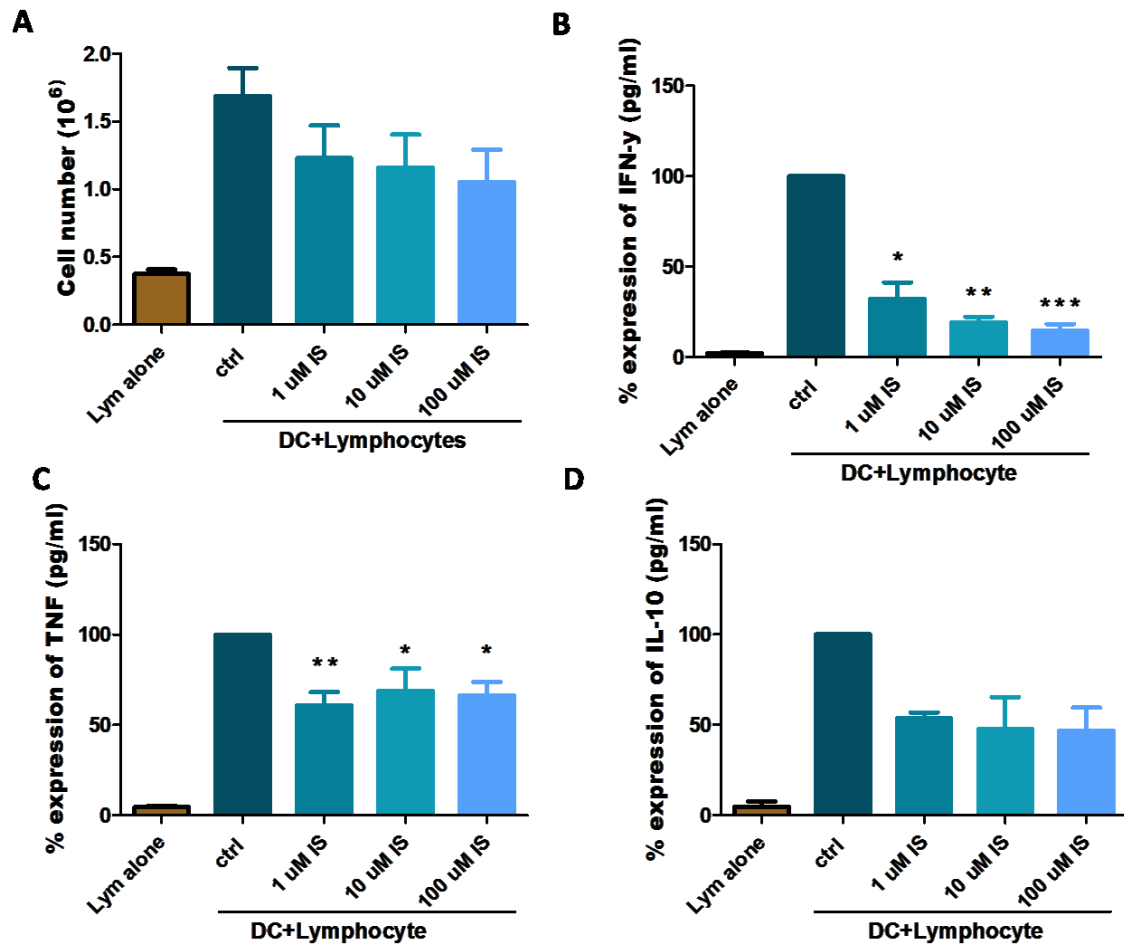
Figure 5.31: Co-culture of I3S treated mDCs with allogeneic T cells.
DCs treated with/without I3S were cocultlured with allogenic T cells at 1:10 ratio. A. Proliferated T cells were counted on day 6 by means of CASY for n= 8 MLR settings. B, C&D. T cell mediated cytokines were accessed on day 5 by means of ELISA for IFN (n=8), TNF (n=8), and IL-10 (n=3) respectively. Bars show the mean + s.e.m. *p<0.05, **p<0.01, ***p<0.001, * show significant differences between control and treatment (Kruskal Wallis and post-hoc by Dunn's Multiple Comparison Test).

6 Discussion and conclusion

6.1   Immune cell infiltrates during acute GI-GvHD

The mucosa of gastro intestinal tract is unique among tissues in that it is in continuous contact with super dynamic microbial community and is populated by heterogeneous composition of immune cells which have crucial function in protection and immune homeostasis[156]. The major form of adaptive immunity in the gut is humoral immunity via B cells and cell mediated immunity via T cells[2]. T cells are found within the gut epithelial layer, spread throughout the lamina propria and submucosa, and within peyer's patches. In GI tract, different subsets of effector CD4^{+} T cells are induced by and protect against different microbial species. The helper CD4^{+} T cells secret different cytokines that are specialized for particular types of antimicrobial responses[2]. In humans most the the intraepitheilal T cells are CD8^{+} T cells which are responsible for direct cytolysis of foreign organisms or cells with altered antigen expression. The reason for CD8^{+} T cell abundance can be attributed to the fact that GI tract is continuously exposed to antigens and that more CD8^{+} T cells are required to keep control of invasion of harmful organisms. It is well accepted that mature donor T lymphocytes present in stem cell inoculum during stem cell transplantation is the major cause of graft vs host disease but at the same time these T cells promote hematopoietic engraftment, reconstitute T cell immunity and mediate potent beneficial anti-tumor effect i.e. graft vs leukemia effect[157].

6.1.1   Infiltration of CD4^{+} T cells and CD8^{+} T cells during acute GI GvHD

Both CD4^{+} and CD8^{+} T cells have critical roles in the pathogenesis of GvHD. Of note, GvHD is the result of naïve T cell response and that memory T cells do not include GvHD[158,159]. The pathogenicity of helper T cells has been attributed to CD4^{+} T cell subsets like Th1, Th2 and Th17 that act via proinflammatory cytokines production. The pathogenicity of CD8^{+} T cells has widely been attributed to perforin and granzyme pathway[160].

Infiltration of CD4^{+} T cells was analyzed in 199 patients after stem cell transplantation by applying single antibody immunohistochemistry. No significant difference existed between GvHD and non GvHD patients in terms of CD4^{+} T cells infiltration but we found that the CD4^{+} T cells expression was highly correlated with apoptosis of epithelial cells and infiltration of CD8^{+} T cells. In one study, Landfired et al. reported in cohort of 64 transplanted patients that the infiltration of CD4^{+} T cells (as well as neutrophils) significantly reduced in NOD2/CARD15 SNP patients when compared to wildtype recipient[161]. In another study, Holler and co-workers elegantly demonstrated that NOD2/CARD15 polymorphism associated with GvHD and overall survival after ASCT[162,163]. Therefore it can be well noted that NOD2 polymorphism and reduction of CD4^{+} T cells infiltrates is associated with GvHD. We however did not see significant change in overall CD4^{+} T cell infiltrates according to GvHD grades but the correlation of CD4^{+} T cell infiltrates with CD8^{+} T cells and epithelial apoptosis clearly suggest indirect participation of CD4^{+} T cells in exacerbation of GvHD preferentially via FasL/TNF dependent mechanisms or by helping CD8^{+} T cells. Furthermore, it can also be hypothesised that the majority of CD4^{+} T cells could be effector or memory T cells that is known to participate in GVL effect but not GvHD which could possibly explain why there is no difference in CD4^{+} T cells infiltrates during GvHD but strong correlation exists with CD8^{+} T cells and apoptosis of epithelial cells in the gut.

When CD8^{+} T cells were analyzed in 197 transplanted patient's gut biopsies, there was a significant increase of these cytotoxic T cells along with exacerbation of GvHD. In addition, CD8^{+} T cells infiltrates were significantly correlated with infiltration of CD4^{+} T cells, loss of crypts in gut and the apoptosis of epithelial cells in gut. This suggests i) strong interaction of CD4^{+} T cells and CD8^{+} T cells in gut; ii) strong cytolytic activity of CD8^{+} T cells in destruction of crypts (Paneth cells) and epithelial cells of gut. Therefore, increase in CD8^{+} T cells could indicate strong inflammation rendering crypt and epithelial destruction. As a matter of fact infiltration of CD8^{+} T cell is a well established hallmark of GvHD, therefore our result confirms CD8^{+} T cell mediated cytotoxicity in the gut of large number of patients after stem cell transplantation.

6.1.2 Infiltration of Foxp3^{+} and IDO^{+} cells during acute GI GvHD

As clear as it is that GvHD is caused by uncontrolled T cell mediated inflammation, it is unambiguously known that Foxp3^{+} regulatory T cells are responsible for subsiding uncontrolled T cell response thus mantianing self-tolerance[42]. For the first time in the science of stem cell transplantation, we showed the status of Tregs infiltrates in 199 gut biopsies of transplanted patient by performing Foxp3 immunohistochemistry and found that Tregs significantly increases during GvHD. Body of literatures demonstrated loss of Tregs frequency subsequent to GvHD[59,164-167]. Our result is in contrast with existing literatures and hypothesis that extreme GvHD is partly due to loss of Tregs leading to compromised regulation in the inflammatory milieu. We observed increase of Foxp3 protein in the gut of ASCT patients. This result was further supported by the increase of FOXP3 at mRNA level as well and the strong correlation of Foxp3 at protein and mRNA level. One main reason for these differences in our data and previous data is that most of the previous studies evaluated Tregs in peripheral blood. Our study is entirely focused on the intestinal tissue which is the major organ to be damaged in acute GI GvHD. We observed that infiltration of Tregs were significantly higher in patients who showed histological and clinical signs of GvHD. To our knowledge, there are only three reports till now on Foxp3 expression on intestinal tissue[59-61]. Two of these studies[60,61] reported that Foxp3 increases during GvHD and are in harmony with our observation. It can be speculated that the increase in Foxp3^{+} cells in response to inflammation is a counter regulatory mechanism of T cells to subside inflammation during GvHD. It could also reflect a greater degree of systemic T cell activation in this population. Another possible explanation would be the exhaustion of Tregs. Given that the GI tract is a secondary lymphoid organ where immune cells can differentiate de novo based on environmental cues, we can speculate that these Tregs are rather induced de novo in response to pronounced inflammation. Unfortunately, natural and induced Tregs could not be individualized in this study due the lack of marker/s that differentiates natural and induced Tregs.

Next, we were interested to find out the cellular source of Foxp3. For this, single immunofluorescence for Foxp3, CD4 and CD8 was individually established. Double immunofluorescence was performed for CD4 and Foxp3 together. It was

observed that the huge proportion (90%) of Foxp3^{+} cells were CD4 positive. When these double positive cells were analyzed on 22 patients, CD4^{+}Foxp3^{+} double positive cells were upregulated in GvHD and were almost significant supporting immunohistochemistry result of Foxp3 expression. To our surprise, CD4 negative Foxp3^{+} cells were detected insinuating the existence of new population of Foxp3^{+} cells that are not of CD4 origin. When double immunofluorescence was performed for CD8 and Foxp3 together, we found CD8 positive Foxp3^{+} cells that showed increasing trend with the exacerbation of GvHD. CD8^{+}Foxp3^{+} Tregs has been previously described in literatures and found to be capable of supressing T cell responses in experimental model of autoimmunity of allergen exposure[56,168]. In terms of GvHD, Beres and co-workers demonstrated that the suppressive population of CD8^{+} Foxp3^{+} Tregs are induced early during GvHD in mice model. Analysis of these Tregs population are highly missing in clinical spectrum of GvHD however Zheng and colleagues recently reported that human CD8^{+}Foxp3^{+} T cells that were induced *in vitro* were able to supress GvHD in a humanized mouse model[169]. Therefore it can be noted that human CD8^{+} Foxp3^{+} Tregs might have suppressive ability in clinic. In our study, although CD8^{+} Foxp3^{+} Tregs were only up to 10% compared to total Foxp3^{+} Tregs, this small population might have serious contribution in amelioration of GvHD. Furthermore, induction of CD8^{+} Foxp3^{+} Tregs was observed only after grade 2 GvHD with huge variation in cells per HPF due to steroid treatment. Patients who received more than 20 mg/kg of steroids depicted less CD8^{+} Foxp3^{+} Tregs than the paitents who received 0-20 mg/kg steroids per day (data not shown). This suggests that protective CD8^{+} Foxp3^{+} Tregs are compromised in patients who receive high dose steroids and are susceptible to GvHD related death. Similarly, lesser CD4^{+} Foxp3^{+} Tregs were observed in grade 2-4 patients receiving high dose steroids (data not shown). These findings provide preliminary evidence that silencing the immune system by steroids has adversary effect on protective Tregs population in GvHD patients.

Next, indoleamine-2,3 deoxygenase (IDO) was analyzed by single antibody immunohistochemistry in gut of 193 patients after stem cell transplantation. We observed significant upregulation of IDO with increasing GvHD. Increase in IDO at protein level is supported by significant increase of IDO mRNA (n=190) at

transcriptional level and a significant correlation of between IDO protein and mRNA expression. Increased IDO production during GvHD related inflammation may reflect a reactive release of immunosuppressive mediators which is perhaps initiated to balance immune reactions. Significant correlation between IDO expression and Foxp3 expression both at protein and mRNA level indicates that immunosuppressive IDO might have favoured Foxp3 expression as IDO is well-known to induce peripheral tolerance by increasing Tregs[80,81]. IDO catabolizes essential amino acid tryptophan into kynurenine, an agonist for Aryl Hydrocarbon Receptor (AHR). AHR is necessary for generating Tregs[67]. As AHR is an agonist for several bacterial metabolites including indole and their derivatives, it may turn out well to state that the balanced bacterial diversity is required for toleregenic Tregs generation.

Of note, infiltration of neutrophils highly correlated with Foxp3 and IDO expression in this study. Neutrophils are known to interefere with T-cell proliferation as neutrophilic myeloid-derived suppressor cells (MDSCs)[170]. Recently, Pillay and colleagues reported that the subset of mature human neutrophils that can be systematically induced in response to acute inflammation are able to suppress T cell function[171]. Experimental models have demonstrated that the prolonged antibiotic treatment leads to reduced neutrophil number[172] and a severe neutropenia occurs in germ-free animals [173] suggesting a close link between microbiota and neutrophils. Recent evidence suggests that the bacterial metabolites such as SCFAs regulate neutrophil-mediated inflammation through GPR43 expression at high levels by neutrophils[174]. In this light, we can hypothesize that the neutrophilic MDCSs are highly regulated by intact microbome. MDSCs not only suppress T cell activity but also stimulate Tregs[175]. In one recent observation by Jitschin and colleagues, monocytic MDSCs were able to suppress T cells and induce Tregs presumably via increased IDO activity[176]. Taking into account that we observed strong correlation between neutrophils, Foxp3$^+$ cells, and IDO$^+$ cells, it can be hypothesized that MDSCs infiltrate to the site of acute inflammation during GvHD trying to subside T cell mediated inflammation by enhancing IDO and Tregs, and could be potential target in GvHD treatment.

6.1.3 Infiltration of IL-17^{+} cells during acute GI GvHD

IL-17 received considerable attention in past few years when several literatures reported inflammatory response of IL-17 in GvHD mice model[102,103]. Contrary to the belief that IL-17 increases and possess severe inflammation during GvHD, we found significant downregulation of IL-17 protein when IHC was performed on gut samples of 197 transplanted patients. Furthermore, at mRNA level, the transcription factor of IL-17- *RORC*, also significantly downregulated along with increasing GvHD in 197 patients. We reported that GvHD is attributed to loss of IL-17. In addition, IL-17 protein and *RORC* mRNA significantly correlated with each other and that the transplant related mortalityoccured more frequently in the patients expressing low IL-17 and low *RORC*. Our observations do not obey the dogmatic belief that IL-17 contributes to GvHD. Our findings suggest that IL-17 cells are diminished in GvHD and their loss contributes to higher GvHD and greater transplant related mortality. This is a first report to demonstrate loss of IL-17 in patient's gut biopsies in a large number of patients. However, a possible solution of the obvious discrepancy might be IL17 production by non-T cell populations.

We therefore exploited double immunofluorescence on colon biopsies to find out cellular source of IL-17 cells. For this 39 samples were analyzed for IL-17^{+}CD4^{+} double staining. Surprisingly, no double positive cells were observed. All the IL-17^{+} cells identified in the colon were CD4 negative. This is the first clinical evidence to state that IL-17 production in colon is not mediated by Th17. It is known that gamma-delta T cells[177] and invariant natural killer T cells[178] are other major source of IL-17 production. To clarify if IL-17 belongs to other T cell types, we again exploited double immunofluorescence of IL-17^{+}CD3^{+} and analyzed 39 heterogeneous colon samples. Again to our surprise, IL-17 signal did not colocalize with CD3 signal providing first clinical evidence that IL-17 cell in colon are produced by non T cells are perhaps are of innate origin. Due to the complexity of double immunofluorescence technique on formalin fixed paraffin embedded (FFPE) biopsies we could not differentiate between low IL-17 expression and background. Therefore we might have omitted cell with low IL-17 expression (if any) that resembled background. Only the bright distinct IL-17 signals were chosen that were reliable enough to be a true signal. Our study

accounts for distinct and clean IL-17 expression that was both CD4 negative and CD3 negative. It is however quite unlikely to have true technical error as we clearly observed CD4$^+$IL-17$^+$ in the colon of Crohn's disease patients which was distinctly bright and clean. The overall IL-17 expression was analyzed by two different analysers and observed significant downregulation of IL-17 during GvHD. This confirms the specificity of IL-17 antibody and that immunofluorescent staining is in harmony with immunohistochemical staining.

Recently, a whole new set of immune cells have been identified, termed as innate lymphoid cells (ILCs) which plays central role to preserve epithelial integrity and tissue immunity[81]. ILCs mirrors helper T cell function by producing similar cytokines and expressing similar transcription factors for their development but lacks lineage marker[83]. Perhaps innate immunity alone is not sufficient to combat very early infections and that T cell related cytokines are required to mount effective immune response which is supplemented by ILCs. This could be one of the reasons why ILCs exists.

In past 10 years, there was a rise of influential works in understanding ILCs with the major focus on group 3 ILCs. Group 3 ILCs express *RORC* as a major transcription factor and produce IL-17 and IL-22[83]. Recent work by Hanash and colleagues demonstrated ILCs that produce IL-22 were associated with protection of the intestinal stem and progenitor cell compartment and mature epithelium from inflammatory tissue damage in an experimental model of GvHD[41]. However, during GVHD, there is loss of the IL-22-producing ILCs necessary for limiting that inflammatory tissue damage. We were however unable to establish IL-22 staining. Nevertheless, IL-22 producing ILCs also produce IL-17[179], and in our study these IL-17 are lost, we hypothesized that innate lymphoid cells are the major source of IL-17 and the decreased frequency of IL-17 producing ILCs renders higher GvHD. For this, IL-17 was colabelled with CD117 (c-kit), a well-known marker for group 3 ILCs. Majority of IL-17 signal colocalized with CD117 signal suggesting that IL-17$^+$ cells are probably group 3 innate lymphoid cells that are involved in tissue repair and immune homeostasis. At the same time, we found very few IL-17$^+$ cells that were negative for CD117 marker. This confers the heterogeneity of innate IL-17 population and confirms that there are several innate immune cells responsible of IL-17 production. Our findings have several limitations. Since mast cell also express CD117 and produce IL-17, we cannot

ascertain that all the CD117$^+$ IL-17$^+$ cells are ILCs. These could be a mix population of ILCs and mast cells. Furthermore, ILCs cannot be directly demonstrated by microscopy due to the lack of definite marker. If only one could combine IL-17 and CD117 together with CD127, group 3 ILCs can be confirmed. We were unable to establish CD127 staining and we were unable to establish triple staining due to the complexity of immunofluorescence on FFPE slides.

It is necessary to explore the heterogeneity of innate IL-17 to understand its role in GvHD. Triple staining may help us to decode several different IL-17 producing cells broadening our understanding in the pathogenesis of GvHD.

6.2   Differential gene regulation during acute GI GvHD

Several reports have intensified the importance of determining the gene expression profiling which helps identify the candidate genes involved in disease diagnosis, prognosis and outcome of GvHD[180-182]. In this study, an advanced digital PCR 'Fluidigm' was used to monitor gene profiling. Firstly, the accuracy and the reproducibility of Fluidigm were determined by repeating few genes that were previously analyzed in University Hospital Regensburg. We found that digital PCR Fluidigm readily reproduce the conventional qPCR data which are indifferent to the primer sets. We and others[141] reported that mRNA analysis by Fluidigm is as accurate as routinely followed qPCR and that Fluidigm technique should be incorporated in scientific research that substitute multiple PCRs at a time.

To our knowledge, this is the first study to evaluate gene profile in gut biopsies of GvHD patients. Out of several profiled genes, *CYP27A1*, *CYP27B1*, *VDR* and *PXR* turned out to be differentially regulated in GI tract of GvHD patients. CYP27A1-an enzyme associated with vitamin D synthesis, and vitamin D receptor were significantly downregulated in GvHD. Patients with less of these mRNAs displayed significantly higher TRM. Based on these results we hypothesize that during GvHD vitamin D metabolism is altered due to reduced *CYP27A1* which might lead to reduced systemic vitamin D level. Loss of *VDR* may reflect the fact that GvHD patients are vulnerable to vitamin D deficiency even when external supplementation is provided. A recent study study from

Meckel and colleagues revealed an interesting fact that serum 25(OH)D3 concentration is inversely related to the disease severity in the cohort of 230 ulcerative colitis patients[183]. They also showed that serum 25(OH)D had a dirct association with expresson of colonic mucosal VDR and tight junction proteins[183]. In another study, using VDR knock-out mice, authors illustrated that VDR is essential for epithelial tight junction protein associated gene-claudin 2 (CLDN2). Together with these recent findings one might hypothesize that the loss of CYP27A1 leads to reduced 25(OH)D level: in combination with the loss of VDR, epithelial junction might be compromised which might support the development of severe GvHD. Taken together, our results indicate the need to supplement patients undergoing stem cell transplantation with vitamin D since this might help to preserve epithelial structures and therefore ameliorate gut GvHD. Few studies have reported that vitamin D deficiency is related to development of chronic GvHD[184,185]. Kreutz et al. demonstrated the marked decline of vitamin D metabolites in the course of allogenic stem cell transplantation[145] providing emphasis on role of vitamin D on pathophysiology of GvHD. Furthermore, Kaplan-Meier estimates showed that the incidence of transplant related mortality is higher in patients expressing low level of CYP27A1 and VDR. It is worth to speculate that these vitamin D related parameters may represent the potential biomarkers and therefore further studies are required to find out the mechanism of loss of CYP27A1 and VDR which might contribute to vitamin D related therapy in future. It is well realized that the polymorphism in VDR is associated with poor survival following GvHD[186]. Subsequently, cyp polymorphism is associated with increased TRM after SCT[187]. Therefore it is perhaps noteworthy to study the vitamin D related gene expression with respect to SNPs. In addition, the cellular source of these changes needs to be clarified.

On the other hand, CYP27B1 upregulated in GvHD and was associated with increased mortality and reduced survival. CYP27B1 is responsible for the synthesis of biologically active form of vitamin D[188]. Few reports suggest that CYP27B1 upregulates in inflammatory phenomena**[147,148]**. Our finding is in line with the concept that CYP27B1 might indicate the inflammatory mediator of GvHD and could be used as a marker to predict GvHD mediated inflammation.

Pregnane-X-Receptor (PXR) turned out to be another possible candidate as a biomarker for GvHD progression. PXR is able to sense and metabolize xenobiotic compounds and suppresses inflammation[149]. This study showed significant downregulation of *PXR* mRNA in patients who suffered from GvHD. Deceased patients depicted relatively less PXR expression. It can be noted that PXR acts as an anti-inflammatory mediator which are lost during GvHD related inflammation. Recent study suggests that rifaximin (a rifamycin-derivative frequently used for treatment of traveler's diarrhea) is a potential ligand for PXR[189]. In one report, Weber et al. demonstrated that rifaximin treated patients had preserved intestinal microbial balance in ASCT patients[190]. This suggests the involvement of PXR in balanced microbial diversity. Although insignificant, our findings that rifaximin treated patients showed higher *PXR* mRNA expression when compared to ciprofloxacin treated patients is in line with Mencarelli and co-workers who reported that rifaximin increases the expression of *PXR* in the *in vitro* model of human epithelial cell[191]. *PXR* mRNA expression however did not show any differences in Kaplan-Meier estimates therefore we were not able to predict patient's survival with *PXR* mRNA expression.

6.3 Role of bacterial metabolites in GI GvHD

Human body harbors a dynamic community of nearly 100 trillion intestinal bacteria that are inevitable for the development, education and normal function of immune system[192]. Bacterial metabolites such as short chain fatty acids (SCFAs), indoles and their derivatives are essential to maintain immune balance in mice and men [36,113,155,193]. Since body of literatures have provided evidence that microbes and microbial metabolites are important for the maintenance of immune tolerance, in this study we hypothesized that indoxyl 3-sulfate, a bacterial metabolite, have immunomodulatory effects on human dendritic cells.

Here we reported that the bacterial metabolite I3S promotes anti-inflammatory and immunoregulatory DCs *in vitro*. So far, I3S is best known marker for chronic kidney diseases and cardiovascular diseases in patients during renal failure and this metabolite is toxic for epithelial and endothelial cells at the concentration of CKD patients [194]. However, our results appear to support the findings that microbes-derived indole and derivatives thereof, such as indole-3-carbinol (I3C)

and indiriubin-3'-oxime (IO) modulates the immune function by altering the function of DCs [155]. Unlike epithelial and endothelial cells, DCs maturation and viability remained unaffected in the presence of I3S which perhaps suggests a symbiotic survival mechanism of indoxyl 3-sulfate producing bacteria (clostridia species) and immune cells. The maturation process and antigen presenting ability of DCs was also unaltered by I3S suggested by normal expression of HLA-DR. However, co-stimulatory molecules CD80 and CD86 were downregulated under the influence of I3S. CD1a and CD83 on the other hand were not affected. Taken together, these data suggests that the bacterial metabolite I3S does not alter first signal of T cell activation i.e. antigen presentation by HLA-DR molecule but strongly alters second signal i.e. downregulation of co-stimulatory molecules on DCs that are necessary for T cell activation.

The third signal, cytokine production by DCs, was accessed by ELISA. Secretion of pro-inflammatory cytokines, IL-12 and IL-6 was strongly downregulated in presence of I3S whereas, IL-10, an anti-inflammatory cytokine strongly upregulated in presence of I3S. Our results further supports the findings by Benson and colleagues reported that the indole derivatives can alter cytokine production by DCs thus induce immunoregulatory nature [155]. Downregulation of surface marker CD80 and CD86 and the suppression of IL-6 production is in line with the findings by Orabona and colleagues that IL-6 production requires CD80 and CD86 expression [195]. Furthermore, *IL12A* and *IL12B* mRNA decreased at transcriptional level implicating that I3S uses IL-12 pathway to suppress inflammation mediated by DCs. Expression of IκB protein (inhibitor of NF-kB) in presence of I3S suggests that NF-kB pathway is possibly inhibited by I3S thus DCs acquire anti-inflammatory properties. It is known that I3S is a ligand of aryl hydrocarbon receptor (AhR) [196] and that AhR regulates NF-kB pathway [197]. We, however, did not observe alteration of AhR at transcriptional level but the slight alteration of suppressor of NF-kB reveals that I3S can modulate DC function partly by altering NF-kB perhaps via AhR independent pathway. This hypothesis is supported by the findings by Benson and co-workers where alteration in murine DC surface marker expression, cytokine production, and gene transcription were not entirely dependent on AhR [155].

To further explore whether these immunomodulatory DCs alter function of lymphocytes, I3S treated mDCs were co-cultured with lymphocytes isolated from healthy subjects. In the set of allogenic mixed leukocyte reaction, flow cytometry

revealed no difference in proliferation and expression of CD4$^+$ ^{T} cells and CD8$^+$ T cells (data not shown). There were no alterations in the proliferation of CD4$^+$CD25$^+$FOXP3$^+$ cells along with unaltered expression of AhR at transcriptional level. Bacterial metabolites (species of Clostridia) such as short chain fatty acid, namely butyrate, are potential Tregs inducers [51,198]. Indole and its derivatives, which are also produced by the species of Clostridia are reported to generate Tregs *in-vitro* [199]. Indoxyl 3-sulfate, however, did not seem to affect the differentiation of Tregs. This can be partially explained by unaltered AhR, as it is known that AhR is necessary to develop Tregs [200]. Finally, we have found strong reduction in cytokine production in MLR settings. IFN-y and TNF were significantly downregulated when lymphocytes were differentiated with I3S treated mDCs. Reduction of IFN-y production could be the result of decreased IL-12 production by mDCs followed by decreased T cell proliferation. To our surprise, IL-10 also depicted trend of downregulated in our MLR settings similar to the findings of Bansal and colleagues[199]. We assume that the regulatory criteria of lymphocytes is defined by the extent of inflammatory criteria, that is, in reduced inflammatory milieu, regulatory milieu also declines.

Collectively, we have demonstrated that I3S is beneficial to induce anti-inflammatory and immunoregulatory dendritic cells. The alteration in DC phenotype and function is possibly IL-12 pathway dependent. Altogether, we showed that I3S can modulate immune function by modulating cytokine levels. Our result supports the findings by Weber and colleagues that microbiota-derived indole and metabolites thereof are relevant counterpart of human immune system in protection against inflammation and for complex immune balance. It is however still hard to explain how the complex immune balance is achieved. In a much broader term we hypothesize that the bacterial metabolites like indoxyl 3-sulfate is a classic example of commensality. Tolerogenic immune system firstly prevents immune reaction against the bacteria itself which provides them a survival advantage. Secondly, the tolerogenic immune environment influences the inflammatory host immune system in general to avoid excess inflammation.

6.4　Conclusion and Perspective

Since the early beginnings, in the 1950's, hematopoietic stem cell transplantation (HSCT) has become an established curative treatment for an increasing number of patients with life-threatening hematological, oncological, hereditary and immunological diseases. This has become possible due to worldwide efforts of preclinical and clinical research focusing on issues of transplant immunology, reduction of transplant-associated morbidity and mortality and efficient malignant disease eradication. In the light of GvHD, gastrointestinal tract represents the major target organ of GvHD related inflammation. In spite of our broad understanding on the pathophysiology of GvHD, the actual GvHD biology of GI-tract remains poorly understood which is dominantly due to the lack of biopsies from GI tract of patients. In this study, we exploited huge number of gut biopsies from transplanted patients and analyzed several relevant players in GvHD.

Likewise, treatment has not improved in the last 20 years and the outcome of steroid resistant acute GvHD remains poor with only 30-40% survival which also reflects the insufficient understanding of pathophysiology[201].
The results of our study show that rather than effector cell population, immunoregulation seems to be most prognostic in GvHD. This seems to be true for the observed IDO – Foxp3 pathway, but also for the potential role of IL17^{+} cells.

Increase of regulatory proteins such as Foxp3 and IDO with increase in GvHD severity represents previously unrecognized regulatory loop in GvHD. Existence of CD8^{+} Foxp3^{+} Tregs provides novel insight in existence of different population of Tregs that may well turn out to be previously unrecognized protective cells in GvHD, but further studies are needed which also address the question of involvement of natural versus induced Tregs. Association of Foxp3^{+} Treg infiltrate with IDO strongly suggests that the majority of cells observed in our study are inducible Tregs but confirmation by more complex staining is needed.

Understanding of regulatory T cells has advanced significantly in both preclinical and clinical models for GvHD. Our data do not argue against the clinical application of natural Tregs where the next big challenge is to generate large and

pure enough Tregs with stable Foxp3-expression in a cost effective way. A further clinical problem is the optimal time point of Tregs application – if Tregs are applied to treat refractory GvHD there may be a substantial delay between indication and application and dampen the chance of successful interference due to irreversible damage. Furthermore, the impact of ongoing immunosuppressive drugs on Treg function has to be considered in clinical trials as it is also suggested by the effect of higher doses of steroid treatment on regulatory cell expression.

Therefore a deeper understanding of function of the different subpopulations of Foxp3$^+$ Tregs preferentially induced and natural Tregs is still needed and crucial to understand the role of these immunosupressors in allogeneic HSCT. Furthermore the role of CD8$^+$ Tregs still remains unclear. As Tregs may undergo changes depending on the inflammatory environment they are facing, modulation of a Treg promoting environment seems important in addition to therapeutic and prophylactic application.

The fact that IL-17$^+$ cells are of innate origin demands a further extended vision in pathophysiology of GvHD and approaches shall be introduced to protect innate IL-17$^+$ cells which may have crucial role in intestinal epithelial cell protection.

A still unresolved question is the role of steroid treatment on some of the observed effects. It may well be that FoxP3 expression and regulatory T cells are affected by steroids and that the treatment of GvHD in this way contributes to further loss of immunoregulation. As we used only onset or screening biopsies for our analysis of TRM, however, a steroid effect on these data is unlikely.

Bacterial diversity shapes immune system. Therefore effort shall be made to analyze immune cell in relation to the bacterial diversity which will clarify the importance of microbiota in influencing immune cells. Here we showed the bacterial metabolite indoxyl sulfate induce tolerogenic DCs *in vitro.* We observed that indoxyl sulfate is involved in downregulation of pro-inflammatory cytokines and upregulation of anti-inflammatory cytokine. It is well accepted that correct bacterial diversity is required for immune homeostasis. Bacterial metabolites like short chain fatty acids are involved in maintaining the integrity of epithelial cells, generate Tregs, induce tolerance and maintain immune balance. Therefore it is

quite possible that immune cell infiltrates are highly controlled by diversity of bacteria. It seems very important to understand why and how tiny micro-organism can alter entire immune response in human beings. Understanding the effective role of protective bacteria and their metabolites in inflammatory diseases like GvHD and attempt to preserve the bacterial diversity may contribute well to establish immune homeostasis in ASCT patients. The immunomodulating effects of bacterial metabolites as shown for 3IS in this study strongly suggests that the microbial environment is a major player in this context, and it is well possible that restoration of a protective microbiome needs to precede Tregs application or other immunoregulatory interventions.

Furthermore, biomarkers that allow early identification of patients at risk are urgently needed. This will help clinicians to choose right treatment early on time before the major changes have already damaged target organs. We showed that vitamin D related genes such as *CYP27A1* and *VDR* could be a potential biomarker in future for which further research is needed. Biopsy derived markers have to be evaluated against newly established serum markers[117] in prospective studies. A special effort should be made to detect early biomarkers as they might allow risk adapted early treatment and thus prevent irreversible damage.

7 Summary

Acute Graft vs Host Disease (aGvHD) after allogenic stem cell transplantation is caused by activated donor T cells after recognition of recipient minor or major HLA antigens, which are presented after conditioning mediated inflammation or activation of danger signals. Donor T cells attack epithelial structures on target organs, especially in the GI tract. Damage of target organs is attributed to cytotoxic T cells along with helper T cells and their pro-inflammatory cytokines. Natural regulatory T cells are able to dampen GvHD, but their exact role in prophylaxis and treatment has not yet been defined. Our current view of the pathophysiology of GvHD is summarized in Figure 7.1.
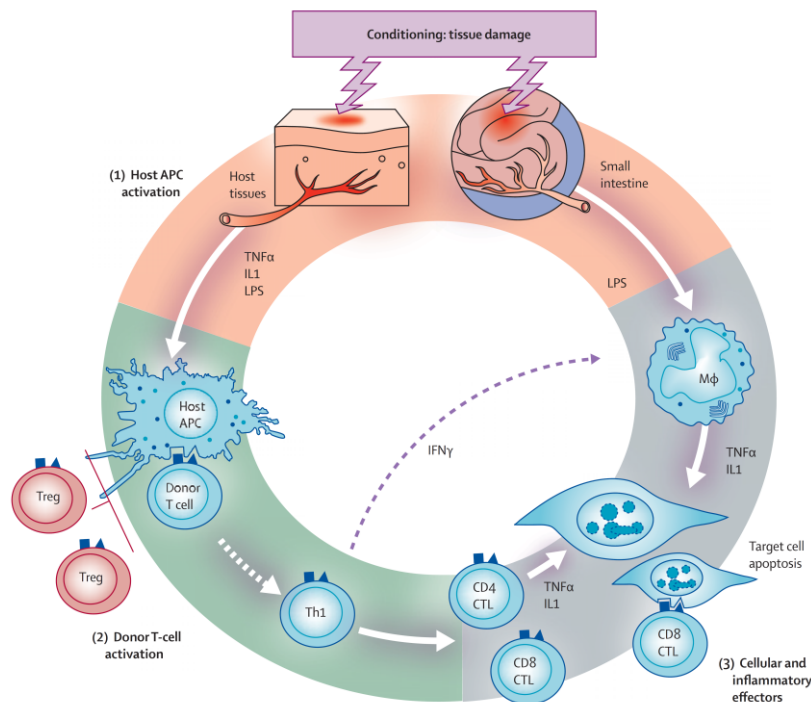

Figure 7.1: Pathophysiology of acute GvHD.
Pathophysiology of acute GvHD is summarized into three steps. 1. Conditioning regimen prior to transplantation damages and activates host tissues, especially the intestinal mucosa. DAMPs are released as a consequence; leading to inflammatory cytokine release and activation of host APCS. 2. Host APCs activate donor T cells in draining lymph nodes. 3. Activated macrophages along with T cells secret inflammatory cytokines that cause target cell apoptosis.

Our understanding in GvHD biology has advanced substantially; yet, the pathophysiology of gut GvHD is poorly understood partially due to the lack of gut biopsies for research and the difficulties to directly translate data from murine experiments into humans. The aim of this dissertation was therefore to analyze immune cell infiltrates and biomarkers in gut biopsies of patients after allogenic stem cell transplantation and to explain some of the newer findings on the role of the microbiome by analyzing bacterial metabolites *in vitro* .

CD4$^+$ T cells and CD8$^+$ T cells were analyzed by means of single antibody immunohistochemistry (IHC). CD4$^+$ T cells were found to be correlated with CD8$^+$ T cell infiltration and epithelial apoptosis whereas CD8$^+$ T cells were upregulated in GvHD and correlated with crypt loss and epithelial apoptosis confirming the primacy of T cell infiltrates in development and exacerbation of GvHD.

Foxp3$^+$ and IDO$^+$ cells were analyzed by IHC in gut biopsies of ASCT patients and the respective mRNA expression was analyzed by qPCR. Both Foxp3$^+$ cells and IDO$^+$ cells significantly upregulated at protein and mRNA level with exacerbation of GvHD, and, Foxp3 and IDO expression strongly correlated to each other suggesting an immunoregulatory loop reactively activated to dampen the T cell response. Using double immunofluorescence, existence of both, the expected CD4$^+$Foxp3$^+$ and the new population of CD8$^+$ Foxp3$^+$ Tregs were discovered which may be crucial for GvHD resolution.

IL-17$^+$ cells were analyzed by IHC and immunofluorescence in colon biopsies of ASCT patients which were significantly downregulated in GvHD. In line with protein expression, the transcription factor *RORC* significantly downregulated in GvHD. Double immunofluorescence depicted these cells are non T cells but co-express CD117 (c-kit) confirming the innate origin of IL-17$^+$ cells, more likely to be type 3 innate lymphoid cells. This suggests that IL17$^+$ cells beyond TH17 cells exist also in humans which may be protective in GvHD by production of protective IL22.

First phase of gene profiling revealed four possible candidate genes: *CYP27A1*, *CYP27B1*, *VDR* and PXR that were highly regulated in GvHD and two genes: *VDR* and *CYP27A1* could be a future biomarker. The predominance of Vitamin D dependent genes as significant biomarkers in GI tissue further supports the central role of immunoregulation in GvHD related inflammation.

As many of these regulatory loops are activated by the interplay between intestinal microbiota and immune cells, we revealed the importance of bacterial metabolite indoxyl sulfate as a potential immunomodulator that inhibited maturation and activation of human monocyte-derived dendritic cells *in vitro*.

Based on our findings we propose a new hypothesis on the pathophysiology of GvHD which is shown in fig 7.2
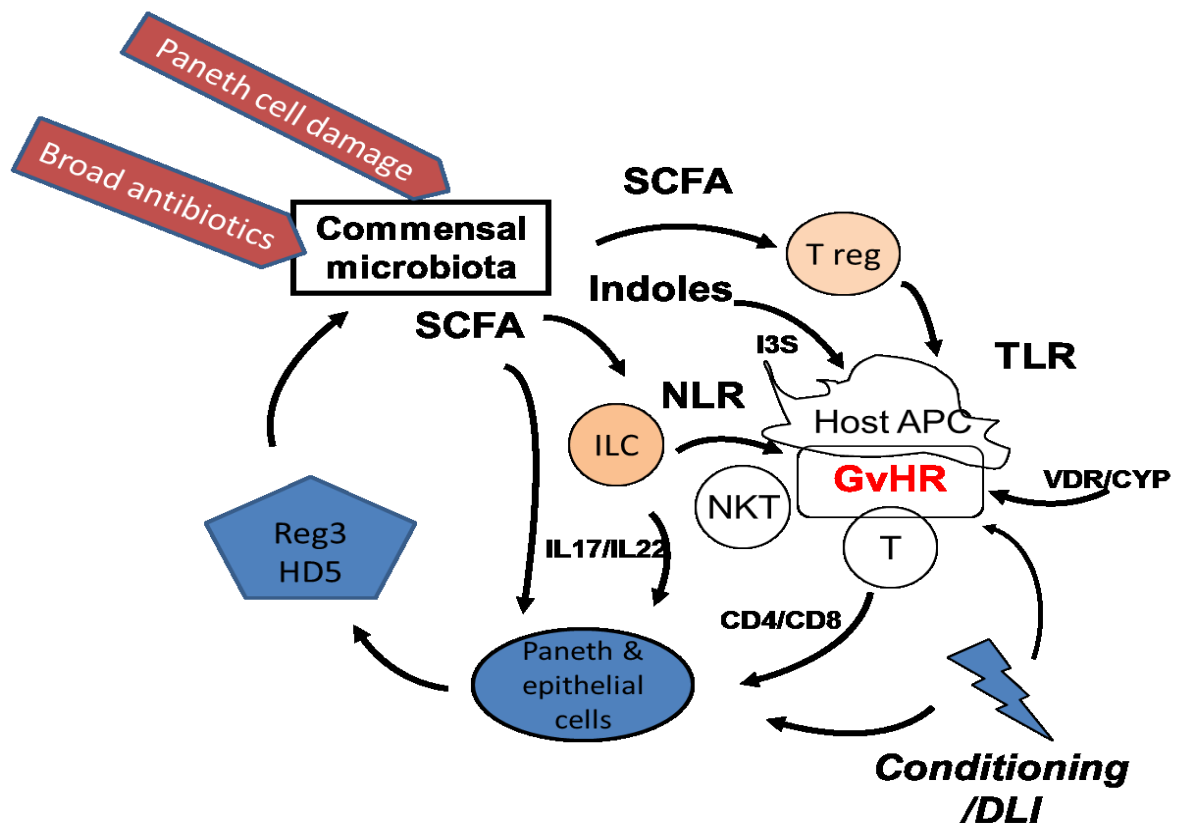
Figure 7.2: Pathophysiology of acute GvHD.
In a steady state, balanced microbiome and microbial metabolites maintains epithelial integrity and immune homeostasis. Once microbial diversity is destroyed initially due to broad antibiotics, epithelial barrier is broken and at the same time, bidirectional communication between Paneth cell and microbiome is hampered leading to compromised Reg proteins and defensins. Conditioning mediated toxicities leads to production of ATPs and uric acid which work together with PAMPs and DAMPs to indcue recipient antigen expression in antigen presenting cells. This leads to severe graft vs host reaction with increased CD8+ T cell activation. Both CD4+ and CD8+ T cells work synergistically to further destroy Paneth cells and epithelium. MDSC, Tregs, IDO+ cells, and toleregenic APCs try to dampen the inflammation but due to the lack of beneficial bacterial metabolites, complete regulation is obstructed and control of GvHD cannot be achieved. Alongside, IL17/IL22 producing protective ILCs, and vitamin D related parameters are lost in the course of inflammation. These phenomena lead to severe tissue destruction in lethal graft vs host disease.

In summary, our data underline that GvHD is a result of an imbalance between alloreactive T cells and protective regulatory cells and ILCs. Strategies aiming to restore immunoregulation are of central importance and may be either applied directly or by changing the balance of microbiota as bacterial metabolites play a major role in intestinal immunoregulation.

8 Zusammenfassung

In der Pathophysiologie der GvHD stand bis vor kurzem die Aktivierung alloreaktiver zytotoxischer T Zellen des Spenders durch major und minor HLA Antigene des Empfängers im Vordergrund. In einer ersten Phase werden diese auf Empfänger Antigenpräsentierenden Zellen nach Aktivierung durch die Konditionierung und Danger Associated Patterns stimuliert. In der Effektorphase werden die Targetorgane der GvHD über zytotoxische Mechanismen, aber auch über FasL und von CD4 Zellen produzierte proinflammatorische Zytokine geschädigt. Natürliche regulatorische T Zellen können die Entstehung der GvHD verhindern bzw abschwächen.

Die exakte Rolle der Immunregulation und der beteiligten Zellpoulationen im Patienten bei der GvHD ist z.T. durch die Schwierigkeit der Untersuchungen von Biopsien, aber auch durch die mangelnde Übertragbarkeit aus dem Mausmodell bisher unzureichend charakterisiert. Ziel dieser Arbeit war es deshalb, an einer großen Serie intestinaler Biopsien mittels Immunhistologie und -fluoreszenz sowie auf mRNA Ebene die regualatorischen Zellpopulationen genauer zu untersuchen und als möglichen Mechanismus der Immurnegaulation die Interaktion eines von der Arbeitsgruppe diagnostisch beschriebenen bakteriellen Metaboliten mit Immunzellen zu chrakterisieren.

Die Dominanz zytotoxischer T Zellen konnte durch die Korrelation der CD8 Infiltrate mit der Apoptose bestätigt warden, CD4 Zellen waren im Sinne einer T-Zellhilfe damit assoziiert.

Anders als erwartet waren Foxp3 positive Zellen und die Foxp3 mRNA bei Auftreten einer GvHD heraufreguliert. In Zusammenschau mit der gleichzeitigen Aktivierung IDO positive Zellen muss von einer immunregulatorischen Reaktion auf die T-Zellaktivierung ausgegangen warden. Als neue Population wurden neben den bekannten CD4$^+$Foxp3$^+$ Zellen auch CD8$^+$Foxp3$^+$ Zellen beschreiben, die als regulatorische Zellen im intestinalen Gewebe bei anderen Erkrankungen bekannt sind.

Entgegen der Erwartungen waren IL17 positive Zellen bei der GvHD vermindert. Das Paradoxon, dass TH17-Zellen bei der GvHD vermehrt sein sollten, konnte dadurch aufgeklärt warden, dass die IL17$^+$ Zellen keine T Zellmarker trugen, sondern dass sie wegen der Positivität für cKit vermutlich Innate Lymphoid Cells vom Typ 3 sind. Die verminderte Expression des Transkriptionsfaktors RoRy unterstützt diese Befunde.Diesen Zellen wird eine wichtige Rolle bei der Dämpfung der intestinalen Inflammation, vermutlich über IL22, zugeschrieben.

In der Genexpressionsanalyze stachen Enzyme des Vit D Stoffwechels sowie der VitDR als prognostische Marker hervor, was die zentrale Rolle der Immunregulation bei der intestinalen GvHD weiter unterstreicht.

Viele dieser regulatorischen Mechansimen warden durch die Interaktion mit dem intesitnalen Mikrobiom aktiviert. In der Untersuchung des in der Diagnostik wichtigen Indoxlysulfats konnte gezeigt werden, dass dieser Metabolit die Aktivierung von Immunzellen supprimiert und zur Immunregaultion über IL10 führt.

Zusammenfassend zeigen diese Untersuchung auf mehreren Ebenen, dass die GvHD als Dysblance zwischen Aktivierung zytotoxischer T Zellen und der Suppression regulatorischer Populationen wie T regs und ILCs verstanden werden kann. Die Entwicklung von Strategien zur Wiederherstellung der Immunregulation scheint von zentraler Bedeutung für die Verbesserung der GvHD Porphylaxe und Therapie zu sein. Dies kann entweder direkt geschehen oder durch Wiederherstellung einer balanzierten Zusammensetzung der intestinalen Mikrobiota, deren Metabolite einen erheblichen Anteil an der intestinalen Immunregulation tragen.

9 References

1   Ferrara, J. L., Levine, J. E., Reddy, P. & Holler, E. Graft-versus-host disease. *The Lancet* **373**, 1550-1561 (2009).
2   Abbas, A. K., Lichtman, A. H. & Pillai, S. *Cellular and molecular immunology*. (Elsevier Health Sciences, 2011).
3   Caceres-Cortes, J., Mindeni, M., Patersoni, B. & Caligiuri, M. A. A cell initiating human acute myeloid leukaemia after transplantation into SCID mice. *Nature* **367**, 17 (1994).
4   Dean, M., Fojo, T. & Bates, S. Tumour stem cells and drug resistance. *Nature Reviews Cancer* **5**, 275-284 (2005).
5   Bleakley, M. & Riddell, S. R. Molecules and mechanisms of the graft-versus-leukaemia effect. *Nature Reviews Cancer* **4**, 371-380 (2004).
6   Gratwohl, A. *et al.* Current trends in hematopoietic stem cell transplantation in Europe. *Blood* **100**, 2374-2386 (2002).
7   Copelan, E. A. Hematopoietic stem-cell transplantation. *New England Journal of Medicine* **354**, 1813-1826 (2006).
8   Tiercy, J.-M. *et al.* The probability of identifying a 10/10 HLA allele-matched unrelated donor is highly predictable. *Bone marrow transplantation* **40**, 515-522 (2007).
9   Powles, R. *et al.* Allogeneic blood and bone-marrow stem-cell transplantation in haematological malignant diseases: a randomised trial. *The Lancet* **355**, 1231-1237 (2000).
10   Cutler, C. *et al.* Acute and chronic graft-versus-host disease after allogeneic peripheral-blood stem-cell and bone marrow transplantation: a meta-analysis. *Journal of Clinical Oncology* **19**, 3685-3691 (2001).
11   Stewart, B. L. *et al.* Duration of immunosuppressive treatment for chronic graft-versus-host disease. *Blood* **104**, 3501-3506 (2004).
12   Wagner, J., Steinbuch, M., Kernan, N., Broxmayer, H. & Gluckman, E. Allogeneic sibling umbilical-cord-blood transplantation in children with malignant and non-malignant disease. *The Lancet* **346**, 214-219 (1995).
13   Bacigalupo, A. *et al.* Defining the intensity of conditioning regimens: working definitions. *Biology of Blood and Marrow Transplantation* **15**, 1628-1633 (2009).
14   McSweeney, P. A. *et al.* Hematopoietic cell transplantation in older patients with hematologic malignancies: replacing high-dose cytotoxic therapy with graft-versus-tumor effects. *Blood* **97**, 3390-3400 (2001).
15   Mattsson, J., Uzunel, M., Remberger, M. & Ringdén, O. T CELL MIXED CHIMERISM IS SIGNIFICANTLY CORRELATED TO A DECREASED RISK OF ACUTE GRAFT-VERSUS-HOST DISEASE AFTER ALLOGENEIC STEM CELL TRANSPLANTATION 1. *Transplantation* **71**, 433-439 (2001).
16   Apperley, J., Carreras, E., Gluckman, E., Gratwohl, A. & Masszi, T. Principles of conditioning. *The EBMT Handbook Haemopoietic Stem Cell Transplantation, 6th edn. European School of Haematology* (2012).
17   Barnes, D., Corp, M., Loutit, J. & Neal, F. Treatment of murine leukaemia with x rays and homologous bone marrow. *British medical journal* **2**, 626 (1956).
18   Billingham, R. The biology of graft-versus-host reactions. (1966).
19   Kernan, N. A. *et al.* Clonable T lymphocytes in T cell-depleted bone marrow transplants correlate with development of graft-v-host disease. *Blood* **68**, 770-773 (1986).
20   Epstein, F. H. *et al.* T-lymphocyte-antigen interactions in transplant rejection. *New England Journal of Medicine* **322**, 510-517 (1990).
21   Martin, P. J. *et al.* A retrospective analysis of therapy for acute graft-versus-host disease: initial treatment. *Blood* **76**, 1464-1472 (1990).
22   Filipovich, A. H. *et al.* National Institutes of Health consensus development project on criteria for clinical trials in chronic graft-versus-host disease: I. Diagnosis and staging working group report. *Biology of Blood and Marrow Transplantation* **11**, 945-956 (2005).
23   Xun, C., Thompson, J., Jennings, C., Brown, S. & Widmer, M. Effect of total body irradiation, busulfan-cyclophosphamide, or cyclophosphamide conditioning on

inflammatory cytokine release and development of acute and chronic graft-versus-host disease in H-2-incompatible transplanted SCID mice. *Blood* **83**, 2360-2367 (1994).

24   Matzinger, P. The danger model: a renewed sense of self. *Science (New York, N.Y.)* **296**, 301-305 (2002).

25   Shlomchik, W. D. *et al.* Prevention of graft versus host disease by inactivation of host antigen-presenting cells. *Science (New York, N.Y.)* **285**, 412-415 (1999).

26   Hill, G. R. *et al.* Total body irradiation and acute graft-versus-host disease: the role of gastrointestinal damage and inflammatory cytokines. *Blood* **90**, 3204-3213 (1997).

27   Markey, K. A., MacDonald, K. P. & Hill, G. R. The biology of graft-versus-host disease: experimental systems instructing clinical practice. *Blood* **124**, 354-362 (2014).

28   Teshima, T. *et al.* Acute graft-versus-host disease does not require alloantigen expression on host epithelium. *Nature medicine* **8**, 575-581 (2002).

29   Newton-Nash, D. K. The molecular basis of allorecognition assessment of the involvement of peptide. *Human immunology* **41**, 105-111 (1994).

30   Markey, K. A. *et al.* Conventional dendritic cells are the critical donor APC presenting alloantigen after experimental bone marrow transplantation. *Blood* **113**, 5644-5649 (2009).

31   Sprent, J., Schaefer, M., Gao, E. & Korngold, R. Role of T cell subsets in lethal graft-versus-host disease (GVHD) directed to class I versus class II H-2 differences. I. L3T4+ cells can either augment or retard GVHD elicited by Lyt-2+ cells in class I different hosts. *The Journal of experimental medicine* **167**, 556-569 (1988).

32   Goulmy, E. *et al.* Mismatches of minor histocompatibility antigens between HLA-identical donors and recipients and the development of graft-versus-host disease after bone marrow transplantation. *New England Journal of Medicine* **334**, 281-285 (1996).

33   Kagi, D. Fas and perforin pathways as major mechanisms of. *Science (New York, N.Y.)* **235**, 458 (1987).

34   Lowin, B., Hahne, M., Mattmann, C. & Tschopp, J. Cytolytic T-cell cytotoxicity is mediated through perforin and Fas lytic pathways. *Nature* **370**, 650-652 (1994).

35   Blazar, B. R., Murphy, W. J. & Abedi, M. Advances in graft-versus-host disease biology and therapy. *Nature Reviews Immunology* **12**, 443-458 (2012).

36   Mathewson, N. D. *et al.* Gut microbiome-derived metabolites modulate intestinal epithelial cell damage and mitigate graft-versus-host disease. *Nature immunology* (2016).

37   Peled, J. U., Jenq, R. R., Holler, E. & van den Brink, M. R. Role of gut flora after bone marrow transplantation. *Nature Microbiology* **1**, 16036 (2016).

38   Edinger, M. *et al.* CD4+ CD25+ regulatory T cells preserve graft-versus-tumor activity while inhibiting graft-versus-host disease after bone marrow transplantation. *Nature medicine* **9**, 1144-1150 (2003).

39   Bollrath, J. & Powrie, F. M. in *Seminars in immunology.* 352-357 (Elsevier).

40   Schneidawind, D. *et al.* Third-party CD4+ invariant natural killer T cells protect from murine GVHD lethality. *Blood* **125**, 3491-3500 (2015).

41   Hanash, A. M. *et al.* Interleukin-22 protects intestinal stem cells from immune-mediated tissue damage and regulates sensitivity to graft versus host disease. *Immunity* **37**, 339-350 (2012).

42   Fontenot, J. D. & Rudensky, A. Y. A well adapted regulatory contrivance: regulatory T cell development and the forkhead family transcription factor Foxp3. *Nature immunology* **6**, 331-337 (2005).

43   Feuerer, M., Hill, J. A., Mathis, D. & Benoist, C. Foxp3+ regulatory T cells: differentiation, specification, subphenotypes. *Nature immunology* **10**, 689-695 (2009).

44   Sakaguchi, S., Yamaguchi, T., Nomura, T. & Ono, M. Regulatory T cells and immune tolerance. *Cell* **133**, 775-787 (2008).

45   Hori, S., Nomura, T. & Sakaguchi, S. Control of regulatory T cell development by the transcription factor Foxp3. *Science (New York, N.Y.)* **299**, 1057-1061 (2003).

46   Cobbold, S. P. *et al.* Induction of foxP3+ regulatory T cells in the periphery of T cell receptor transgenic mice tolerized to transplants. *The Journal of Immunology* **172**, 6003-6010 (2004).

47   Maloy, K. J. & Powrie, F. Regulatory T cells in the control of immune pathology. *Nature immunology* **2**, 816-822 (2001).

48   Vignali, D. A., Collison, L. W. & Workman, C. J. How regulatory T cells work. *Nature Reviews Immunology* **8**, 523-532 (2008).

49   Campbell, D. J. & Koch, M. A. Phenotypical and functional specialization of FOXP3+ regulatory T cells. *Nature Reviews Immunology* **11**, 119-130 (2011).

50   Belkaid, Y. & Rouse, B. T. Natural regulatory T cells in infectious disease. *Nature immunology* **6**, 353-360 (2005).

51   Arpaia, N. *et al.* Metabolites produced by commensal bacteria promote peripheral regulatory T-cell generation. *Nature* **504**, 451-455 (2013).

52   Kingsley, C. I., Karim, M., Bushell, A. R. & Wood, K. J. CD25+ CD4+ regulatory T cells prevent graft rejection: CTLA-4-and IL-10-dependent immunoregulation of alloresponses. *The Journal of Immunology* **168**, 1080-1086 (2002).

53   Joffre, O., Gorsse, N., Romagnoli, P., Hudrisier, D. & Van Meerwijk, J. P. Induction of antigen-specific tolerance to bone marrow allografts with CD4+ CD25+ T lymphocytes. *Blood* **103**, 4216-4221 (2004).

54   Cohen, J. L. & Boyer, O. The role of CD4+ CD25 hi regulatory T cells in the physiopathogeny of graft-versus-host disease. *Current opinion in immunology* **18**, 580-585 (2006).

55   Nguyen, V. H. *et al.* The impact of regulatory T cells on T-cell immunity following hematopoietic cell transplantation. *Blood* **111**, 945-953 (2008).

56   Hahn, B. H., Singh, R. P., La Cava, A. & Ebling, F. M. Tolerogenic treatment of lupus mice with consensus peptide induces Foxp3-expressing, apoptosis-resistant, TGFβ-secreting CD8+ T cell suppressors. *The Journal of Immunology* **175**, 7728-7737 (2005).

57   Robb, R. J. *et al.* Identification and expansion of highly suppressive CD8+ FoxP3+ regulatory T cells after experimental allogeneic bone marrow transplantation. *Blood* **119**, 5898-5908 (2012).

58   Li, Q. *et al.* Decrease of CD4+ CD25+ regulatory T cells and TGF-β at early immune reconstitution is associated to the onset and severity of graft-versus-host disease following allogeneic haematogenesis stem cell transplantation. *Leukemia research* **34**, 1158-1168 (2010).

59   Rieger, K. *et al.* Mucosal FOXP3+ regulatory T cells are numerically deficient in acute and chronic GvHD. *Blood* **107**, 1717-1723 (2006).

60   Lord, J. D. *et al.* Blood and gastric FOXP3+ T cells are not decreased in human gastric graft-versus-host disease. *Biology of Blood and Marrow Transplantation* **17**, 486-496 (2011).

61   Ratajczak, P. *et al.* Th17/Treg ratio in human graft-versus-host disease. *Blood* **116**, 1165-1171 (2010).

62   Strauss, L. *et al.* Selective survival of naturally occurring human CD4+ CD25+ Foxp3+ regulatory T cells cultured with rapamycin. *The Journal of Immunology* **178**, 320-329 (2007).

63   Hippen, K. *et al.* Generation and Large-Scale Expansion of Human Inducible Regulatory T Cells That Suppress Graft-Versus-Host Disease. *American Journal of Transplantation* **11**, 1148-1157 (2011).

64   Hippen, K. L. *et al.* Massive ex vivo expansion of human natural regulatory T cells (Tregs) with minimal loss of in vivo functional activity. *Science translational medicine* **3**, 83ra41-83ra41 (2011).

65   Matsuoka, K.-i. *et al.* Low-dose interleukin-2 therapy restores regulatory T cell homeostasis in patients with chronic graft-versus-host disease. *Science translational medicine* **5**, 179ra143-179ra143 (2013).

66   Furusawa, Y. *et al.* Commensal microbe-derived butyrate induces the differentiation of colonic regulatory T cells. *Nature* **504**, 446-450 (2013).

67   Baban, B. *et al.* IDO activates regulatory T cells and blocks their conversion into Th17-like T cells. *The Journal of Immunology* **183**, 2475-2483 (2009).

68   Mezrich, J. D. *et al.* An interaction between kynurenine and the aryl hydrocarbon receptor can generate regulatory T cells. *The Journal of Immunology* **185**, 3190-3198 (2010).

69   Bessede, A. *et al.* Aryl hydrocarbon receptor control of a disease tolerance defence pathway. *Nature* **511**, 184-190 (2014).

70   Denison, M. S. & Nagy, S. R. Activation of the aryl hydrocarbon receptor by structurally diverse exogenous and endogenous chemicals*. *Annual review of pharmacology and toxicology* **43**, 309-334 (2003).

71   Trzonkowski, P. *et al.* First-in-man clinical results of the treatment of patients with graft versus host disease with human ex vivo expanded CD4+ CD25+ CD127− T regulatory cells. *Clinical immunology* **133**, 22-26 (2009).

72   Brunstein, C. G. *et al.* Infusion of ex vivo expanded T regulatory cells in adults transplanted with umbilical cord blood: safety profile and detection kinetics. *Blood* **117**, 1061-1070 (2011).

73 Mellor, A. L. & Munn, D. H. Ido expression by dendritic cells: tolerance and tryptophan catabolism. *Nat Rev Immunol* **4**, 762-774 (2004).

74 Jasperson, L. K. *et al.* Indoleamine 2, 3-dioxygenase is a critical regulator of acute graft-versus-host disease lethality. *Blood* **111**, 3257-3265 (2008).

75 Fallarino, F. & Grohmann, U. Using an ancient tool for igniting and propagating immune tolerance: IDO as an inducer and amplifier of regulatory T cell functions. *Current medicinal chemistry* **18**, 2215-2221 (2011).

76 Jasperson, L. K. *et al.* Inducing the tryptophan catabolic pathway, indoleamine 2, 3-dioxygenase (IDO), for suppression of graft-versus-host disease (GVHD) lethality. *Blood* **114**, 5062-5070 (2009).

77 Curti, A., Trabanelli, S., Salvestrini, V., Baccarani, M. & Lemoli, R. M. The role of indoleamine 2, 3-dioxygenase in the induction of immune tolerance: focus on hematology. *Blood* **113**, 2394-2401 (2009).

78 Landfried, K. *et al.* Tryptophan catabolism is associated with acute GVHD after human allogeneic stem cell transplantation and indicates activation of indoleamine 2, 3-dioxygenase. *Blood* **118**, 6971-6974 (2011).

79 Grohmann, U. *et al.* CTLA-4–Ig regulates tryptophan catabolism in vivo. *Nature immunology* **3**, 1097-1101 (2002).

80 Guillonneau, C. *et al.* CD40Ig treatment results in allograft acceptance mediated by CD8+ CD45RC low T cells, IFN-γ, and indoleamine 2, 3-dioxygenase. *The Journal of clinical investigation* **117**, 1096-1106 (2007).

81 Hazenberg, M. D. & Spits, H. Human innate lymphoid cells. *Blood* (2014).

82 Spits, H. & Cupedo, T. Innate lymphoid cells: emerging insights in development, lineage relationships, and function. *Annual review of immunology* **30**, 647-675 (2012).

83 Walker, J. A., Barlow, J. L. & McKenzie, A. N. Innate lymphoid cells—how did we miss them? *Nature Reviews Immunology* **13**, 75-87 (2013).

84 McKenzie, A. N., Spits, H. & Eberl, G. Innate lymphoid cells in inflammation and immunity. *Immunity* **41**, 366-374 (2014).

85 Spits, H. *et al.* Innate lymphoid cells—a proposal for uniform nomenclature. *Nature Reviews Immunology* **13**, 145-149 (2013).

86 Moro, K. *et al.* Innate production of TH2 cytokines by adipose tissue-associated c-Kit+ Sca-1+ lymphoid cells. *Nature* **463**, 540-544 (2010).

87 Neill, D. R. *et al.* Nuocytes represent a new innate effector leukocyte that mediates type-2 immunity. *Nature* **464**, 1367-1370 (2010).

88 Allen, J. E. & Sutherland, T. E. in *Seminars in immunology.* 329-340 (Elsevier).

89 Fallon, P. G. *et al.* IL-4 induces characteristic Th2 responses even in the combined absence of IL-5, IL-9, and IL-13. *Immunity* **17**, 7-17 (2002).

90 Monticelli, L. A. *et al.* Innate lymphoid cells promote lung-tissue homeostasis after infection with influenza virus. *Nature immunology* **12**, 1045-1054 (2011).

91 Halim, T. Y. *et al.* Retinoic-acid-receptor-related orphan nuclear receptor alpha is required for natural helper cell development and allergic inflammation. *Immunity* **37**, 463-474 (2012).

92 Mjösberg, J. *et al.* The transcription factor GATA3 is essential for the function of human type 2 innate lymphoid cells. *Immunity* **37**, 649-659 (2012).

93 Luci, C. *et al.* Influence of the transcription factor RORγt on the development of NKp46+ cell populations in gut and skin. *Nature immunology* **10**, 75-82 (2009).

94 Sanos, S. L. *et al.* RORγt and commensal microflora are required for the differentiation of mucosal interleukin 22–producing NKp46+ cells. *Nature immunology* **10**, 83-91 (2009).

95 Satoh-Takayama, N. *et al.* Microbial flora drives interleukin 22 production in intestinal NKp46+ cells that provide innate mucosal immune defense. *Immunity* **29**, 958-970 (2008).

96 Cella, M. *et al.* A human natural killer cell subset provides an innate source of IL-22 for mucosal immunity. *Nature* **457**, 722-725 (2009).

97 Lindemans, C. A. *et al.* Interleukin-22 promotes intestinal-stem-cell-mediated epithelial regeneration. *Nature* (2015).

98 Sonnenberg, G. F. & Artis, D. Innate lymphoid cell interactions with microbiota: implications for intestinal health and disease. *Immunity* **37**, 601-610 (2012).

99 Hazenberg, M. D. & Spits, H. Human innate lymphoid cells. *Blood* **124**, 700-709 (2014).

100 Hams, E., Bermingham, R. & Fallon, P. G. Macrophage and innate Lymphoid Cell interplay in the Genesis of Fibrosis. *Frontiers in immunology* **6** (2015).

101 Gaffen, S. L. Structure and signalling in the IL-17 receptor family. *Nature Reviews Immunology* **9**, 556-567 (2009).

102   Carlson, M. J. *et al.* In vitro–differentiated TH17 cells mediate lethal acute graft-versus-host disease with severe cutaneous and pulmonary pathologic manifestations. *Blood* **113**, 1365-1374 (2009).

103   Kappel, L. W. *et al.* IL-17 contributes to CD4-mediated graft-versus-host disease. *Blood* **113**, 945-952 (2009).

104   Zhao, X. Y., Xu, L. L., Lu, S. Y. & Huang, X. J. IL-17-producing T cells contribute to acute graft-versus-host disease in patients undergoing unmanipulated blood and marrow transplantation. *European journal of immunology* **41**, 514-526 (2011).

105   Ivanov, I. I. *et al.* The orphan nuclear receptor RORγt directs the differentiation program of proinflammatory IL-17+ T helper cells. *Cell* **126**, 1121-1133 (2006).

106   Ferretti, S., Bonneau, O., Dubois, G. R., Jones, C. E. & Trifilieff, A. IL-17, produced by lymphocytes and neutrophils, is necessary for lipopolysaccharide-induced airway neutrophilia: IL-15 as a possible trigger. *The Journal of Immunology* **170**, 2106-2112 (2003).

107   Happel, K. I. *et al.* Cutting edge: roles of Toll-like receptor 4 and IL-23 in IL-17 expression in response to Klebsiella pneumoniae infection. *The Journal of Immunology* **170**, 4432-4436 (2003).

108   Zheng, Y. *et al.* Interleukin-22 mediates early host defense against attaching and effacing bacterial pathogens. *Nature medicine* **14**, 282-289 (2008).

109   Cua, D. J. & Tato, C. M. Innate IL-17-producing cells: the sentinels of the immune system. *Nature Reviews Immunology* **10**, 479-489 (2010).

110   Consortium, H. M. P. Structure, function and diversity of the healthy human microbiome. *Nature* **486**, 207-214 (2012).

111   Cho, I. & Blaser, M. J. The human microbiome: at the interface of health and disease. *Nature Reviews Genetics* **13**, 260-270 (2012).

112   Holler, E. *et al.* Metagenomic analysis of the stool microbiome in patients receiving allogeneic stem cell transplantation: loss of diversity is associated with use of systemic antibiotics and more pronounced in gastrointestinal graft-versus-host disease. *Biology of Blood and Marrow Transplantation* **20**, 640-645 (2014).

113   Weber, D. *et al.* Low urinary indoxyl sulfate levels early after transplantation reflect a disrupted microbiome and are associated with poor outcome. *Blood* **126**, 1723-1728 (2015).

114   Singh, N. *et al.* Activation of Gpr109a, receptor for niacin and the commensal metabolite butyrate, suppresses colonic inflammation and carcinogenesis. *Immunity* **40**, 128-139 (2014).

115   Whitfield-Cargile, C. M. *et al.* The microbiota-derived metabolite indole decreases mucosal inflammation and injury in a murine model of NSAID enteropathy. *Gut microbes*, 1-16 (2016).

116   Shimada, Y. *et al.* Commensal bacteria-dependent indole production enhances epithelial barrier function in the colon. *PLoS One* **8**, e80604 (2013).

117   Levine, J. E. *et al.* A prognostic score for acute graft-versus-host disease based on biomarkers: a multicentre study. *The Lancet Haematology* **2**, e21-e29 (2015).

118   Wolff, D. *et al.* The Treatment of Chronic Graft-Versus-Host Disease. *Dtsch Arztebl Int* **108**, 732-740 (2011).

119   Jagasia, M. H. *et al.* National institutes of health consensus development project on criteria for clinical trials in chronic graft-versus-host disease: I. The 2014 diagnosis and staging working group report. *Biology of Blood and Marrow Transplantation* **21**, 389-401. e381 (2015).

120   Apperley, J., Carreras, E. & Gluckman, E. *Haematopoietic stem cell transplantation*. (European School of Haematology, 2008).

121   Glucksberg, H. *et al.* CLINICAL MANIFESTATIONS OF GRAFT-VERSUS-HOST DISEASE IN HUMAN RECIPIENTS OF MARROW FROM HL-A-MATCHED SIBLING DONOR, S. *Transplantation* **18**, 295-304 (1974).

122   Coons, A. H., Creech, H. J. & Jones, R. N. Immunological properties of an antibody containing a fluorescent group. *Experimental Biology and Medicine* **47**, 200-202 (1941).

123   Coons, A. H. & Kaplan, M. H. Localization of antigen in tissue cells II. Improvements in a method for the detection of antigen by means of fluorescent antibody. *The Journal of experimental medicine* **91**, 1-13 (1950).

124   Dabbs, D. J. *Diagnostic immunohistochemistry*. (Elsevier Health Sciences, 2013).

125   Graw, R., Herzig, G., Eisel, R. & Perry, S. Leukocyte and platelet collection from normal donors with the continuous flow blood cell separator. *Transfusion* **11**, 94-101 (1971).

126   Johnson, W., Mei, B. & Cohn, Z. A. The separation, long-term cultivation, and maturation of the human monocyte. *J Exp Med* **146**, 1613-1626 (1977).

127   Sanderson, R. J., Shepperdson, F. T., Vatter, A. E. & Talmage, D. W. Isolation and enumeration of peripheral blood monocytes. *The Journal of Immunology* **118**, 1409-1414 (1977).

128   Meierhoff, G., Krause, S. W. & Andreesen, R. Comparative analysis of dendritic cells derived from blood monocytes or CD34+ hematopoietic progenitor cells. *Immunobiology* **198**, 501-513 (1998).

129   Bain, B., VAS, M. R. & LOWENSTEIN, L. The development of large immature mononuclear cells in mixed leukocyte cultures. *Blood* **23**, 108-116 (1964).

130   Laemmli, U. K. Cleavage of structural proteins during the assembly of the head of bacteriophage T4. *nature* **227**, 680-685 (1970).

131   Shapiro, A. L., Viñuela, E. & Maizel, J. V. Molecular weight estimation of polypeptide chains by electrophoresis in SDS-polyacrylamide gels. *Biochemical and biophysical research communications* **28**, 815-820 (1967).

132   Hummel, S. *et al.* Telomere shortening in enterocytes of patients with uncontrolled acute intestinal graft-versus-host disease. *Blood* **126**, 2518-2521 (2015).

133   Shedlock, D. J. & Shen, H. Requirement for CD4 T cell help in generating functional CD8 T cell memory. *Science* **300**, 337-339 (2003).

134   Sun, J. C. & Bevan, M. J. Defective CD8 T cell memory following acute infection without CD4 T cell help. *Science (New York, N.Y.)* **300**, 339-342 (2003).

135   Bremm, M. *et al.* Advanced flowcytometric analysis of regulatory T cells: CD127 downregulation early post stem cell transplantation and altered Treg/CD3+ CD4+-ratio in severe GvHD or relapse. *Journal of immunological methods* **373**, 36-44 (2011).

136   Beres, A. J. *et al.* CD8+ Foxp3+ regulatory T cells are induced during graft-versus-host disease and mitigate disease severity. *The Journal of Immunology* **189**, 464-474 (2012).

137   Mellor, A. L. & Munn, D. H. IDO expression by dendritic cells: tolerance and tryptophan catabolism. *Nature Reviews Immunology* **4**, 762-774 (2004).

138   Puccetti, P. & Grohmann, U. IDO and regulatory T cells: a role for reverse signalling and non-canonical NF-κB activation. *Nature Reviews Immunology* **7**, 817-823 (2007).

139   Bettelli, E., Oukka, M. & Kuchroo, V. K. TH-17 cells in the circle of immunity and autoimmunity. *Nature immunology* **8**, 345-350 (2007).

140   Dong, C. Diversification of T-helper-cell lineages: finding the family root of IL-17-producing cells. *Nature Reviews Immunology* **6**, 329-334 (2006).

141   Spurgeon, S. L., Jones, R. C. & Ramakrishnan, R. High throughput gene expression measurement with real time PCR in a microfluidic dynamic array. *PloS one* **3**, e1662 (2008).

142   Jang, J. S. *et al.* Quantitative miRNA expression analysis using fluidigm microfluidics dynamic arrays. *BMC genomics* **12**, 1 (2011).

143   Sigmundsdottir, H. & Butcher, E. C. Environmental cues, dendritic cells and the programming of tissue-selective lymphocyte trafficking. *Nat Immunol* **9**, 981-987, doi:10.1038/ni.f.208 (2008).

144   van Etten, E. & Mathieu, C. Immunoregulation by 1, 25-dihydroxyvitamin D 3: basic concepts. *The Journal of steroid biochemistry and molecular biology* **97**, 93-101 (2005).

145   Kreutz, M. *et al.* Variations in 1 alpha,25-dihydroxyvitamin D3 and 25-hydroxyvitamin D3 serum levels during allogeneic bone marrow transplantation. *Bone Marrow Transplant* **33**, 871-873, doi:10.1038/sj.bmt.1704448 (2004).

146   Prosser, D. E. & Jones, G. Enzymes involved in the activation and inactivation of vitamin D. *Trends in biochemical sciences* **29**, 664-673 (2004).

147   Miller, J. & Gallo, R. L. Vitamin D and innate immunity. *Dermatologic therapy* **23**, 13-22 (2010).

148   Schauber, J. *et al.* Injury enhances TLR2 function and antimicrobial peptide expression through a vitamin D–dependent mechanism. *The Journal of clinical investigation* **117**, 803-811 (2007).

149   Mencarelli, A. *et al.* Inhibition of NF-kappaB by a PXR-dependent pathway mediates counter-regulatory activities of rifaximin on innate immunity in intestinal epithelial cells. *European journal of pharmacology* **668**, 317-324, doi:10.1016/j.ejphar.2011.06.058 (2011).

150   Wahli, W. A gut feeling of the PXR, PPAR and NF-kappaB connection. *Journal of internal medicine* **263**, 613-619, doi:10.1111/j.1365-2796.2008.01951.x (2008).

151 Levine, J. E. *et al.* Low Paneth cell numbers at onset of gastrointestinal graft-versus-host disease identify patients at high risk for nonrelapse mortality. *Blood* **122**, 1505-1509 (2013).

152 Ott, S. *et al.* Reduction in diversity of the colonic mucosa associated bacterial microflora in patients with active inflammatory bowel disease. *Gut* **53**, 685-693 (2004).

153 Turnbaugh, P. J. *et al.* An obesity-associated gut microbiome with increased capacity for energy harvest. *nature* **444**, 1027-1131 (2006).

154 Holmes, E. *et al.* Human metabolic phenotype diversity and its association with diet and blood pressure. *Nature* **453**, 396-400 (2008).

155 Benson, J. M. & Shepherd, D. M. Dietary ligands of the aryl hydrocarbon receptor induce anti-inflammatory and immunoregulatory effects on murine dendritic cells. *Toxicological Sciences*, kfr249 (2011).

156 Duerkop, B. A., Vaishnava, S. & Hooper, L. V. Immune responses to the microbiota at the intestinal mucosal surface. *Immunity* **31**, 368-376, doi:10.1016/j.immuni.2009.08.009 (2009).

157 Shlomchik, W. D. Graft-versus-host disease. *Nature reviews. Immunology* **7**, 340-352, doi:10.1038/nri2000 (2007).

158 Anderson, B. E. *et al.* Memory CD4+ T cells do not induce graft-versus-host disease. *The Journal of clinical investigation* **112**, 101-108, doi:10.1172/jci17601 (2003).

159 Zhang, P., Wu, J., Deoliveira, D., Chao, N. J. & Chen, B. J. Allospecific CD4(+) effector memory T cells do not induce graft-versus-host disease in mice. *Biology of blood and marrow transplantation : journal of the American Society for Blood and Marrow Transplantation* **18**, 1488-1499, doi:10.1016/j.bbmt.2012.07.009 (2012).

160 Voskoboinik, I., Whisstock, J. C. & Trapani, J. A. Perforin and granzymes: function, dysfunction and human pathology. *Nature Reviews Immunology* **15**, 388-400 (2015).

161 Landfried, K. *et al.* Recipient NOD2/CARD15 status affects cellular infiltrates in human intestinal graft-versus-host disease. *Clinical and experimental immunology* **159**, 87-92, doi:10.1111/j.1365-2249.2009.04049.x (2010).

162 Holler, E. *et al.* Prognostic significance of NOD2/CARD15 variants in HLA-identical sibling hematopoietic stem cell transplantation: effect on long-term outcome is confirmed in 2 independent cohorts and may be modulated by the type of gastrointestinal decontamination. *Blood* **107**, 4189-4193, doi:10.1182/blood-2005-09-3741 (2006).

163 Holler, E. *et al.* Both donor and recipient NOD2/CARD15 mutations associate with transplant-related mortality and GvHD following allogeneic stem cell transplantation. *Blood* **104**, 889-894, doi:10.1182/blood-2003-10-3543 (2004).

164 Mielke, S. *et al.* Reconstitution of FOXP3+ regulatory T cells (Tregs) after CD25-depleted allotransplantion in elderly patients and association with acute graft-versus-host disease. *Blood* **110**, 1689-1697 (2007).

165 Miura, Y. *et al.* Association of Foxp3 regulatory gene expression with graft-versus-host disease. *Blood* **104**, 2187-2193 (2004).

166 Rezvani, K. *et al.* High donor FOXP3-positive regulatory T-cell (Treg) content is associated with a low risk of GVHD following HLA-matched allogeneic SCT. *Blood* **108**, 1291-1297 (2006).

167 Zhai, Z. *et al.* Correlation of the CD4+ CD25high T-regulatory cells in recipients and their corresponding donors to acute GVHD. *Transplant International* **20**, 440-446 (2007).

168 Tsai, Y.-G., Yang, K. D., Niu, D.-M., Chien, J.-W. & Lin, C.-Y. TLR2 agonists enhance CD8+ Foxp3+ regulatory T cells and suppress Th2 immune responses during allergen immunotherapy. *The Journal of Immunology* **184**, 7229-7237 (2010).

169 Zheng, J. *et al.* Human CD8+ regulatory T cells inhibit GVHD and preserve general immunity in humanized mice. *Science translational medicine* **5**, 168ra169-168ra169 (2013).

170 Scapini, P. & Cassatella, M. A. Social networking of human neutrophils within the immune system. *Blood* **124**, 710-719, doi:10.1182/blood-2014-03-453217 (2014).

171 Pillay, J. *et al.* A subset of neutrophils in human systemic inflammation inhibits T cell responses through Mac-1. *The Journal of clinical investigation* **122**, 327-336 (2012).

172 Deshmukh, H. S. *et al.* The microbiota regulates neutrophil homeostasis and host resistance to Escherichia coli K1 sepsis in neonatal mice. *Nature medicine* **20**, 524-530, doi:10.1038/nm.3542 (2014).

173 Kanther, M. *et al.* Commensal microbiota stimulate systemic neutrophil migration through induction of serum amyloid A. *Cellular microbiology* **16**, 1053-1067, doi:10.1111/cmi.12257 (2014).

174 Maslowski, K. M. *et al.* Regulation of inflammatory responses by gut microbiota and chemoattractant receptor GPR43. *Nature* **461**, 1282-1286, doi:10.1038/nature08530 (2009).

175 Hoechst, B., Gamrekelashvili, J., Manns, M. P., Greten, T. F. & Korangy, F. Plasticity of human Th17 cells and iTregs is orchestrated by different subsets of myeloid cells. *Blood* **117**, 6532-6541, doi:10.1182/blood-2010-11-317321 (2011).

176 Jitschin, R. *et al.* CLL-cells induce IDOhi CD14+HLA-DRlo myeloid-derived suppressor cells that inhibit T-cell responses and promote TRegs. *Blood* **124**, 750-760, doi:10.1182/blood-2013-12-546416 (2014).

177 Sutton, C. E. *et al.* Interleukin-1 and IL-23 induce innate IL-17 production from γδ T cells, amplifying Th17 responses and autoimmunity. *Immunity* **31**, 331-341 (2009).

178 Michel, M.-L. *et al.* Identification of an IL-17–producing NK1. 1neg iNKT cell population involved in airway neutrophilia. *The Journal of experimental medicine* **204**, 995-1001 (2007).

179 Wojno, E. D. T. & Artis, D. Innate lymphoid cells: balancing immunity, inflammation, and tissue repair in the intestine. *Cell host & microbe* **12**, 445-457 (2012).

180 Bouazzaoui, A. *et al.* Chemokine and chemokine receptor expression analysis in target organs of acute graft-versus-host disease. *Genes and immunity* **10**, 687-701 (2009).

181 Novota, P. *et al.* Expression profiling of major histocompatibility and natural killer complex genes reveals candidates for controlling risk of graft versus host disease. *PLoS One* **6**, e16582 (2011).

182 Sadeghi, B. *et al.* Early-phase GVHD gene expression profile in target versus non-target tissues: kidney, a possible target&quest. *Bone marrow transplantation* **48**, 284-293 (2013).

183 Meckel, K. *et al.* Serum 25-hydroxyvitamin D concentration is inversely associated with mucosal inflammation in patients with ulcerative colitis. *The American journal of clinical nutrition* **104**, 113-120, doi:10.3945/ajcn.115.123786 (2016).

184 Glotzbecker, B. *et al.* Low levels of 25-hydroxyvitamin D before allogeneic hematopoietic SCT correlate with the development of chronic GVHD. *Bone Marrow Transplant* **48**, 593-597, doi:10.1038/bmt.2012.177 (2013).

185 von Bahr, L. *et al.* Increased incidence of chronic GvHD and CMV disease in patients with vitamin D deficiency before allogeneic stem cell transplantation. *Bone Marrow Transplant* **50**, 1217-1223, doi:10.1038/bmt.2015.123 (2015).

186 Middleton, P. G. *et al.* Vitamin D receptor gene polymorphism associates with graft-versus-host disease and survival in HLA-matched sibling allogeneic bone marrow transplantation. *Bone Marrow Transplant* **30**, 223-228, doi:10.1038/sj.bmt.1703629 (2002).

187 Elmaagacli, A. H. *et al.* Cytochrome P450 2C19 loss-of-function polymorphism is associated with an increased treatment-related mortality in patients undergoing allogeneic transplantation. *Bone Marrow Transplant* **40**, 659-664, doi:10.1038/sj.bmt.1705786 (2007).

188 Lopes, N. *et al.* Alterations in Vitamin D signalling and metabolic pathways in breast cancer progression: a study of VDR, CYP27B1 and CYP24A1 expression in benign and malignant breast lesions Vitamin D pathways unbalanced in breast lesions. *BMC cancer* **10**, 1 (2010).

189 Ma, X. *et al.* Rifaximin is a gut-specific human pregnane X receptor activator. *Journal of Pharmacology and Experimental Therapeutics* **322**, 391-398 (2007).

190 Weber, D. *et al.* Rifaximin preserves intestinal microbiota balance in patients undergoing allogeneic stem cell transplantation. *Bone marrow transplantation* (2016).

191 Mencarelli, A. *et al.* Pregnane-X-receptor mediates the anti-inflammatory activities of rifaximin on detoxification pathways in intestinal epithelial cells. *Biochemical pharmacology* **80**, 1700-1707, doi:10.1016/j.bcp.2010.08.022 (2010).

192 Hooper, L. V. & Macpherson, A. J. Immune adaptations that maintain homeostasis with the intestinal microbiota. *Nature Reviews Immunology* **10**, 159-169 (2010).

193 Nastasi, C. *et al.* The effect of short-chain fatty acids on human monocyte-derived dendritic cells. *Scientific reports* **5** (2015).

194 Vanholder, R., Schepers, E., Pletinck, A., Nagler, E. V. & Glorieux, G. The uremic toxicity of indoxyl sulfate and p-cresyl sulfate: a systematic review. *Journal of the American Society of Nephrology* **25**, 1897-1907 (2014).

195 Orabona, C. *et al.* CD28 induces immunostimulatory signals in dendritic cells via CD80 and CD86. *Nature immunology* **5**, 1134-1142 (2004).

196   Schroeder, J. C. *et al.* The uremic toxin 3-indoxyl sulfate is a potent endogenous agonist for the human aryl hydrocarbon receptor. *Biochemistry* **49**, 393-400 (2009).

197   Vogel, C. F. *et al.* Aryl hydrocarbon receptor signaling regulates NF-κB RelB activation during dendritic-cell differentiation. *Immunology and cell biology* **91**, 568-575 (2013).

198   Smith, P. M. *et al.* The microbial metabolites, short-chain fatty acids, regulate colonic Treg cell homeostasis. *Science* **341**, 569-573 (2013).

199   Bansal, T., Alaniz, R. C., Wood, T. K. & Jayaraman, A. The bacterial signal indole increases epithelial-cell tight-junction resistance and attenuates indicators of inflammation. *Proceedings of the national academy of sciences* **107**, 228-233 (2010).

200   Gandhi, R. *et al.* Activation of the aryl hydrocarbon receptor induces human type 1 regulatory T cell-like and Foxp3+ regulatory T cells. *Nature immunology* **11**, 846-853 (2010).

201   Martin, P. J. *et al.* Endpoints for clinical trials testing treatment of acute graft-versus-host disease: a joint statement. *Biology of blood and marrow transplantation : journal of the American Society for Blood and Marrow Transplantation* **15**, 777-784, doi:10.1016/j.bbmt.2009.03.012 (2009).

10 Acknowledgements

Ich danke Sven Heymann für seine großartige Unterstützung. Vielen Dank für dein Vertrauen und deine Geduld in guten und schlechten Zeiten. Vielen Dank auch an Klaus Heymann und Christiane Heymann für die elterliche Liebe und Unterstützung.

Finally, I like to thank my family for believing in me especially my mother. I owe my entire success and achievement to my mother. I thank you for letting me choose my own path. Thank you for everything.